The University Of Sheffield.

Thesis Title

Investigating the Role of the Yeast Dynamin-like protein Vps1 in Endocytosis

By:

Laila Moushtaq

A thesis submitted in partial fulfilment of the requirements for the degree of Doctor of Philosophy

The University of Sheffield
Faculty of Pure Science
School (or Department) of Molecular Biology and Biotechnology

Submission Date
18.12.2015

Acknowledgement

First and for all, I would like to thank Prof. Kathryn Ayscough for giving me this opportunity to undertake my PhD research in her Lab. Thank you for your continuous guidance and support, for always being there when needed and most importantly for believing in me. You have been an amazing supervisor and a wonderful Boss and I wouldn't have made it without your support.

Secondly, I would like to give a big thanks to my forever-beloved husband, Ashkan. Thank you for all your patience, support and understanding throughout the years. Thank you for always being there when I needed you. Thank you for the late driving to and from the lab when I had work to finish. Thank you for babysitting Ali when you were most tired so I could get my work done. Thank you for your words that only made me a stronger woman. They say, behind every great man is a great woman; but I also believe that behind every great woman is a very patient man. You and our son Ali are the bright light of my days and I wouldn't have made it without your belief in me.

Great love, respect and appreciation to my wonderful parents, who even though are miles away, their prayers have always been with me. Thanks for your continuous words of encouragement and support. I love you and I miss you both.

Finally, I would like to thank past and present members of the Ayscough and Winder lab for their help, guidance and advices. You guys were great.

Abstract

Endocytosis is a highly regulated process in most eukaryotic cells, and is essential for the cell to appropriately respond to changes in its environment. It is critical for recycling plasma membrane proteins and lipids and for the uptake/down-regulation of cell-surface receptors and cargo molecules ensuring appropriate membrane composition. Clathrin-mediated endocytosis (CME) is the best-studied form of endocytosis occurring in both mammals and in yeast. Stages of CME involve the formation of a clathrin-coated pit (CCP), which undergoes progressive invagination before scission occurs forming a clathrin-coated vesicle (CCV). Dynamins are a conserved family of large GTPases whose function is best understood in the context of CME specifically in the vesicle scission process. Mutations in dynamin have been implicated in various neurological disorders such as Epilepsy, Charcot-Marie Tooth and many others. There are no classical dynamins in yeast however, Vps1, a dynamin-like-protein has been shown to perform similar functions to the classical mammalian dynamins. The work in this thesis aimed to use yeast as a model system to increase our understanding of dynamins and their endocytic function. Specifically, mutations corresponding to disease causing mutations in dynamin1 and 2 were generated and studied in yeast Vps1. Attempts were also made to investigate whether mammalian Dynamin-2 can complement deletion of *vps1* in any of its membrane trafficking roles. A chimeric construct was generated comprising vps1 with the InsertB region replaced by the Dynamin-2 PH domain to determine whether this was able to localize and function in yeast. Finally, the generation of stable cells with integrated Vps1 endocytic mutations allowed a screen to be carried out to identify genes, which when overexpressed rescue the temperature sensitivity

associated with one of these endocytic mutations and thereby indicate cell processes or pathways that might impact on Vps1 function during endocytosis.

List of Abbreviations

Amp	Ampicillin
APS	Ammonium persulphate
BLAST	Basic local alignment search tool
BSA	Bovine serum albumin
BSE	Bundle signaling element
CCV	Clathrin coated vesicle
CME	Clathrin mediated endocytosis
CMT	Charchot-Marie-Tooth
CNM	Centronuclear Myopathy
CPY	Carboxypeptidase Y
DLP	Dynamin-like protein
DMSO	Dimethyl sulphoxide
DNA	Deoxyribonucleic acid
Dnm1	Dynamin-related GTPase 1
DRP	Dynamin-related protein
DTT	Dithiothreito
EDTA	Ethylenediaminetetraacetic acid
ECL	Enhanced chemi-luminescence
EGF	Epidermal growth factor
ELC	Exercise-induced collapse
EM	Electron microscope
EPS15	EGFR pathway substrate 15
ESCRT	Endosomal sorting complex required for transport
F-actin	Filamentous actin

FCHO	FCH domain only proteins
FEME	Fast endophilin-mediated endocytosis
G-actin	Globular actin
GED	GTPase effector domain
GFP	Green fluorescent protein
GTP	Guanosine triphosphate
GTPγs	Guanosine 5'-O-[gamma-thio]triphosphate
Kb	Kilo base pair
kDA	Kilo Dalton
Leu	Leucine
LiAc	Lithium acetate
LY	Lucifer yellow
Mgm1	Mitochondrial genome maintenance-1
Min	Minutes
mRNA	Messenger RNA
MTS	Mitochondrial targeting sequence
N-terminal	Amino terminal
PAGE	Polyacrylamide gel electrophoresis
PBS	Phosphate buffered saline
PEG	Polyethylene glycol
PCR	Polymerase chain reaction
PH	Pleckstrin homology
PRD	Proline rich domain
PVDF	Polyvinylidene difluoride
RFP	Red fluorescent protein

RPM	Rounds per minute
SDS	Sodium dodecyl sulfate
SGD	Saccharomyces genome database
SH3	Src-homology 3
TAE	Tris-acetate-EDTA
Taq	Thermus acquaticus
TBST	Tris-buffered saline and Tween-20
TE	Tris EDTA
TEMED	N, N, N', N'-Tetramethylethyl-enediamine
TIFR	Total internal reflection fluorescence
TMD	Transmembrane domain
Tris	Tris(hydroxymethyl)aminomethane
UF	Uranyl formate
Ura	Uracil
UV	Ultra violet
V	Volts
Vps1	Vacuolar protein sorting 1
WT	Wild type
WWW	World wide web
YEp24	Yeast episomal plasmid 24
YPD	Yeast extract peptone dextrose
YT	Yeast extract and tryptone

Table of Content

List of Figures

List of Tables

Chapter 1: Introduction

1.1. Membrane trafficking and eukaryotic cell compartmentalization

An important feature of eukaryotic cells is the presence of internal membrane bound compartments and organelles to which proteins must be correctly targeted in order to maintain appropriate function of these compartments. Synthesized proteins usually contain sorting signals through which they are recognized. They get trafficked passing through a series of organelles, including the endoplasmic reticulum (ER) and the Golgi apparatus on their way to the plasma membrane or the extracellular space [figure 1.1]. While exocytosis ensures that appropriate material is trafficked to the cell surface, material also needs to be constantly removed from the surface to allow protein and lipid remodelling. Nutrient transporters and signalling receptors need their levels to be regulated to ensure these are appropriate for the cell environment. This inward movement of proteins and lipids happens via the process of endocytosis. In the case of some integral membrane proteins which carry ligands between different cellular compartments, they have to be constantly shuttled making up to 300 round trips during their lifetime [Trowbridge and Collawn 1993]. Therefore, controlling these processes is essential to regulate the steady state of cellular organelles and to maintain the correct signaling response required by the cell [Bonifacino and Glick, 2004].

1.2. Endocytosis

Endocytosis is an important and highly regulated process that occurs in most eukaryotic cells. It involves the invagination of plasma membrane into the cell resulting in a vesicle, which can then fuse with the endosomes and enter the endo-lysosomal membrane system [Robertson *et al.* 2009]. Endocytosis is important for recycling plasma membrane proteins and lipids ensuring appropriate membrane composition, and for the uptake or down-regulation of cell-

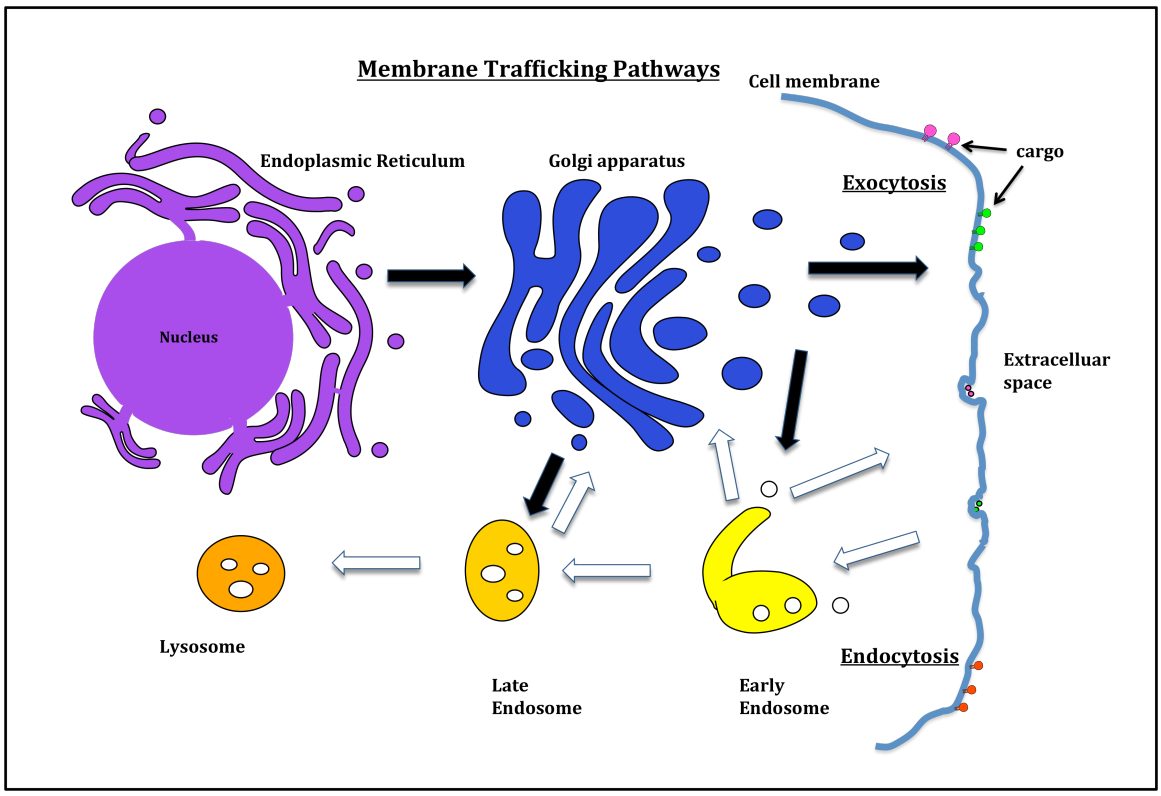

Fig.1.1. Membrane trafficking. The diagram represents a broad summary of the membrane trafficking pathways. Through several steps of fission and fusion events, secretory vesicles form at the ER and move through the Golgi complex until they reach the plasma membrane where the cargo gets removed to the extracelluar space or stay at the plasma membrane. The Black arrows in the diagram represent this pathway, which is known as exocytosis. In some cases the secretory vesicles can be targeted to other compartments such as the early or late endosomes for cargo recycling or degradation. On the other hand, various proteins, lipids and extracelluar materials get internalized via the formation of plasma membrane invagination, which bud off forming vesicles that carry the cargo molecules to the early endosomes for appropriate sorting or to the late endosomes and the lysosomes for degradation. The white arrows in the diagram represent this pathway, which is known as endocytosis. In some cases the secretory vesicles can be targeted to other compartments such as the Golgi complex.

surface receptors and cargo molecules [Doherty and McMahon 2009], which is essential for allowing the cell to appropriately respond to changes in its environment. Endocytosis is not only involved in the negative regulation of membrane proteins and lipids, but it also plays important roles in the positive regulation of many signaling pathways. An example of the latter is the epidermal growth factor (EGF), where in the case of a reduction in the receptor concentration on the plasma membrane, the EGF receptors are recycled back to the plasma membrane after being internalized via endocytosis allowing for a prolonged signaling [Platta and Stenmark 2011]. Also, in mammalian cells, pathogens such as viruses were shown to use various endocytic routes for internalization into the cell [Marsh and Helenius 2006].

Because endocytosis is a fundamental process, controlling not only the plasma membrane composition and the entrance of various cargoes into the cell, but also in initiating various signaling pathways, its regulation is very important in order to maintain normal function and cell response to environmental cues. Abnormalities in endocytosis were shown to be involved in human diseases including neurodegenerative diseases such as Alzheimer's disease [Wu and Yao 2009], atherosclerosis, diabetes [Zhang 2008] and cancer [Mellman and Yarden, 2013].

1.2.1. Mechanisms of Endocytosis - Clathrin-Mediated Endocytosis:

Several mechanisms of endocytosis have been described, which can be divided into different classes. The best-studied mechanism is the clathrin-mediated endocytosis (CME), where a clathrin-coated pit (CCP) undergoes progressive invagination before scission occurs forming a clathrin-coated vesicle (CCV) [Yarar *et al.* 2004]. Various adaptor and accessory proteins are involved in this process, and these can vary between different compartments and organisms [Le Roy and Wrana 2005]. In terms of cargoes, it was shown that in some cells, cargoes that get packaged into a vesicle are

limited whereas in other cells e.g. in synapses, up to 20 different cargoes can be present in the same vesicle [Doherty and McMahon 2009]. Real-time fluorescence microscopy studies established that specific proteins are sequentially recruited to endocytic sites to drive membrane invagination and vesicle scission [Smaczynska-de Rooij *et al.* 2010].

Based on ultrastructural analysis and cellular observations the formation of a CCV was defined to go through five stages, these are; initiation of pit formation, cargo selection, coat assembly, scission and uncoating [figure 1.2] [McMahon and Boucrot, 2011]. The first stage in CME, the formation of membrane invagination or a pit, was thought to be mediated by the AP2 protein complex, however studies have shown that this stage is initiated by the FCH domain only (FCHO) proteins, EGFR pathway substrate 15 (EPS15) and intersectins [McMahon and Boucrot, 2011]. These proteins are thought to recruit AP2, which mediates cargo selection along with other cargo specific adaptor proteins. Once cargo selection has taken place, clathrin gets recruited to the plasma membrane from the cytoplasm directly by AP2 and other accessory adaptor proteins [Le Roy and Wrana 2005] and clathrin triskelia assemble into a polygonal lattice, which along with the action of other accessory proteins result in the formation of a coated vesicle [McMahon and Boucrot, 2011]. As the coat assembly takes place, the BAR domain proteins such as amphiphysin, endophilin and sorting nexin 9 (SNX9) get recruited to help form the neck of the pit. Finally the CCV vesicle gets released upon GTP hydrolysis of dynamin, which is a major scission protein (see later). Once released into the interior of the cell, the CCV is uncoated with the action of specific proteins e.g. Auxilin and Hsc70 (in mammals) and the vesicle is trafficked into the early endosome, which is the primary sorting station for proteins [Le Roy and Wrana 2005].

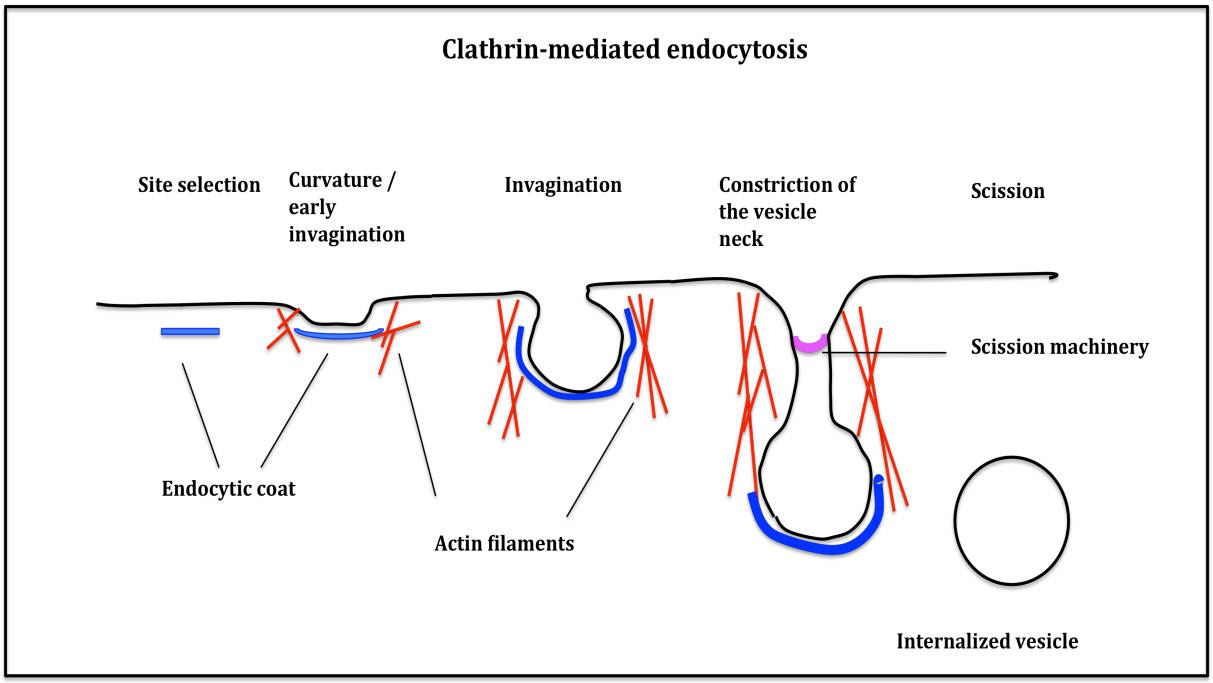

Figure.1.2. Clathrin-mediated endocytosis. A schematic diagram representing the different stages of clathrin mediated endocytosis including initiation of pit formation, coat assembly, invagination of the plasma membrane and vesicle scission.

Once in the early endosome, the proteins are either recycled back into the plasma membrane or are targeted for degradation via the late endosome and the lysosome.

Many of the endocytic proteins were shown to be highly conserved from mammals to yeast [Kaksonen *et al.* 2005]. The role of clathrin in endocytosis in mammalian cells was established in 1975 [Pearse, 1975], however its importance in yeast endocytosis was accepted much later [Kaksonen *et al.* 2005, Newpher *et al.* 2005].

Although CME occurs in both mammals and yeast, some obvious differences have been pointed out. First of all, in yeast, CME results in the formation of tubular invaginations with clathrin localizing only to the distal tips of the tubules, which suggests that clathrin might play a role in stabilizing the curvature of the vesicle during its inward growth [Robertson *et al.* 2009]. Another difference is the presence of F-actin at an early stage, which is not evident in mammals. F-actin was shown to be essential for appropriate plasma membrane invagination in yeast [Aghamohammadzadeh and Ayscough 2009]. As a result, the presence of F-actin in the early endocytic stages provides a strong framework to support the force generation required to invaginate plasma membrane against the turgor pressure [Aghamohammadzadeh and Ayscough 2009].

1.2.2. Other endocytic routes: clathrin independent endocytosis

In mammalian cells an increasing number of clathrin independent endocytic routes have been described [figure 1.3]. For example, a recently defined endocytic pathway is the fast endophilin-mediated endocytosis (FEME) pathway [Boucrot *et al.* 2015]. This pathway is triggered upon the activation, either directly or in-directly, of membrane-bound receptors.

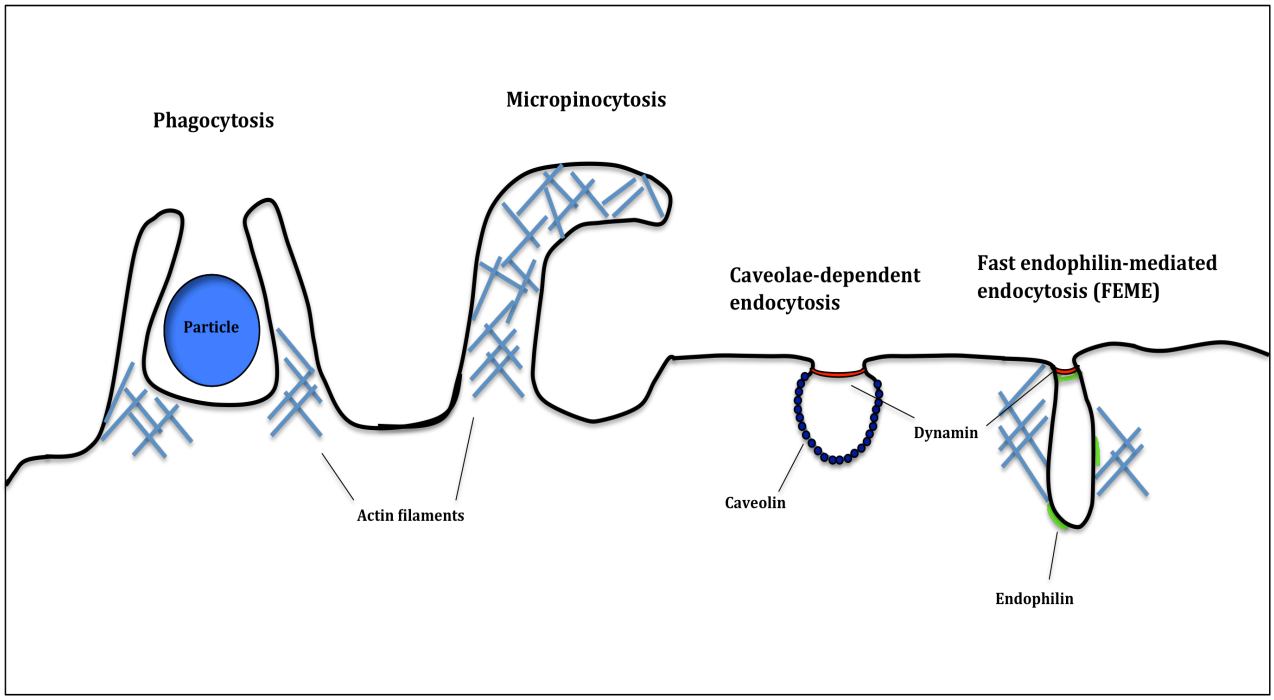

Fig.1.3. Summary of some Clathrin independent endocytic pathways. A schematic diagram representing some of the clathrin independent endocytic pathways including phagocytosis, micropinocytosis, caveolae dependent and fast endophilin-mediated endocytosis.

This activation triggers the formation of the phospholipid PI(3,4)P2 from PI(4,5)P2 that binds to a protein known as lamellipodin, a protein distributed at the leading edge of a migrating cell [Boucrot *et al.* 2015, Haucke, 2015]. Lamellipodin binds to endophilin allowing for its recruitment to the cell membrane, which in turn induces membrane invagination forming tubules, which then snip off forming a vesicle [Boucrot *et al.* 2015, Haucke, 2015].

Caveolae dependent endocytosis is another clathrin-independent pathway characterized by 60-80nm wide pits in the plasma membrane, containing specific lipid rafts coated with caveolins. Although in caveolae dependent endocytosis flask-shaped invaginations of the plasma membrane have been described, caveolae appeared as an open cup with a wide opening rather than a constricted neck as observed in cryo-fixed material and form a flask-shaped invaginations of the plasma membrane [Hansen and Nichols 2010, Parton and del Pozo, 2013]. Caveolae dependent endocytosis was reported to be especially abundant in smooth muscle cells, fibroblasts, adipocytes and endothelial cells [Parton and Simons, 2007].

Macropinocytosis [Swanson and Watts 1995] and phagocytosis [Aderem and Underhill 1999] are other endocytic mechanisms, however, these are involved in the uptake of larger membrane areas compared to other mechanisms. Macropinocytosis is a method of internalizing large amounts of solutes and extracellular fluids where it forms at highly ruffled sites of the plasma membrane [Swanson and Watts 1995, Doherty and McMahon, 2009]. On the other hand phagocytosis is involved in internalizing large particles via the formation of invaginations around the cargo to be internalized [Doherty and McMahon, 2009].

In yeast, CME has been well characterized, however the fact that endocytosis still takes place in clathrin-null cells and in the absence of other CME required genes e.g. Las17, although at a reduced rate, have suggested the existence of other endocytic routes that are clathrin independent [Kaksonen *et al.* 2005]. Growing evidence has been emerging describing alternative endocytic pathways in yeast. For example, Prosser *et al.* 2011 described a Rho1-dependent pathway which works through the GTPase Rho1 and the formin Bni1 and works independently of the key elements of CME such as clathrin, actin bundling proteins and Arp2/3-mediated actin polymerization. Another work published by the Ayscough lab [Aghamohammadzadeh *et al.* 2014] described an Abp1mediated pathway, in which this endocytic pathway was shown to be dynamin independent and functions in the presence of low levels of latrunculin-A, a drug known to disrupt the actin cytoskeleton [Morton *et al.* 2000].

1.3. Dynamins

Dynamins are a conserved family of large GTPases that have been implicated in a wide range of cellular processes including vesicle trafficking, vesicle scission, synaptic vesicle recycling, organelle division, viral resistance and cytokinesis (Praefcke and McMahon 2004). The importance of dynamin was first highlighted in *Drosophila melanogaster*, where mutations in the *shibire* gene (later discovered to encode dynamin) caused paralysis at high temperature by reversibly blocking endocytosis at nerve terminals, which prevents membrane cycling and as a result, depletes synaptic vesicles (Van der Bliek and Meyerowrtz 1991).

1.3.1. Members of the Dynamin Superfamily

Although members of the dynamin superfamily have some structural similarity, they seem to have diverse functional roles. Therefore, based on structural and functional

properties, members of the dynamin superfamily have been divided into several families. These include:

Classical dynamins – characterized as having five domains; an N-terminal GTPase domain (also known as G-domain), a middle domain, a pleckstrin homology (PH) domain, a GTPase effector domain (GED) and finally a C-terminal proline rich domain (PRD) [Ramachandran 2011]. The GTPase domain is relatively large (~ 300 residues) compared to other GTPases [Ramachandran 2011], and it contains GTP-binding motifs (G1-G4) that are required for nucleotide binding and hydrolysis, where these motifs are conserved except for the G4 (Praefcke and McMahon 2004). The middle domain and the GED domain are both important in self-assembly as they are involved in the dimerization and oligomerization of dynamin [Ramachandran 2011]. The PH domain is involved in binding membrane lipids, specifically phosphatidylinositol-4,5-bisphosphate (PIP_2), while the PRD domain (more than 30% proline residues) [Smirnova *et al.* 1998] contains sites for binding the Src-homology 3 (SH3) domain of accessory proteins, including the amphiphysins, endophilin, calcineurin and cortactin, which then target dynamin to different action sites in the cell [Ramachandran 2011].

Dynamin-like-proteins (also known as dynamin-related proteins) – are similar to the classical dynamins except that they lack both the PH and PRD domains. However, some members of this family still show lipid-binding properties, e.g. the *A.thaliana* ADL2 was shown to bind specifically to phosphatidylinositol-4-phosphate (PtdIns(4)P) [Kim *et al*. 2001].

Mx proteins - are only conserved in vertebrates and, like the dynamin related proteins, lack both the PH and PRD domains. Their expression in humans is induced by type 1 interferons, where MxA results in a strong protection against viral infections

and block the replication of many viruses at various sites in the cell [Staeheli *et al.* 1986].

OPA proteins – contain all the domains present in classical dynamins except for the PRD domain. In addition, they contain an N-terminal mitochondrial import sequence followed by a predicted transmembrane domain [Praefcke and McMahon 2004]. These proteins were shown to be involved in mitochondrial fusion as they are found between the inner and outer mitochondrial membranes [Olichon *et al.* 2001].

Mitofusin proteins - these proteins contain a predicted transmembrane domain in place of the PH domain and the C-terminal domain was predicted to be helical. Also, the GED domain of mitofusins shows weak homology to the classical dynamin GED domain [Praefcke and McMahon 2004]. Mitofusins were shown to be involved in mitochondrial dynamics, where they localize to the cytoplasmic side of the outer mitochondrial membrane [Praefcke and McMahon 2004].

Guanylate-binding proteins (GBPs) – contain recognisable GTPase, middle and GED domains, however, these domains have only a weak sequence homology to the classical dynamins. GBPs play a role in resistance against intracellular pathogens, which is similar but less efficient compared to the Mx proteins [Anderson *et al.* 1999].

In this review, the main focus will be on the function and properties of classical dynamins and on dynamin-like proteins in endocytosis, therefore the other members of the dynamin superfamily will not be addressed any further.

1.3.2. Dynamin structure

As mentioned above, classical dynamins have been described to consist of five main domains based on their primary sequence, including a large GTPase domain (also known as G-domain), a middle domain, a PH domain, a GED and PRD domains [Ramachandran 2011]. The increased information on the structure of dynamin including the crystal structure of dynamin (lacking the PRD) has introduced some modifications to our understanding of the dynamin domains, which better reflects the three-dimensional folding of the protein [Figure 1.4]. These are summarized below.

The G-domain contains four highly conserved G-motifs (G1 to G4), which are required for the binding and hydrolysis of GTP, where only one molecule of GTP binds per G-domain [Praefcke and McMahon 2004]. The G1 motif coordinates the GTP phosphates, a threonine residue in the G2 motif is involved in GTP hydrolysis, a glycine residue in the G3 motif forms a hydrogen bond with the γ-phosphate of GTP, and the G4 motif plays a role in guanine and ribose coordination [Gonzalez-Jamett *et al.* 2013]. The conformational changes regulating dynamin assembly and disassembly are accompanied by cycles of GTP binding and hydrolysis [Marks *et al*. 2001].

The GED has a regulatory role in which it stimulates the protein's GTPase activity [Muhlberg *et al.* 1997]. An arginine residue located at position 725 was shown to be involved in GTP hydrolysis suggesting that the GED acts as an intra-molecular GTPase activating protein [Sever *et al.* 2000, Gonzalez-Jamett *et al.* 2013]. Helices at the amino- and carboxy-terminal of the G-domain and a carboxy-terminal helix from GED come together forming the bundle signaling element (BSE) [Chappie *et al.* 2009]. The BSE was suggested to sense and transmit the conformational changes associated with dynamin assembly to the GTPase domain [Chappie *et al.* 2009].

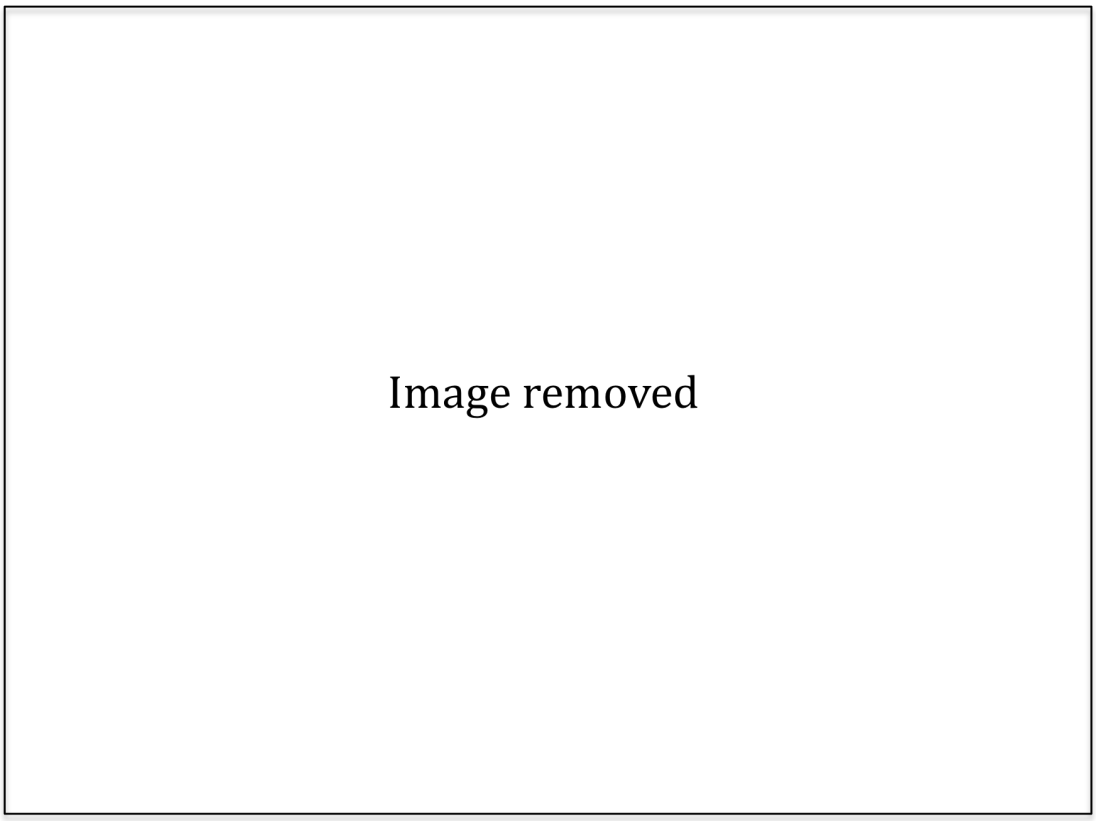

Fig.1.4. Structure of Nucleotide-Free Human Dynamin-1 (Faelber *et al*. 2011). A) Different domains of classical Dynamin-1. The numbers at the top represent the amino acids. B) Representation of human Dynamin-1 as resolved by Faelber *et al*. 2011. Regions not resolved in the crystal structure are indicated by dotted lines. Lipid-binding residues are indicated as o.

The middle domain and parts of the GED form the stalk region, which is critical for mediating oligomerization of dynamin into higher ordered structures [Faelber *et al.* 2011]. Stalk regions from neighboring dynamin monomers assemble in a cross-like manner via a conserved central interface known as interface-2 [Ford *et al.* 2011, Faelber *et al.* 2011, Chappie *et al.* 2011] yielding dynamin dimers in which the two G-domains are positioned in opposite directions [Faelber *et al.* 2011, Ford *et al.* 2011].

The stalk dimers oligomerize into higher ordered structures via interface-1 and interface-3. Mutations in the interface-3 region of the dynamin protein were shown to disturb the ability of dynamin to assemble into rings or helical structures [Faelber *et al.* 2011]. The PRD on the other hand contains a number of amino acid motifs (PxxP), which interact specifically with SH3 domains of various proteins. This interaction has been demonstrated to be essential for localizing dynamin to endocytic sites [Okamoto *et al.* 1997].

1.3.3. Biochemical properties of classical dynamins

Members of the dynamin family have some unique biochemical properties that differ from the smaller GTPases that have been studied such as Ras. It has been proposed that dynamins function as mechanochemical enzyme where upon the hydrolysis of GTP results in a conformational change in the protein important to drive membrane scission [Ferguson and Camilli, 2012]. Unlike other GTPase proteins, dynamins have a low affinity for GTP (10-25 μM) but a high basal rate of GTP hydrolysis (K_{cat} 8-30 x10^{-3} sec^{-1}) compared to ras, which has a basal rate of GTP hydrolysis of (K_{cat} 3.4 x10^{-4} sec^{-1}) [Sever *et al.* 2000]. Dynamins also have a very high stimulated GTP hydrolysis activity (K_{cat} 1-5 sec^{-1}) and since the rate of guanine nucleotide association and dissociation

are very rapid in dynamins, the GTP hydrolysis was suggested to be the rate-limiting step in it's GTPase cycle [Sever *et al.* 2000].

Dynamins are able to bind membrane lipids and form helical tubes that constrict and vesiculate in the presence of GTP [Sweitzer and Hinshaw 1998]. This induced self-assembly of dynamin was demonstrated to stimulate the GTPase activity by up to 100-fold [Gonzalez-Jamett *et al.* 2013]. Other factors that can induce dynamin oligomerization such as low-ionic strength solutions, negatively charged tubular templates, such as microtubules and actin bundles were also shown to stimulate dynamin's GTPase activity [Gonzalez-Jamett *et al.* 2013]. The fact that dynamin is able to self assemble *in-vitro* without the requirement for any additional proteins indicates that the protein is able to form all the required binding interactions for self-assembly [Smirnova *et al.* 1998] and act as its own guanine nucleotide-exchange factor (GEF) when in an oligomerized state [Muhlberg *et al*. 1997].

Dynamin was shown to bind to Inositol phospholipids, specifically phosphatidylinositol 4,5-bisphosphate (PtdIns (4,5) P2) [Salim *et al.* 1996, Lin *et al.* 1997]. It was reported that dynamin is capable of inserting itself into the lipid bilayer via a hydrophobic variable-loop 1 (VL1) of the PH domain which is critical for its self-assembly generation of high membrane curvature and membrane fission [Ramachandran *et al.* 2009]. This study also revealed the importance of the PH domain as another factor that can stimulate the dynamin GTPase activity.

1.4. Function of classical dynamins

In mammals, three dynamin genes are present which encode for Dynamin-1, 2 and 3 proteins, all of which have the same domain organization but differ in their expression patterns [Cao *et al.* 1998]. Dynamin-1 is mainly expressed at high levels in neuronal

cells [Nakata *et al.* 1991], Dynamin-2 is ubiquitously expressed and Dynamin-3 is found in the brain, although at much lower levels than Dynamin-1, in the testis, and in some other tissues such as the lungs [Cao *et al.* 1998]. It was suggested that the differences between the dynamin isoforms include affinities for SH3-domain-containing proteins, rates of GTPase activity, oligomerization efficiency and lipid binding properties [Ferguson and Camilli 2012]. For example, one of the main differences between Dynamin-1 and 2 was reported to involve differences in lipid binding characteristics, which introduces differences in their membrane fission activity [Liu *et al.* 2011]. This is fundamental to accommodate the differences in the proteins roles where Dynamin-1 mediates rapid endocytosis at the synapse while Dynamin-2 regulates early and late events in CME in non-neuronal cells [Liu *et al.* 2011].

1.4.1. Endocytic functions of classical dynamins

Despite dynamin having several cellular roles, its function is best understood in the context of CME [Van der Bliek *et al.* 1993]. During endocytosis, scaffold proteins (e.g. Eps15 and intersectin) and clathrin adaptors (e.g. the AP-2 complex) are recruited to the plasma membrane [Traub, 2009]. The different endocytic proteins cluster cargo, induce membrane curvature and actin nucleation [McMahon and Boucrot, 2011]. The clathrin lattice continues to form around the endocytic coat with more cargo adaptors and endocytic proteins assembling at the endocytic site [McMahon and Boucrot, 2011]. Actin polymerization is important in the invagination of the clathrin coated vesicle (CCV), which is accompanied by the recruitment of BAR-domain-containing proteins and since dynamin is important in the scission step of the vesicle, it is thought

to rapidly accumulate in the last steps of vesicle formation to mediate fission [Taylor *et al.* 2011, Ferguson and Camilli, 2012].

Three models [Ramachandran 2011] have been proposed that might explain the exact mechanism through which dynamin performs its role in vesicle scission. The first being the mechanochemical model, which proposes that dynamin forms a collar around the neck of a CCV, which upon GTP hydrolysis constricts, stretches or twists resulting in the release of the vesicle. The second model is the lipid-partitioning model, which suggests that dynamin assembly on the membrane results in an increase of PIP2. Upon GTP-dependent helix constriction, PIP2 become separated from the bulk membrane, which destabilizes the membrane leading to spontaneous membrane fission. The third model is known as the effector recruitment model suggests that the co-assembly of dynamin with membrane-curvature-generating BAR proteins such as, SNX9 and syndapin, which function cooperatively with the actin network together drive membrane fission and the vesicle release.

Although classical dynamins were best studied in CME, it was shown that they are not limited to CME, but also play a role in caveolae mediated endocytosis [Henley *et al.* 1998], phagocytosis [Gold *et al.* 1999] and in fast endophilin mediated endocytosis (FEME) [Boucrot *et al.* 2015].

1.4.2. Non-endocytic functions of classical dynamins

In addition to its role in endocytosis, dynamin was also shown to function in vesicle budding from the Golgi and endosomes (Jones *et al.* 1998, Nicoziani *et al.* 2000), regulation of microtubule stability (Thompson *et al.* 2002) in actin cytoskeleton dynamics (Mooren *et al*. 2009, Gu *et al*. 2010) and in cytokinesis [Ishida *et al.* 2011].

Various live cell analysis and immunofluorescence studies have shown a colocalization of dynamin with actin meshworks in lamellipodia, membrane ruffles, invadopodia, podosomes and actin comets [Ferguson and Camilli, 2012]. A direct interaction between dynamin and actin has also been reported [Gu *et al.* 2010], however it was suggested that the importance of this interaction is a reflection for the important role of dynamin in endocytosis.

Initially, dynamin was identified as a microtubule-binding protein, where it was shown to interact with microtubules in-vitro [Shpetner and Vallee 1989]. However the growing data supporting its role in endocytosis put its role with microtubules under a question. More recent work [Tanabe and Takei, 2009] has revealed for the first time a role for Dynamin-2 in the regulation of dynamic instability of microtubules in-vivo, a function that is essential for microtubule-dependent membrane transport and organelle motility. Since dynamin was shown to regulate microtubule dynamics by a mechanism independent of membrane traffic [Tanabe and Takei, 2009], the implication of this function in cell cycle progression, which requires dynamic instability of microtubules [D'Avino *et al.* 2005] was addressed by [Ishida *et al.* 2011]. Through interactions of its PRD, Dynamin-2 was found to localize at the mitotic spindle, and deletion of this region resulted in defects in cytokinesis but had no severe effects on endocytosis. Also, deleting the middle domain in dynamin, which binds to γ-tubulin, impaired the entry into mitosis. Their data suggest that dynamin may regulate cytokinesis by two distinct pathways, membrane traffic and microtubule dynamics.

1.4.3. Function of dynamin-related-protein 1 (Drp-1)

Similar to classical dynamin, the dynamin-related proteins (DRPs) contain the N-terminal GTPase domain, the middle domain, and the C-terminal GED [Williams and

Kim 2014, Vater *et al.*1992, Van der Bliek 1999] but lack the PH and PRD domains. Drp1 was suggested to specifically function in mitochondrial fission [Smirnova *et al.* 1998] where it performs scission in a similar manner to the classical dynamins, i.e. via the oligomerization into helices and the formation of ring-like structure [Smirnova *et al.* 2001, Williams and Kim 2014]. Drp1 was also reported to tubulate liposomes [Yoon *et al.* 2001] and to constrict lipid bilayers in the presence of GTP [Frohlich *et al.* 2013, Francy *et al.* 2015] even though no lipid binding regions are known to be present in the protein, suggesting that these proteins have the capacity to function in a similar manner to the classical dynamins.

1.5. Dynamins and human disease

It has been well documented that different mutations in classical dynamins are involved in various diseases. In mice, the knockout of Dynamin-2 gene was shown to result in embryonic lethality suggesting an essential role during embryonic development [Ferguson *et al.* 2009], while the knockout of Dynamin-1 gene resulted in a reduced life span in mice mainly due to defects in synaptic vesicle endocytosis [Ferguson *et al.* 2007]. On the other hand, Dynamin-3 knockout mice showed no apparent phenotype, however it worsened the Dynamin-1 knockout phenotype, resulting in a perinatal lethality and a more severe defect in activity-dependent synaptic vesicle endocytosis [Raimondi *et al.* 2011].

Mutations in Dynamin-2 were shown to result in congenital diseases in humans with the best-studied examples being the Charcot-Marie-Tooth (CMT) neuropathy [Zuchner *et al*. 2005] and Centronuclear Myopathy (CNM) both which are autosomal dominant disorders. CMT is characterized by progressive muscle weakness and wasting, where most of the mutations were shown to localize to the N-terminal region of the PH

domain, specifically to a 'lipid-binding pocket' [Bohm *et al.* 2012], which includes three hydrophobic variable loops (VL1-VL3) that are involved in membrane scission and in the insertion of dynamin into lipid membranes [Heymann and Hinshaw 2009, Bethoney *et al*. 2009, Ramachandran *et al.* 2009 and Gonzalez-Jamett *et al.* 2013]. Mutations outside the PH region have also been reported in CMT [Claeys *et al.* 2009]. The mechanism by which these mutations affect the cellular function of dynamin is still not fully understood, and despite the fact that many of the CMT linked mutations were shown to affect clathrin mediated endocytosis (CME), some mutations showed normal function of CME, suggesting that CMT mutations could affect other cellular mechanisms other than CME [Gonzalez-Jamett *et al.* 2013].

CNM on the other hand, is a slowly progressive congenital myopathy characterized by a progressive weakness and atrophy of the skeletal muscles [Jeannet *et al.* 2004, Fischer *et al.* 2006] and the presence of centrally located nuclei in muscle fibres [Bitoun *et al.* 2005 and Durieux *et al.* 2010]. A number of Dynamin-2 mutations linked to CNM are localized to the C-terminal helix of the PH domain [Bohm *et al*. 2012], which coordinates lipid binding with the GTPase activity [Kenniston and Lemmon 2010]. In this case, these mutations show an enhanced GTPase activity in the presence of lipids compared to the wild-type dynamin [Kenniston and Lemmon 2010]. Other Dynamin-2 mutations linked to CNM were also localized to the middle domain [Ramachandran *et al.* 2007], where they were also shown to have an increased GTPase activity, suggesting that the pathogenic mechanism of this disorder could be a result of a gain-of-function (Bohm *et al.* 2012, Gonzalez-Jamett *et al.* 2013].

Mutations in Dynamin-1 gene have also been associated with various diseases, including epilepsy. Fitful, is a mutation in mouse that was shown to result in epilepsy [Boumil *et al.* 2010]. Fitful mice were shown to have recurrent seizures in addition to other neurological defects, including impaired hearing. The mutation was shown to localize to the middle domain, which is important for the oligomerization of the protein into higher orders and it was shown to distort the self-assembly of Dynamin-1 as well as endocytosis [Boumil *et al.* 2010].

Mutations in the GTPase domain in Dynamin-1 were also shown to be responsible for reversible collapse, which is characterized by a deficiency in sustained synaptic transmission during high neural activity [Heymann and Hinshaw 2009]. Also, Exercise-induced collapse (EIC) in Labrador retrievers is another disorder caused by mutations in the Dynamin-1 gene [Patterson *et al*. 2008], where upon intense exercise or excitement, this mutation results in an acute and severe muscle weakness that can become life threatening to the otherwise healthy dogs [Patterson *et al*. 2008]. Although this mutation maps specifically to the GTPase domain, its effect on the GTPase activity remains unclear. The number of various mutations mapping to Dynamin-1 and -2 resulting in diseases is greatly increasing, however our understanding of the impact of these mutations on the biochemical properties and functions of dynamin and the resulting phenotype remains poorly understood.

1.6. Yeast as a model of membrane trafficking and endocytosis

Yeast is a common term used to describe *Saccharomyces cerevisiae*, one of the most studied and best-characterized eukaryotic model organisms and the first eukaryotic organism to have its entire genome sequenced [Goffeau *et al.* 1996]. Despite the fact that

S.cerevisiae is a single-celled organism, it offers several advantages that make it the most useful model organism to study many fundamental cellular processes such as DNA replication and recombination, cell cycle, cell signaling, membrane trafficking and much more.

In addition to the fact that it is easily handled, *S.cerevisiae* has a generation time of about 1.5 – 2 hrs when grown in rich medium and one of its main advantages is that it shares its complex intracellular organization with higher eukaryotic organisms [Sherman 2002]. *S.cerevisiae* can exist stably as either diploids or haploids and with the rapid advances in molecular biology techniques, various genetic modifications can be easily introduced into its genome such as gene deletions, gene mutations, creation of fusion proteins etc. In addition to genomic modifications, genetic information can also be introduced into it on plasmids.

With the completion of the human genome sequencing project [Lander *et al.* 2001, McPherson *et al.* 2001] it became clearer that thousands of proteins are conserved in both yeast and man sharing amino acid sequence similarity, many of which are implicated in various human diseases. All this makes yeast an important organism for studying the bases of complex problems in various human disorders.

1.7. The yeast dynamin-like proteins

In yeast there are no classical dynamins, however, there are three dynamin-like proteins (DLPs); mitochondrial genome maintenance-1 (Mgm1), dynamin-related GTPase 1 (Dnm1) and vacuolar protein sorting-1 (Vps1), all of which contain the conserved N-terminal GTPase domain, the middle domain and the C-terminal GTPase effector domain GED [Praefcke and McMahon 2004].

1.7.1. Dnm1

Dnm1 is an 85 kD protein homologous to Drp-1 in mammals [Williams and Kim 2014]. Like Dlp1, Dnm1 was reported to localize to the mitochondria and function in mitochondrial fusion and fission [Ingerman *et al.* 2005, Cerveny *et al.* 2007] as well as playing a role in controlling peroxisome abundance [Kuravi et al. 2006]. In addition to the three domains it shares with classical dynamins, Dnm1 also contains a region known as Insert B, between the middle and GED domains. This region is thought to facilitate the binding of Dnm1 to adaptor proteins, which is essential for its recruitment to the mitochondrial membrane [Bui *et al.* 2012]. Besides its function at the mitochondria, early studies have also suggested that Dnm1 plays a role in post scission endosomal trafficking [Gammie *et al.* 1995] however no further work was carried out in that area.

1.7.2. Mgm1

Mgm1 is a 94 kD mitochondrial GTPase protein considered to be mainly involved in maintaining mitochondrial genome and inheritance, where mutations in the *MGM1* gene resulted in temperature sensitive loss of mitochondrial DNA [Jones and Fangman 1992]. In addition to the three domains that Mgm1 shares with classical dynamins, it also contains a mitochondrial targeting sequence (MTS) that confers mitochondrial localization of Mgm1, and a transmembrane domain (TMD), which anchors the protein in the inner membrane of the mitochondria. Mgm1 was shown to be homologous to the mammalian DLP Opa1, where mutations in Opa1 were linked to dominant optic atrophy [Alexander *et al.* 2000].

1.7.3. Vps1

Vps1 is an 80 kD protein [Rothman *et al*. 1989] sharing about 45 % of sequence identity with dynamin (Obar *et al.* 1990). Vps1 was originally identified in screens for genes involved in vacuolar protein sorting in *S.cerevisiae* [Rothman *et al*. 1989, Vater *et al.* 1992]. Similar to Dnm1 and Mgm1, Vps1 also lacks both the PH and the PRD domains but alternatively it contains a region within the GED domain known as Insert B [figure 1.5]. Although no PH domain is present in Vps1, it was still shown to be able to bind to, and tubulate liposomes [Smaczynska-de Rooij *et al.* 2010].

Vps1 has been shown to play a role in several processes including membrane protein trafficking and retention in the Golgi compartment [Wilsbach and Payne 1993, Nothwehr *et al*. 1995, Yu and Cai 2004], endosomal recycling [Hayden *et al.* 2013], sorting of soluble vacuolar proteins [Vater *et al.* 1992], peroxisomal inheritance [Hoepfner *et al.* 2001] and in clathrin-mediated endocytosis [Smaczynska-de Rooij *et al.* 2010].

Since Vps1 is the main subject of this thesis, the remaining of the introduction will only address Vps1.

1.8. Role of Vps1 in yeast

Of the three DLPs in yeast, Vps1 is the most functionally diverse protein, performing fusion and fission roles in a number of membrane trafficking stages including Golgi to endosome, endosomal recycling, vacuolar fusion, and endocytosis as well as in peroxisomal fission . Some of these functions are addressed below.

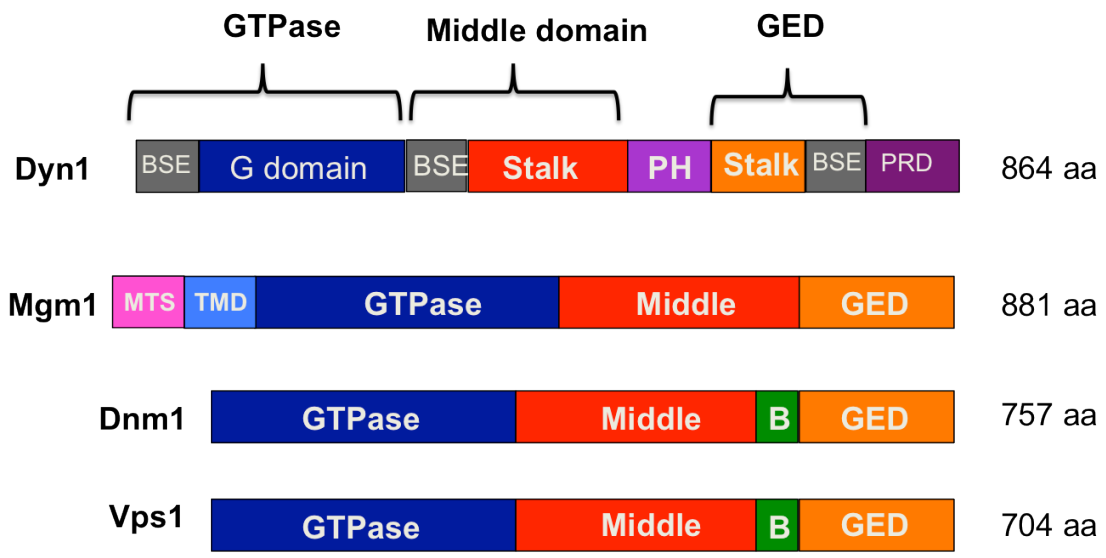

Fig.1.5. Domain structure comparison of Classical Dynamin and the three DLPs in yeast. The human Dynamin-1 (Dyn1) contains the five classical domains, including the GTPase domain, middle domain, Pleckstrin homology (PH) domain, GTP effector domain (GED), and proline-rich domain (PRD). (BSE) refers to the bundle signaling element. The yeast DLPs all have a GTPase, middle, and GED domain. Both Vps1 and Dnm1 contain a region upstream the GED known as Insert B (B). In addition, Mgm1 contains a mitochondrial targeting sequence (MTS) and a transmembrane domain (TMD). The lengths of each of the proteins are shown on the right as the number of amino acids.

1.8.1. Vps1 in membrane trafficking

Many studies have revealed a significant role for Vps1 in endosomal trafficking after the analysis of post-endocytosed patches. It was shown that in cells lacking Vps1, the rate of the endocytic patch inward movement was reduced [Nannapaneni *et al.* 2010]. A disruption in the actin cytoskeleton in cells lacking Vps1 was also observed which is correlated with the reduced patch motility [Nannapaneni *et al.* 2010]. In addition, Vps1 was shown to be involved in the disassembly of endocytic components [Wang *et al.* 2011].

A role for Vps1 in early endosome to Golgi trafficking was also recently reported (Lukehart *et al.* 2013). Using the vesicle membrane receptor protein (v-SNARE) Snc1, which gets continuously recycled back to the plasma membrane through the early endosomes and Golgi [Lewis *et al.* 2000] it was shown that cells lacking Vps1 or carrying mutations in the GTPase domain resulted in the accumulations of Snc1 in the cytoplasm [Smaczynska-de *et al*. 2010). In addition, genetic interaction studies revealed that Vps1 interacts with 4 recycling factors Ric1, Gyp1, Ypt6 and Rcy1, all of which are involved in the trafficking from the early endosomes to the Golgi [Hoppins *et al*. 2011, Lukehart *et al.* 2013, Tong *et al.* 2004].

A study by Hayden *et al.* 2013 reported a role for Vps1 in trafficking from the late endosomes to vacuole where it was shown that cells lacking Vps1 had an accumulation of late endosomes in the cytoplasm. Using FM4-64 pulse chase and dual-labeling it was shown that a large fraction of Vps1 localized to the late endosomes. A genetic interaction between Vps1 and several endosomal sorting complex required for transport (ESCRT) proteins was reported [Hayden *et al.* 2013] and it was suggested

that Vps1 may participate along with the ESCRT proteins for intraluminal vesicle formation at the late endosome.

1.8.2. Vps1 in vacuolar fusion and fission and peroxisomal division

The process of fission and fusion in yeast is important for maintaining vacuolar homeostasis. Mutations in Vps1 were shown to lead to defective phenotypes in vacuolar morphology. Cells lacking Vps1 were classified into the F class of vacuolar morphology with one large vacuole surrounded by numerous smaller ones (Raymond *et al.* 1992). Since the one large vacuole was an indication of defective vacuolar fission and the numerous smaller vacuoles were an indication of defective fusion event, it was suggested that Vps1 is involved in both processes [Peters *et al.* 2004, Williams and Kim 2014].

Vps1 was also shown to play a role in peroxisome division, where cells lacking Vps1 showed aberrant peroxisomal phenotype characterized by a reduction in the number and an increase in the size of peroxisomes (Hoepfner *et al.* 2001, Vizeacoumar *et al.* 2003, Kuravi *et al*. 2006).

1.8.3. Vps1 in endocytosis

While the high level of homology between Vps1 and mammalian dynamins might indicate a role in endocytosis, the lack of clear localization to sites of clathrin at the plasma membrane, coupled with its roles in other steps of membrane trafficking, meant that a function in endocytosis was not recognized until recently. However, accumulated circumstantial evidence as well as co-localization with endocytic reporters using TIRF microscopy has meant that Vps1 is now considered part of the endocytic machinery. A study by Yu and Cai (2004) showed that *vps1Δ* conferred synthetic lethality when combined with *sla1Δ. S*la1 is an adaptor protein required for

the cortical actin patch structure and organisation in *S.cerevisiae* [Ayscough *et al.* 1999] and is essential in coupling endocytosis with the actin cytoskeleton via interacting with several actin-binding proteins including Sla2, Abp1 and Las17 [Warren *et al.* 2002]. Results from two-hybrid interaction analysis showed that Vps1 interacts directly with Sla1 via its C-terminal domain (GED plus some additional upstream sequences) [Yu and Cai 2004]. The work also showed that *vps1Δ* mutant was hypersensitive to Latrunculin-A (Lat-A), which is a drug known to bind actin monomers and inhibit their polymerization [Coue *et al*. 1987]. Lat-A sensitivity has been used as a marker for actin cytoskeleton integrity [Ayscough *et al.* 1997] and so from the results which show that the loss of the Vps1 leads to instability of actin filaments, it was suggested that Vps1, specifically the C-terminus, is important for the normal organization of actin cytoskeleton in yeast.

Further support for an endocytic role for Vps1 came again from the study by Yu and Cai 2004, using the Ste3p receptor as a marker for endocytosis. Their results showed that in *vps1Δ* the Ste3 receptor internalization from the cell membrane into the vacuole was impaired. Nannapaneni *et al.* (2010) also investigated the role of Vps1 in endocytosis using the fluorescent lipophilic dye FM4-64, with the aim to identify the exact stage of endocytosis at which the protein functioned. The results revealed that in *vps1Δ,* the majority of vesicles remained on the membrane after a 5min pulse-chase, compared to only 10% of cells containing wild-type Vps1, suggesting that Vps1 was required for the normal internalization of endocytic vesicles. Furthermore, the study looked at the effect of *vps1Δ* on various endocytic proteins including Las17, Ede1 and Abp1. Both Las17 and Ede1 which are early endocytic proteins, stayed immobile once recruited to cortical patches and showed nearly 2-fold increase in their lifetime

compared to wild-type Vps1. The same was true for the late endocytic protein Abp1 which showed a 2-3 fold increase in its lifetime compared to wild-type, suggesting that Vps1 functioned in patch assembly starting at an early stage. In addition, it was shown that Abp1 showed slow and random motions upon internalization compared to the wild-type Vps1, which showed movements in directional motions. This was explained by the fact that actin cables are usually short and fragmented in *vps1Δ* and so patches are unable to move as fast compared to when wild type protein is present [Nannapaneni *et al.* 2010].

A study from the Ayscough lab, by Smaczynska-de Rooij *et al.* (2010) also investigated the role of Vps1 in endocytosis. Using live cell imaging techniques of fluorescently tagged endocytic reporters they measured the lifetime of Vps1-GFP on membrane which was found to be 8.7 seconds. Vps1-GFP also colocalised with Abp1-mRFP suggesting that Vps1 is indeed present at endocytic sites. They observed that Vps1 arrived to endocytic patches about 5 seconds after Abp1 suggesting a role at the onset of/or during invagination of the vesicle. In trying to address a question of the possible mechanism of action for Vps1, Smaczynska-de Rooij *et al.* (2010) investigated the behaviour of various endocytic proteins in *vps1Δ.* It was found that the lifetime of 5 endocytic proteins, Sla2, Ent1, las17, Abp1 and Sac6 were markedly increased with aberrant inward movement of patches and patch retraction, confirming the fact that deletion of Vps1 severely disrupts endocytosis.

Vps1 was found to interact with the amphiphysin protein Rvs167 both genetically [Nannapaneni *et al.* 2010] and physically [Smaczynska-de Rooij *et al.* 2012]. In the study by Nannapaneni *et al.* 2010, *vps1Δ* cells were crossed with *Rvs161Δ* or *Rvs167Δ* cells and the results revealed a synthetic lethality in the *vps1Δ / Rvs167Δ* cells at the

non-permissive temperature (37 ^{0}C), suggesting a genetic interaction between these two proteins and a possible role for Vps1 in vesicle scission. The fact that upon deletion of Rvs167 there was only about 25% decrease in the successful vesicle scission [Kaksonen *et al.* 2005] suggested that the amphiphysins were important but are not be the only scission proteins. A physical interaction between Vps1 and Rvs167 was confirmed using Yeast-Two hybrid analysis and bimolecular fluorescence complementation [Smaczynska-de Rooij *et al.* 2012]. In addition, mutagenesis revealed that a proline residue at position 564 in Vps1 was found to interact with the SH3 domain of Rvs167. A P564A mutation resulted in an endocytic defect but all other functions of Vps1 were rescued. Previous mammalian work showed that the amphiphysin proteins link Dynamin-1 to the clathrin coat during endocytosis of synaptic vesicles and form a ring like structures around tubules in the presence of GTP [Takie *et al.* 1999] suggesting a close functional relationship between the amphiphysins and dynamin in mammals.

1.9. Project aims

In this thesis, three projects have been undertaken. The aims of each of the projects are summarized below.

Project 1.

Investigating whether yeast can be used as a model to understand specific dynamin mutations and explain the mechanistic defects causing diseases. Functions of dynamin critical in endocytosis but not in its other membrane associated roles are also investigated.

Based on sequence analysis, it was shown that three different dynamin mutations that have been implicated in neurological diseases were in regions conserved in yeast Vps1. For this purpose, these three dynamin mutations were introduced into the yeast Vps1 protein and their effect on the protein's function was studied using various in-vitro and in-vivo assays. Table 1 summarizes the dynamin mutations used in this work, their Vps1 equivalents and the diseases it has been implicated in.

Vps1 Mutations	**Equivalent Mutations in Mammals**	**Linked Diseases**
R298L	R256L in *DNM1*	Exercise Induced Collapse
G397R	G358R in *DNM2*	Charcot-Marie Tooth
A447T	A408T in *DNM1*	Epilepsy

Table.1. The three Vps1 mutations used in this project along with their analogues mammalian dynamin mutations that have been implicated in different neurological diseases

Project 2.

Investigate whether the human dynamin gene can complement to some level the yeast Vps1. In this work, the mammalian Dynamin-2 gene was used. In addition, a chimeric protein was constructed where the Vps1 InsertB region was replaced by the Dynamin-2 PH domain to determine whether this was able to localize and function in yeast.

Project 3.

Using a genetic screen to identify suppressors of a Vps1 endocytic mutation. Performing the screen would allow the identification of gene/genes that can rescue the defects caused by the Vps1 mutations affecting endocytosis. In this work, a YEp24 library screen was undertaken to identify suppressors of a temperature sensitive phenotype shown by the Vps1 RR456-7EE endocytic mutant.

Chapter 2 – Materials and Methods

2.1. Strains, plasmids antibodies and oligonucleotides:

2.1.1. List of bacterial strains:

Strain	Genotype	Origin
XL10-Gold	Tet^r*Δ(mcrA) 183Δ (mcrCB-hsdSMR-mrr) 173 endA1 supE44 thi-1 recA1 gyrA96 relA1 lac Hte*	Agilent Technologies
C41	F – *ompT hsdSB (rB- mB-) gal dcm* (DE3)	Lucigen
C43	F – *ompT hsdSB (rB- mB-) gal dcm* (DE3)	Lucigen
DH5α	*supE44 Δlac 169 (ϕ80 lacZ ΔM15) hsdR17 recA1 endA1 recBC gyr96 thi-1 relA*	Lab strain

2.1.2. List of yeast strains:

Strain name	Genotype	Origin
KAY 389	*MATa, his3-Δ200, leu2-3, 112 lys 2-801 ura 3-52, trp 1-1,*	Lab strain
KAY447	Research genetic strain BY4742 *MATα his3Δ1, leu2Δ0, lys2Δ, ura3Δ0* (wild type)	GE Life Sciences
KAY1095	KAY477 *MATα his3Δ1, leu2Δ0, lys2Δ, ura3Δ0 vps1Δ::KanMx*	E.Hettema
KAY1096	KAY477 *MATα his3Δ1, leu2Δ0, lys2Δ, ura3Δ0 dnm1Δ::KanMx vps1Δ::HIS5*	E.Hettema
KAY1337	*MATa, Rvs167-GFP::HIS3, his3Δ1, leu2Δ0, met15Δ0, ura3Δ0 vps1Δ::LEU2*	KA Lab
KAY1368	*MATα, Sac6-RFP::KanMX vps1Δ::Leu*	KA Lab
KAY1459	*MATa, Sla2-GFP::HIS3, his3Δ1, leu2Δ0, met15Δ0, ura3Δ0 vps1Δ::LEU2*	KA Lab
KAY1462	*MATa his3Δ1, leu2Δ0, lys2Δ, ura3Δ0* + integrated GFP-Snc1-SUC2 *URA*	Smaczynska-de Rooij et al. 2010

KAY1756	*MATa, his3-Δ200, leu2-3/112, ura3-52, trp1-1, lys2-801, vps1Δ::URA3*	KA Lab

2.1.3. List of antibodies:

Antibody	Western Blot	Source
Anti-αCPY primary	1:500	Chemicon International
Anti-Vps1 mouse primary	1:2000	K.Ayscough
Anti-Dyn2 primary	1:4000	Elizabeth Smythe
Anti-Dyn 2 primary	1:1000	Abcam
Anti-Vps1 rat primary	1:20,000	K.Ayscough
Anti-rat horse radish peroxidase conjugate IgG secondary antibody	1:10,000	Sigma
Anti-rabbit horse radish peroxidase conjugate IgG secondary antibody	1:10,000	Sigma
Anti-mouse horse radish peroxidase conjugate IgG secondary antibody	1:10,000	Sigma
Anti-Sheep horse radish peroxidase conjugate IgG secondary antibody	1:10,000	Sigma

2.1.4. List of Plasmids:

Plasmid name	Description	Origin
pKA526	pTpi - mcs - 3xHA *URA3*	E.Hettema (Univ of Sheffield)
pKA527	pTpi - mcs - 3xHA *LEU2*	
pKA528	pKA527 with HA replaced by GFP *LEU2*	Iwona Smaczynska-de Rooij
pKA544	*URA3 CEN* empty plasmid	E.Hettema
pKA549	pAS040 Tpi *URA3 CEN*	Iwona Smaczynska-de Rooij
pKA677	pKA544 Vps1 under its own promoter *URA3 CEN*	Iwona Smaczynska-de Rooij
pKA701	pKA677 Vps1 I649K *URA3 CEN*	Iwona Smaczynska-de Rooij
pKA760	pKA677 Vps1 P564A *URA3 CEN*	Iwona Smaczynska-de Rooij
pKA768	Vps1-GFP *LEU2 CEN*	Iwona Smaczynska-de Rooij
pKA770	pKA677 Vps1 K642A *URA3 CEN*	Iwona Smaczynska-de Rooij
pKA796	pKA677 Vps1 A447T *URA3 CEN*	This study
pKA797	pKA677 Vps1 G397R *URA3 CEN*	This study
pKA798	pKA677 Vps1 R298L *URA3 CEN*	This study
pKA819	pKA850 His-tag Vps1 R298L	This study
pKA820	pKA850 His-tag Vps1 G397R	This study
pKA821	pKA850 His-tag Vps1 A447T	This study
pKA836	pKA768 Vps1 G357G-GFP *LEU2 CEN*	Iwona Smaczynska-de Rooij
pKA850	His-tag Vps1 (wild type)	Iwona Smaczynska-de Rooij

pKA943	pKA677 Vps1 RR457-8EE *URA3 CEN*	Iwona Smaczynska-de Rooij
pKA945	pKA677 Vps1 E461K *URA3 CEN*	Iwona Smaczynska-de Rooij
pKA964	pKA836 Vps1-GFP P532V ((introduces SalI site 5' InsertB region) *LEU2 CEN*	This study
pKA966	pKA964 Vps1-GFP V620L (introduces SacI site 3' InsertB region) *LEU2 CEN*	This study
pKA970	pKA966 insBΔ +Dyn2 PH domain fragment *LEU2 CEN*	This study
pKA1227	pKA526 + Dyn2	This study
pEH010	Ycplac111 His3 promoter, GFP-PTSI, PGK1 term *LEU2 CEN*	E.Hettema

2.1.5. List of Oligonucleotides:

Oligonucleotide Number	Use	Company
712	Vps1 genome integration check - forward	Operon molecules for life
713	Vps1 genome integration check - reverse	Operon molecules for life
832	Vps1 check 1 forward primer	Eurofins
833	Vps1 check 1 reverse primer	Eurofins
834	Vps1 check 2 forward primer	Eurofins
835	Vps1 check 2 reverse primer	Eurofins
1138	Vps1P532V_forward primer	Eurofins
1139	Vps1P532V_reverse primer	Eurofins
1140	Vps1V620L_forward primer	Eurofins
1141	Vps1V620L_reverse primer	Eurofins
1150	Dynamin-2 XbaI forward primer	Eurofins

1151	Dynamin-2 HindIII reverse primer	Eurofins
1152	Dynamin-2 control sequencing primer 1 – forward	Eurofins
1153	Dynamin-2 control sequencing primer 2 – reverse	Eurofins
1154	Dynamin-2 control sequencing primer 3 – forward	Eurofins
1155	Dynamin-2 control sequencing primer 4– reverse	Eurofins
1161	Vps1 allele exchange forward	Eurofins
1162	Vps1 allele exchange reverse	Eurofins
1282	YEp24_forward	Eurofins
OKA152	YEp sequencing primer_reverse	MWG oligo Syn Report

2.2. Bacterial Methods:

2.2.1. Bacterial growth media

2xYT media (1.6% Tryptone, 1% Yeast extract, 0.5% NaCl and 2% Agar only for solid media) was used to grow *Escherichia coli (E.coli)* C41 and C43 competent cells (Lucigen) used in this study. The bacterial strains used in the experiments conferred ampicillin resistance, therefore, the media was supplemented with the antibiotic ampicillin (100mg/ml stock) to a final concentration of 0.1mg/ml. Media was autoclaved before being used. C41 cells were grown at 37^0C whilst C43 cells were grown at 30^0C. The liquid cultures were incubated at the appropriate temperature in an orbital shaking incubator (Certomat BS-1).

2.2.2. Transformation of chemically competent *E.coli* cells

To transform the C41 and C43 competent cells with the appropriate plasmid, cells were removed from the -80^0C freezer and thawed at room temperature. 1μl of

plasmid was added to 50μl of competent cells and the cells were incubated on ice for 30mins. Cells were heat shocked for 40sec, placed back on ice for 2 min and then 400μl of 2xYT was added. Cells were incubated at the appropriate temperature for 1 hr in a shaking incubator before being plated onto 2xYT plates with 0.1mg/ml ampicillin (200μl per plate), which were then incubated overnight at the appropriate temperature (37^0C for C41 and 30^0C for C43).

2.2.3. Glycerol stocks of bacteria

For long-term storage of bacterial cells, glycerol stocks were prepared by mixing equal volumes of the overnight culture with 50% of sterile glycerol in a cryovial. Tubes were snap frozen in liquid nitrogen and stored in the -80^0C freezer.

2.3. Yeast Methods:

2.3.1. Yeast growth medium

Saccharomyces cerevisiae (*S.cerevisiae*) stains used in this study were grown in autoclaved YPD media (1% Yeast extract, 2% peptone, 0.02% adenine, 2% Glucose, 2% agar only for solid media). When selecting for a plasmid containing a marker that compensates for auxotrophic deficiencies, cells were grown in drop-out media containing the appropriate drop-out mix (0.67% nitrogen base without amino acids, drop-out mix of amino acids, 2% glucose and 2% agar for solid media). Yeast cells were grown at 30^0C. The liquid cultures were incubated in an orbital shaking incubator (Certomat BS-1).

2.3.2. Yeast transformation

2.3.2.1. Quick method of yeast transformation

200 μl of overnight culture grown at 30 ^{0}C was taken and added to a microfuge tube. Cells were spun for 1 min at 5000 rpm (Eppendorf centrifuge 5415) and the pellet was resuspended in 100 μl CH buffer (0.1M DTT, 200 mM of Lithium acetate, 800 μl of 50% PEG_{400}). 5 μl of Herring sperm single stranded DNA (HssDNA) (10 mg/ml) was added to the cells after being incubated at 100 ^{0}C for 15 min, following with 1μl of plasmid DNA. The cells were vortexed briefly and then incubated for 30 min at 45 ^{0}C. Cells were then plated onto appropriate drop-out plates and incubated at 30 ^{0}C until colonies become visible (usually after 2days).

2.3.2.2. Lithium acetate method of yeast transformation

From an overnight culture, 250 μl of cells was re-inoculated into 4.75 ml of fresh media and incubated at 30^{0}C for cells to reach early log phase. Cells were spun down for 3 min at 3000 rpm (Hettich Zentrifugen 1619) , resuspended in 5 ml of 1x Tris-EDTA (TE) buffer (10 mM Tris-HCL pH7.5, 1 mM EDTA pH8, dH_2O), spun down again for 3 min at 3000 rpm (Hettich Zentrifugen 1619), resuspended in 5ml of 1x lithium acetate (LiAC) (100 mM) in 1x TE buffer. Samples were spun down again for 3 min at 3000 rpm and the pellets resuspended in 100 μl of 1x LiAc in TE buffer. 15 μl of HssDNA (10 mg/ml) was added followed by 1 μl of plasmid DNA or 20 μl of deletion cassette. Samples were vortexed and 700 μl of 40% Polyethylene glycol (PEG) in LiAc TE was added followed by 1 hr incubation at room temperature on a rolling carousel. Cells were heat shocked at 42 ^{0}C for 15 min, spun down for 3 min at 3000 rpm (Hettich Zentrifugen 1619) and pellets

were resuspended in 200 µl of dH_2O. Cells were finally plated on appropriate plates and incubated at 30^0C.

2.3.3. Yeast plasmid miniprep – Zymoprep I (Zymo Research)

The procedure was followed exactly as stated in the user manual p.2 (catalog #D2001). Briefly, 1 ml of an overnight yeast culture was aliquoted into a 1.5 ml microcentrifuge tube and spun down at 600 xg for 2 min. The pellet was resuspended with 150 µl of digestion buffer (solution 1) followed by 2 µl of Zymolyase. Sample was vortexed and incubated at 37 °C for 30 min. 150 µl of lysis buffer (solution 2) was added into the microcentrifuge tube followed 150 µl of neutralizing buffer (solution 3). The sample was centrifuged at maximum speed for 2 min and 400 µl of isopropanol was added. The sample was centrifuged again at maximum speed for 8 min and the supernatant was removed by aspiration. The plasmid pellet was resuspended in 35 µl of TE buffer.

2.3.4. Glycerol stocks of yeast

For long-term storage of yeast cells, glycerol stocks were prepared by mixing 900 µl of overnight culture with 900 µl of 50% of sterile glycerol in a cryovial and stored at -80^0C freezer.

2.4. Molecular Biology Methods:

2.4.1. Bacterial plasmid DNA miniprep (Bioline plasmid mini kit)

Several bacterial colonies were picked, inoculate into 5 ml of 2xYT medium containing 10 µl of 25 mg/ml of ampicilin and incubated overnight at 37 ^0C. A plasmid miniprep kit from Bioloine (catalog #Bio-52056) was used and the method was followed exactly as stated in the protocol p.9-10. The plasmid DNA

was eluted in 30 µl of distilled H_2O (dH_2O) and 1 µl of each purified sample was ran on a 1% agarose gel at 100V for about 30 min to check for the presence of the plasmid (see 2.4.2.)

2.4.2. Agarose gel electrophoresis

DNA samples were analysed using agarose gel electrophoresis, mostly using a 1% gel (1g agarose in 100 ml of 1% Tris-acetate-EDTA (TAE) buffer (40 mM Tris OH, 20 mMAcetic Acid and 1 mM EDTA) and 0.5 ug/ml of ethidium bromide). DNA samples were loaded onto agarose gel after mixing with orange loading dye and samples were run at 100V for 35 minutes before being visualized using a short wave UV transilluminator and the images were taken on high-density thermal matt paper (110 mm x 20 m from Mitsubishi electric).

2.4.3. Extraction of DNA from Agarose gel (Qiagen)

The QIAquick gel extraction kit (Qiagen) was used (catalog #28704) and the procedure was followed as described in the user handbook p. 24-25. Briefly, the DNA fragment was excised from the agarose gel, weighted and dissolved in the QG buffer. Isopropanol was added to the sample, which was then applied to the QIAquick column and centrifuged for 1 min. 0.75 ml of buffer PE was added to the column and centrifuged for 1 min. The flow through was discarded and the column was centrifuged for a further 1 min. The QIAquick column was placed into a clean 1.5 ml microcentrifuge tube and the DNA was eluted with 30 ml of dH_2O.

2.4.4. Restriction Endonuclease digestion of DNA

Plasmid DNA (200 ng) or PCR products were digested with suitable restriction enzymes (20,000 U/ml) (New England Biolabs) using 10x restriction buffers (1x

final concentration) and dH_2O. Restriction digestion was carried out at 37 ^{0}C for 1-4 hrs.

2.4.5. DNA Mutagenesis - QuickChange Lightning Site-directed mutagenesis (Agilent)

Specific mutagenic oligonucleotide primers were designed following the guidelines on p.5 of the user manual (catalog #210518). The procedure was followed exactly as stated in the user manual p. 7 – 10. Briefly, a reaction mix was prepared using 10-100 ng of template DNA. 2 µl of DpnI enzyme was added into the amplified reaction and was incubated for 5 min at 37 ^{0}C. 2 µl of DpnI treated DNA was then transformed into XL10-Gold ultracompetent cells (see p.9-10 of the user manual). Transformed cells were plated onto 2xYT with 25 mg/ml of amp and incubated at 37 ^{0}C overnight.

2.4.6. Polymerase Chain Reaction (PCR)

2.4.6.1. PCR using *Taq* polymerase (from Bioline)

DNA fragments were amplified using plasmid DNA as a template using polymerase chain reaction (PCR). Specific oligonucleotide primers were designed to bind specifically to upstream and downstream regions of the sequences to be amplified. The following reagents were used at the stated volumes for a total reaction volume of 50 µl;

5 µl 10x NH_4^+ reaction buffer

1 µl 50 mM of magnesium chloride ($MgCl_2$)

1 µl 25mM dNTPs mix

1 µl Forward primer (100 ng/ µl)

1 µl Reverse primer (100 ng/ µl)

0.5 µl *Taq* polymerase (5U/ µl)

1 µl 1:10 dilution of plasmid DNA (100 pmol)

39.5 µl dH_2O

Cycle	Temperature (°C)	Time (sec)
Initial denaturation	94	2 min
Denaturation	94	1
Annealing	55-65 (depending on primers used)	30
Extension	72	60 sec /kb
Final extension	72	5 min
Hold	10	-

PCR cycles for gene amplification using the *Taq* polymerase.

2.4.6.2. Colony PCR

For colony PCR using bacterial cells, a small amount of cells from a single colony was collected using a toothpick and added to a PCR tube followed by 25 µl of the PCR master mix prepared as stated below;

10x NH_4^+ reaction buffer, 50 mM of magnesium chloride ($MgCl_2$), 25mM dNTPs mix, forward primer (100 ng/ µl), reverse primer (100 ng/ µl), *taq* polymerase (5U/ µl), 1:10 dilution of plasmid DNA (100 pmol) and dH_2O (to make up a total volume of 50 µl)

For yeast colony PCR, a small amount of yeast cells taken from a single colony was added to an eppendorf tube containing 20 µl of 0.02 M NaOH and was incubated at 100 ^{0}C for 15 min. 2.2 µl of the cell suspension was then added to 22.5 µl of PCR master mix (same as stated above).

2.4.7. PCR sample purification (Qiagen)

The QIAquick PCR purification kit (Qiagen) was used (catalog #28704) and the procedure was followed as described in the user handbook p18-19. Briefly, 5 volumes of buffer PB were added to 1 volume of the PCR sample, which was then applied to the QIAquick column and centrifuged for 1 min. To wash, 0.75 ml of buffer PE was added to the column and centrifuged for 1 min. The flow through was discarded and the column was centrifuged for a further 1 min. The QIAquick column was placed into a clean 1.5 ml microcentrifuge tube and the DNA was eluted with 30 ml of distilled H_2O.

2.5. Protein assays

2.5.1. Purification of His-tagged protein

2 L of cell culture (C41/C43 competent cells transformed with Vps1 WT, R298L, G397R and A447T containing plasmids) were grown in 2xYT media overnight and centrifuged (Beckman Coulter, Avanti J-26 XP centrifuge) at 7000 rpm for 12 min at 4 ^{0}C. Cells were harvested into 50 ml falcon tubes and pellets were stored at -14^{0}C.

For protein purification, protein pellets were resuspended in 10 ml of Start buffer (20mM Sodium phosphate NaH_2PO_4, 0.5 M NaCl and 10 mM Imidazole pH7.4) and stored on ice. Cells were sonicated (to disrupt the cells) 3 times for 30 seconds at

15 microns Amplitude. 200 μl of (50x) EDTA free protease inhibitor (from Roche, cat. no. 04693132001) was added and the pellets were centrifuged at 21000 xg for 45 minutes. After centrifugation the supernatant was passed through a 0.2 μm filter and 1 mM DTT (Dithiothreitol**)** was added to it before it was applied to the His-Trap HP 1 ml column (GE Healthcare Life Sciences).

Before the His-Trap column was used it had to be washed with 5 ml of Start buffer containing 500mM imidazole pH7.4 followed by 5 ml of distilled water. 0.5 ml of 100 mM nickel sulphate was then added to regenerate the column followed by 5 ml of distilled water and 5 ml of Start buffer. Once the column was washed, the protein fractions were applied to the column followed by 5 ml of Start buffer. The column was then washed several times with Start buffer containing an increasing concentration of imidazole, starting with 5 ml of Start buffer with 60 mM imidazole, 5 ml of Start buffer with 80 mM imidazole, 5 ml of Start buffer with 100 mM imidazole and then finally the protein was eluted with 5 ml of Start buffer with 500 mM imidazole

2.5.2. Measuring protein concentration using the Bradford assay

Protein concentration was measured using the Bradford reagent (from Bio-Rad). A BSA (Bovine serum albumin) standard curve was made using a range of concentrations (between 2 and 9 mg/ml). 20 μl of each BSA concentration was added to 1 ml of 1 in 5 diluted Bradford reagent and the OD was measured at 595nm. A XY graph was then generated using the OD values in Excel, which gave the slope and the Y intercept values, which were then used to calculate the protein concentration.

Absorbance = x + Y intercept / Slope

X = Absorbance – Y intercept / Slope = answer in mg/ml

To convert the protein concentration from mg/ml into μM;

([Protein in mg/ml]/molecular weight) x 1000 x 1000

2.5.3. Protein separation by SDS PAGE

Proteins were separated by size using the sodium dodecyl sulfate (SDS-PAGE) gel electrophoresis. A 10% resolving gel was prepared by mixing 4 ml of dH_2O, 3.3 ml of 30% acrylamide, 2.5 ml resolving buffer (1.5 M Tris-HCl pH8.8 and 0.4% SDS), 100 μl 10% ammonium persulphate (APS) and 4 μl N, N, N', N'-Tetramethylethyl-enediamine (TEMED). The mix was poured between two glass plates sealed together with a rubber strip and held together by two clips, and was left at room temperature for 30 minutes for the gel to set. While the resolving gel was setting, 5 % of stacking gel was prepared by mixing 2.7 ml of distilled water, 670 μl of 30% acrylamide, 500 μl stacking buffer (1 M Tris-HCl pH6.8 and 0.4% SDS), 40 μl 10% APS and 4 μl TEMED. The stacking gel was then poured on top of the resolving gel and a comb was immediately inserted to form the gel wells. The gel was left for another 30 minutes to set before the clips, the comb and the rubber seal were removed. The gel was placed into a gel tank (ATTO Slab Gel Electrophoresis Chamber) and the tank filled with 1 x SDS running buffer (0.025 M Tris, 0.192 M glycine and 0.1 % SDS pH 8.6). 50 μl of sample buffer (50 mM Tris HCL pH 6.8, 2 % SDS, 10 % glycerol, 1 % β-mercaptoethanol, 0.02 % bromophenol blue) was added to 50 μl of each protein sample, before heating them for 5 minutes at 100 ^{0}C and 25 μl of each sample was loaded onto an SDS

PAGE gel. The gel was run at 150 V (Volts) for 2 hours, stained with the Coomassie safe stain (80 mg of Coomassie Brilliant Blue G-250 in 1L of dH_2O and 3ml concentrated HCL for 30 minutes and destained in dH_2O.

2.5.4. Western Blotting – Semi Dry Transfer

Samples were run on a 10% sodium dodecyl sulfate (SDS) gel, which was run at 150 V for 2 hrs. The proteins were transferred onto a polyvinylidene difluoride (PVDF) membrane which was previously soaked in methanol for 5 min before it was left in Tris/glycine buffer (25 mM Tris base, 190 mM glycine and 0.1% SDS). 4 Whatman filter paper previously soaked in Tris/glycine SDS buffer were placed onto the transfer cassette followed by the nitrocellulose membrane, the SDS gel and finally covered with another 4 Whatman papers. The transfer was run for 50 min at 400 mA. The membrane was stained with Ponceau stain (0.2% (w/v) Ponceau S and 5% glacial acetic acid) for about 1 min and destained with dH_2O several times until the stain was removed from the membrane and an image was taken.

The membrane was blocked with 5ml of 1% Tris-buffered saline and Tween-20 (TBST) buffer (20 mM Tris pH 7.5,150 mM NaCl and 0.1% Tween 20) with 5% fat free milk. The membrane was then put into a plastic pouch and 2 ml of 5% fat free milk and primary antibody was added to the membrane. The pouch was sealed and incubated on a moving tray overnight at 4 ^{0}C. After the overnight incubation, the membrane was washed 3 times every 10 min with 5 ml of 1% TBST buffer before it was incubated with 10ml of 5% fat free milk containing 1:10,000 horseradish peroxidase conjugated secondary antibody. The membrane was left

for at least 1 hr on a shaking platform before it was washed again in TBST buffer three times every 10 min. 3 ml of each of ECL I (2.5 μM luminol, 0.396 μM p-coumaric acid, 0.1 M Tris HCL pH 8.5, dH_2O) and ECL II (19.2 % hydrogen peroxide, 0.1 M Tris HCL pH 8.5, dH_2O) were mixed together and applied onto the membrane with light agitation for 30 seconds. The membrane was visualized using Bio-Rad Molecular Imager (Chemi Doc XRS + with image lab software) using the Chemi program where an image was taken every 60 sec for a total of 3600 seconds resulting in a total number of 30 images.

2.5.5. Protein self-assembly assay

A His-tagged protein was purified and buffer exchanged into buffer 1 (20mM Hepes pH7.2, 100mM KCl, 2mM $MgCl_2$ and 1mM DTT). The protein was spun at 90K rpm (Optima TM Ultracentrifuge TL100, Beckman) for 15 minutes to remove any aggregated proteins and the protein concentration of the supernatant was calculated using the Bradford method (see 2.5.2). Ranges of protein concentrations (chosen to be tested) were made up in buffer 1 in a total reaction volume of 50 μl. 0.5 μM of GTPγs was added to the reaction mix followed by sample incubation at room temperature for 15 minutes. The samples were spun down at 80K rpm (Optima TM Ultracentrifuge TL100, Beckman) and the supernatant and pellet were carefully separated, where the pellet was resuspended in 50 μl of buffer 1. 50 μl of sample buffer was added to each of the samples before heating them for 5 minutes at 100 ^{0}C and 25 μl of each sample was loaded onto an SDS PAGE gel, which was run at 150 Volts (V) for 50 min. The gel was stained using the Coomassie safe stain for 30 minutes and destained in dH_2O.

2.5.6. Lipid Binding Assay

2.5.6.1. Preparation of Liposomes

11 μl of 25 mg/ml Folch fraction I (Brain extract from bovine brain from Sigma - Aldrich) was pipetted into a glass vial and washed with 500 μl of chloroform and dried with nitrogen. 500 μl of diethyl ether was added to the glass vial to wash the dried liposomes and then it was dried with nitrogen. Finally the liposomes were resuspended in 200 μl of liposome buffer (20mM Hepes pH7.2, 100mM KCl, 2mM $MgCl_2$ and 1mM DTT) before being placed in a 60 ^{0}C waterbath for 30 minutes with regular agitation. Liposomes could be stored for up to 1 week at 4 ^{0}C.

2.5.6.2. Liposome Co-sedimentation Assay

His-tagged protein was purified and buffer exchanged into liposome buffer (20mM Hepes pH7.2, 100mM KCl, 2mM $MgCl_2$ and 1mM DTT). The protein was spun down at 90K rpm (Optima TM Ultracentrifuge TL100, Beckman) for 15 minutes and the protein concentration was calculated using the Bradford method (see 2.5.2). For a liposome co-sedimentation assay, 20 μl of liposomes, 5 μM Vps1 protein, 1mM GTP, 1mM $CaCl_2$, 5mM $MgCl_2$, 5mM DTT and dH_2O (to make up the reaction volume to a total of 100 μl) was used. Samples were incubated at room temperature for 15 minutes. The samples were spun down at 80K rpm (Optima TM Ultracentrifuge TL100, Beckman) and the supernatant and pellet were carefully separated, where the pellet was resuspended in 100 μl of liposome buffer. 100 μl of sample buffer was added to each of the samples before heating them for 5 minutes at 100 ^{0}C and 25 μl of each sample was loaded onto an SDS

PAGE gel, which was run at 150 Volts (V) for 50 minutes. The gel was stained using the Coomassie safe stain for 30 minutes and destained in dH_2O.

2.5.7. PIP strips:

PIP strips (from Echelon) compose of a 2 cm x 6 cm nitrocellulose membrane containing 100 pmol samples of 15 different phospholipids. In this experiment, the PIP strip membrane was blocked with 5ml of TBST buffer with 5% fat free milk. The membrane was gently agitated for 2 hrs at room temperature before the blocking buffer was discarded and 1 µM of protein in 5% milk and TBST final volume of 500 µl was added. The membrane was incubated for overnight at 4 ^{0}C, washed three times in 5 ml of TBST buffer (each time for 10 minutes) and incubated with an anti-His antibody 1:100 dilution in TBST and 5% milk for 2_hr at room temp on a shaking platform. The membrane was washed again for three times in 5 ml of TBST buffer (each time for 10 minutes) and incubated with anti-mouse IgG-HRP 1:5000 dilution in TBST and 5% milk for 1 hr at room temperature on a shaking platform. The washing step was repeated again and finally 0.5 ml of ECL I and II was added to the membrane with light agitation for 30 seconds before the membrane was visualised using Bio-Rad Molecular Imager (Chemi Doc XRS + with image lab software) using the Chemi program where an image was taken every 60 sec for a total of 3600 seconds resulting in a total number of 30 images.

2.5.8. PIP arrays:

PIP Arrays (from Echelon) are 4 x 5 cm hydrophobic membranes that have been spotted with a concentration gradient of eight phosphoinositides. As with the PIP

strips, His-tagged Vps1WT and R298L proteins were purified using a His-tag column and 1uM of each of the proteins made in 5% fat free milk, final volume of 0.5 ml was added to the PIP array membranes. The procedure was carried out exactly as stated in section 2.5.7.

2.5.9. Yeast Whole cell extraction

Yeast cells (containing appropriate expression plasmid) were inoculated into 5 ml of appropriate media and incubated overnight at 30 ^{0}C. Samples were refreshed by adding 0.5 ml of the overnight culture into 4.5 ml of fresh media and the samples were incubated at 30 ^{0}C for 3-4 hrs. The OD_{600} of the samples was measured in order to calculate the volume of cell suspension required to give a 2 OD_{600} units of cells. Once 2 OD_{600} units of cells were pipetted the samples were spun down at 4000 rpm (Hettich Zentrifugen 1619) for 5 min and the supernatant was discarded. The pellet was resuspended in 1 ml of dH_2O, spun down again at 6000 rpm (Hettich Zentrifugen 1619) for 3 min and the supernatant was discarded again. 100 μl of glass beads and 125 μl of 2x sample buffer was added to the pellet, the samples were vortexed and then left at 100 ^{0}C for 3 min. After the incubation at 100 ^{0}C, the samples were put into a cell disrupter for 3 min, left to cool on the bench for few minutes and then loaded onto a 10% SDS gel which was run at 150 V for about 2 hrs. A semi-dry transfer was then performed (see section 2.5.4.).

2.5.10. Carboxypeptidase Y (CPY) assay

Carboxypeptidase Y (CPY) is a yeast vacuolar protein whose movement from the endoplasmic reticulum (ER) to the Golgi apparatus can be monitored by the

change in protein size from 67 kDa to 69 kDa in the Golgi compartment (Stevens et al. 1982).

For this experiment overnight yeast cultures were reinoculated into fresh media and left to grow to early log phase. Samples were spun down for 3 min at 3000 rpm (Hettich Zentrifugen 1619) and the pellets was resuspended in 5 ml of media with 0.05 mg/ml of cyclohexamide. Samples were incubated at 30 ^{0}C for 30 min before the OD_{600} was measured and the required volumes for 3 U of cell were calculated and pipetted into sterile eppendorf tubes. Samples were then spun down for 3 min at 6000 rpm (Hettich Zentrifugen 1619), washed with 1 ml of dH_2O, spun again for 3 min at 6000 rpm and 100 μl of glass beads was added followed by 125 μl of 2x sample buffer. The samples were vortexed and then boiled in a heat block for 3 min at 100 ^{0}C before being loaded onto a 10% SDS gel which was run at 150 V for about 2 hrs. A semi-dry transfer was then performed (see section 2.5.4.).

2.6. Cell based assays

2.6.1. Temperature sensitivity

Yeast strains grown overnight were reinoculated in fresh drop-out Ura media by adding 250 μl of the overnight culture into 4.75 ml of fresh media and incubated for 3 hrs at 30 ^{0}C. 0.5 OD_{600} units of cells was serially diluted five times in a multi-well plate (1:10, 1:100, 1:1000, 1:10,000, 1:100,000) and 5 μl of each sample was spotted onto fresh drop-out Ura plates which were then incubated at 30 ^{0}C and 37 ^{0}C for 3 days.

2.6.2. Lucifer Yellow

Lucifer yellow is a dye that was used to assess fluid phase endocytosis in yeast [Dulic *et al.* 1991]. An overnight culture was refreshed, where 250 μl of the culture was added to 4.75 ml of fresh YPD media and incubated at 30 ^{0}C in an orbital shaking incubator until the cell density reached 1.4x10^7 cells/ml. 0.4 – 0.6 U of culture at OD_{600} was spun down at 3000 rpm (Hettich Zentrifugen 1619) for 5 min and the pellet was resuspended in 30 μl of drop-out Ura media. 10 μl of 40mg/ml lucifer yellow (LY-CH dilithium salt, Sigma) made up in sterile deionised water was added to the cells and the samples were incubated at 30 ^{0}C in an orbital shaking incubator for 15 minutes to assess early stage endocytosis or 90 minutes to assess late stage endocytosis. Cells were washed three times with 1 ml of ice-cold succinate/azide buffer (50mM succinic acid (Sigma) and 20mM sodium azide (Sigma) buffer (brought to pH5 with NaOH) and the pellet was resuspended in 10 μl of succinate/azide buffer and left on ice until the samples were ready to be viewed. 3 μl of the cell suspension was added onto a microscope slide with a cover slip and images were taken using the 100x oil-immersion objective lens in the Olympus BX-81 fluorescence microscope with a 100 W mercury lamp.

2.6.3. FM4-64 staining

An overnight culture was refreshed, where 250 μl of the culture was added to 4.75 ml of fresh drop-out Ura media and incubated at 30 ^{0}C in an orbital shaking incubator for 4 hrs. 1 ml of log phase culture 0.4 – 0.6 U at OD_{600} was spun down at 3000 rpm (Hettich Zentrifugen 1619) for 3 min and the pellet was resuspended in 250 μl drop-out Ura media. 0.25 μl of 16mM FM4-64 (T3166 from Invitrogen) in

Dimethyl sulphoxide (DMSO) was added to the cell suspension after which it was incubated in a rolling carousel for 15 minutes at 26 ^{0}C. Cells were then spun down at 3000 rpm (Hettich Zentrifugen 1619) for 3mins and resuspended in 1 ml of drop-out Ura media and incubated at 26 ^{0}C shaker for 90 minutes before the cells were harvested by spinning them at 3000 rpm (Hettich Zentrifugen 1619) for 3mins and resuspending the pellet in 150 μl drop-out Ura. 3 μl of the cell suspension was added onto a microscope slide with a cover slip and images were taken using the 100x oil-immersion objective lens in the Olympus BX-81 fluorescence microscope with a 100 W mercury lamp.

2.6.4. Rhodamine Phalloidin

Rhodamine Phalloidin was used to fix and stain yeast cell in order to visualize actin structures. An overnight culture was refreshed by adding 0.5 ml of the culture into 4.5 ml of fresh media and cells were then grown for 4 hrs at 30 ^{0}C. 1 ml of actively growing yeast cells (OD_{600} 0.1-0.3U) were fixed by addition of 134 μl of 37% formaldehyde for 1 hr at room temperature. Cells were spun down for 3 min at 3000 rpm (Hettich Zentrifugen 1619) followed by two washes with 500 μl of wash buffer 1 (1x phosphate buffered saline (PBS) pH 7.4, 1mg/ml BSA and 0.1% Triton TX-100). The pellet was resuspended in 50 μl of wash buffer 1 with 5 μl rhodamine phalloidin and samples were incubated in dark for 30 mins. The cells were spun down at 3000 (Hettich Zentrifugen 1619) and washed twice with 50 μl of wash buffer 2 (1x PBS and 1mg/ml BSA). The pellet was re-suspended in 200 μl of wash buffer 2 and then 2 μl of each sample was spotted onto microscope slide. Images were taken using the 100x oil immersion objective lens in Olympus BX-81 fluorescence microscope 100 W mercury lamp.

2.6.5. Analysis of GFP- and mRFP- tagged reporter proteins

Yeast cells expressing GFP (Green fluorescent protein) or mRFP (Red fluorescent protein) tagged proteins were inoculated into 5 ml of fresh media and grown overnight at 30 ^{0}C. The culture was reinoculated by adding 0.5 ml of the overnight culture into 4.5 ml of fresh media and growing the cells for 3-4 hrs. 3 μl of each sample was then placed onto a microscopic slide and visualized using the 100x oil immersion objective lens in Olympus BX-81 fluorescence microscope 100 W mercury lamp. Time-lapse live-cell imaging was performed with 1 sec time-lapse and 0.5 s exposure.

2.6.5.1. Measuring patch lfetime

The time-lapse videos were analysed using Imaje J software (patch tracking plugin) where the lifetime of individual endocytic patches were measured starting from the appearance of the patch until its disappearance.

2.6.5.2. Measuring patch intensity

The time-lapse videos were analysed using Imaje J software (patch tracking plugin) where the maximum pixel value of each endocytic patch was measured over time from the point of appearance of the patch until its disappearance.

2.6.5.3. Patch tracking

Patch tracking was performed using the Imaje J software (patch tracking plugin) were the X and Y axsis of the each pacth were measured and plotted on appropriate graph using GraphPad Prism 6 software.

2.7. Microscopy methods

2.7.1. Fluorescence microscopy and statistical analysis

Epifluorescence microscopy was performed using Olympus IX-81microscope with a Photometrics Cool Snap HQ camera and 100x 1.40 numerical aperture oil objective. Imaging and image capture was performed using NIS Elements 4.20.01 software. Time-lapse live-cell imaging was performed with 1 sec time-lapse and 0.5 s exposure. Statistical analysis was performed using GraphPad Prism 6 software.

2.7.2. Electron microscopy

2.7.2.1 Vps1 and actin interaction using electron microscopy

To investigate the interaction between Vps1 and actin, actin was polymerized overnight at 4 ^{0}C in F-buffer (500 mM KCl, 10 mM $MgCl_2$, 10 mM EGTA, 100 mM Tris pH 8.0]. 1 μM of Vps1 was mixed with 1.5 μM F-actin in a total volume of 20 μl reaction mix made up with F-buffer. Samples were incubated at room temperature for 15 minutes before a 1 in 10 dilution with F-buffer was made for each sample and the samples were loaded onto carbon coated grids.

2.7.2.2. Negative staining of carbon-coated grids and visualizing grids

5 μl of each sample were adsorbed onto glow discharged (for 25 sec) carbon-coated grids, incubated at room temperature for 2 min before being stained with 0.75 % Uranyl formate (UF). Grids were visualized using the Philips CM-100 electron microscope using a Gatan MultiScan 794 CCD camera.

Chapter 3 - *In-vivo* and *In-vitro* analysis of Vps1 mutations

Chapter 3 - *In-vivo* and *In-vitro* analysis of Vps1 mutations

3.1. Introduction

Vps1 belongs to the family of dynamin-like-proteins and is an important protein that has several essential roles in yeast cells including endocytosis. Although new insights into the role of Vps1 in endocytosis have been made, a lot is still not understood about the functions of its domains and their roles in endocytosis. In this chapter the three chosen Vps1 mutations (Table 1), for which equivalent mutations in dynamin were shown to be linked to neurological disorders, were analyzed using different cell based assays in order to investigate the phenotype of these mutants and determine their effect on the normal function of Vps1 in its different membrane trafficking functions. The effect of the endocytic mutations on the biochemical properties of Vps1 and hence on its roles were also addressed.

This work aimed to help in understanding the nature of the defect that each of the three mutations causes to Vps1 and therefore might help to understand how this affects function in dynamin itself. It would also help to clarify whether the studied mutations result in a general defect or specifically affect endocytosis.

3.2. *In-vivo* analysis

Yeast is a fully functional unicellular organism that allows the study of various proteins and their mutations in their natural cellular environment. The ability to delete, mutate or epitope/GFP tag yeast genes relatively easily, as well as to study the consequence of these changes in a physiological system have all contributed to making yeast a powerful tool for investigating cellular processes.

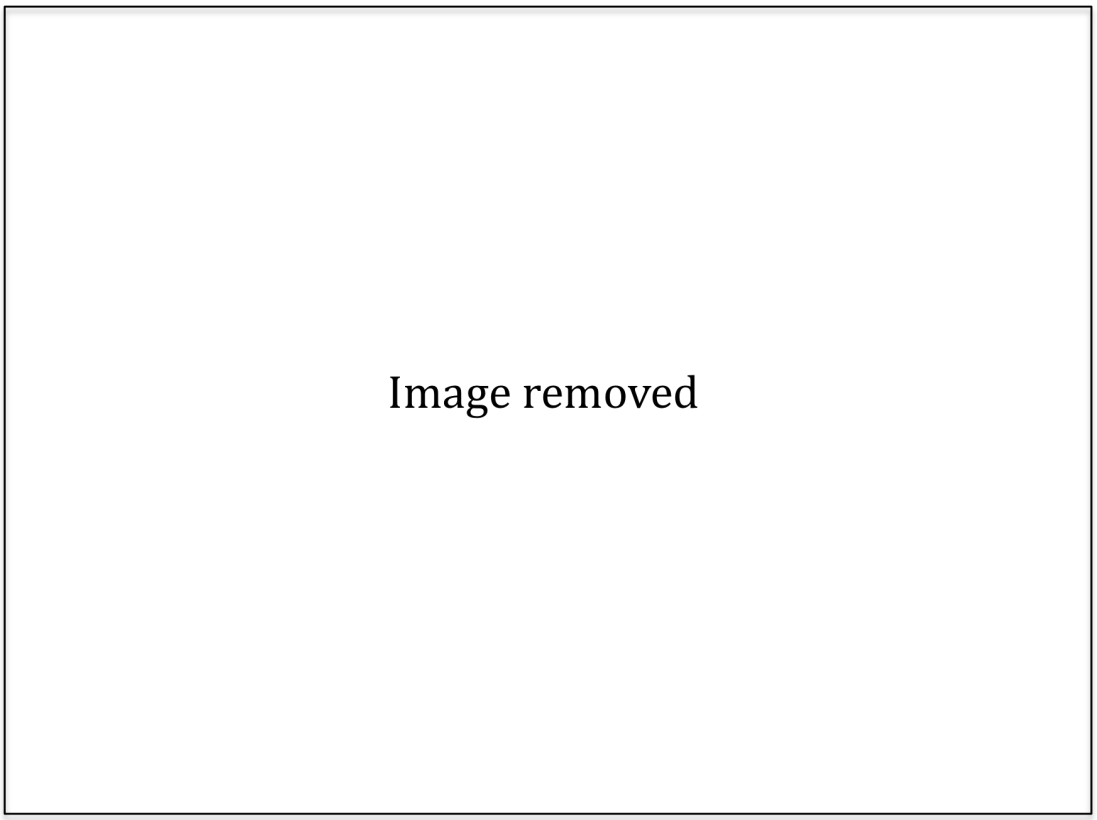

Fig.3.1. Disease mutations annotated on Dynamin-1 structure. A) Different domains of classical Dynamin-1. The numbers at the top represent the amino acids and the arrows indicate the position of the mammalian mutations used in this study. B) Representation of human Dynamin-1 as resolved by Faelber *et al*. 2011. Regions not resolved in the crystal structure are indicated by dotted lines. Lipid-binding residues are indicated as o. The three mutations used in this work are marked on the proposed structure of the human Dynamin-1. This gives an indication of the position of the mutations within the protein. The (m) stands for the mammalian mutations and the (y) stands for the equivalent yeast mutations.

3.2.1. *In-vivo* expression of Vps1 mutations

The first step towards analyzing the R298L (in the GTPase domain), G397R and A447T mutations (in the middle stalk domain) [figure 3.1] was to confirm that the mutations did not affect the protein steady state levels or stability in yeast cells. This was essential so that any effects could be attributed to the mutation rather than to lack of protein. Previously in another project carried out by Laura Beaumont and Iwona Smaczynska-de Rooij, the R298L, G397R and A447T mutations were introduced into the *VPS1* gene on a CEN based plasmid via site-directed mutagenesis and this was confirmed by sequencing.

Cells expressing wild type and mutant Vps1 proteins were grown to exponential growth phase and a yeast whole cell protein extraction was performed. A *vps1Δ* yeast strain (KAY1095) was transformed with a Vps1 wild-type (pKA677) *vps1Δ (*pKA544) , Vps1R298L (pKA798), Vps1G397R (pKA797) and Vps1A447T (pKA796) expression plasmids. An anti-Vps1 mouse primary antibody (generated by the KA lab) and anti-mouse HRP secondary antibody were used to detect Vps1 protein following separation by SDS-PAGE and western blotting. As expected, no Vps1 protein was detected in the *vps1Δ* cell extract but Vps1 was clearly observed in the wild-type cells. The results from the blot confirmed that the three mutant proteins were all expressed in cells with the expression levels being similar to the wild type protein [figure 3.2.A]. A loading control was used [figure 3.2.B] to confirm an equal loading of each of the samples into the gel wells. The experiment was performed twice to confirm the results and an image best representing the results is shown [figure 3.2].

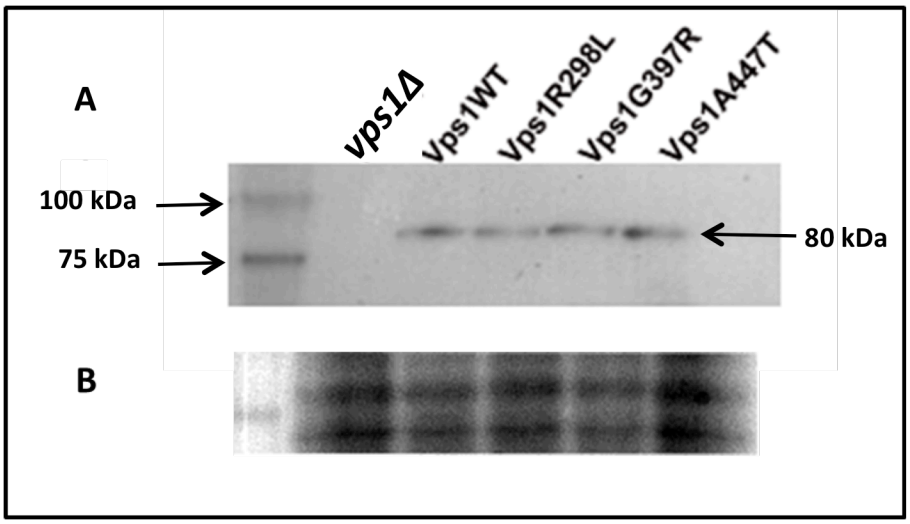

Fig.3.2. Protein expression levels of Vps1 disease mutants in yeast cells. Yeast whole cell protein extraction was performed, where yeast cells containing expression plasmids of Vps1 wild-type, *vps1Δ,* Vps1298L, Vps1G397R and Vps1A447T were used. Samples were loaded onto a 10% SDS gel before being transferred onto a PVDF membrane. A) Western blot was probed with anti Vps1 antibodies showing the expression of the three mutated proteins in yeast cells at similar levels to the wild-type protein. B) A Ponceau staining of the membrane was used as a loading control to allow the protein loading to be compared.

3.2.2 Assessing Growth Phenotype of Vps1 Mutants

Once the expression of the Vps1 mutant proteins in yeast cells was confirmed, a liquid growth phenotype test was performed to assess the effect of the mutations on cell growth. An overnight culture of *vps1Δ* yeast strain (KAY1095) transformed with a Vps1 wild-type (pKA677) *vps1Δ (*pKA544) , Vps1R298L (pKA798), Vps1G397R (pKA797) and Vps1A447T (pKA796) expression plasmids were re-inoculated into fresh media and the optical density was measured using the spectrophotometer. The OD_{600} for all cultures was set at 0.1. Cells were incubated in a shaking incubator at 30 ^{0}C and the OD_{600} of the culture was measured every hour for a total of 11 hours and a growth curve was plotted.

The growth rates of the mutant proteins were shown to be similar to that of the wild type for the first 5-6 hours after which the *vps1Δ* strain showed a slightly reduced growth rate [figure 3.3]. As the cells entered the log phase (after 6 hours of growth) a clear reduction in the growth of the G397R mutant was noticed. A slight reduction in the R298L mutant also became evident whereas the growth of the A447T mutant continued to be similar to the wild-type. The growth graph [figure 3.3] was used to calculate the generation time, where the generation time for Vps1 wild type averaged to 2.4 hrs, 2.8 hrs for *vps1Δ,* 2.6 hrs for R298L, 2.9 hrs for G397R and 2.55 hrs for A447T. This suggested that growth and doubling time in the R298L and A447T mutants were more similar to the wild type compared to the G397R which was more similar to the *vps1Δ* suggesting a possible dominant negative phenotype. Since this experiment was performed once, this difference might be within error.

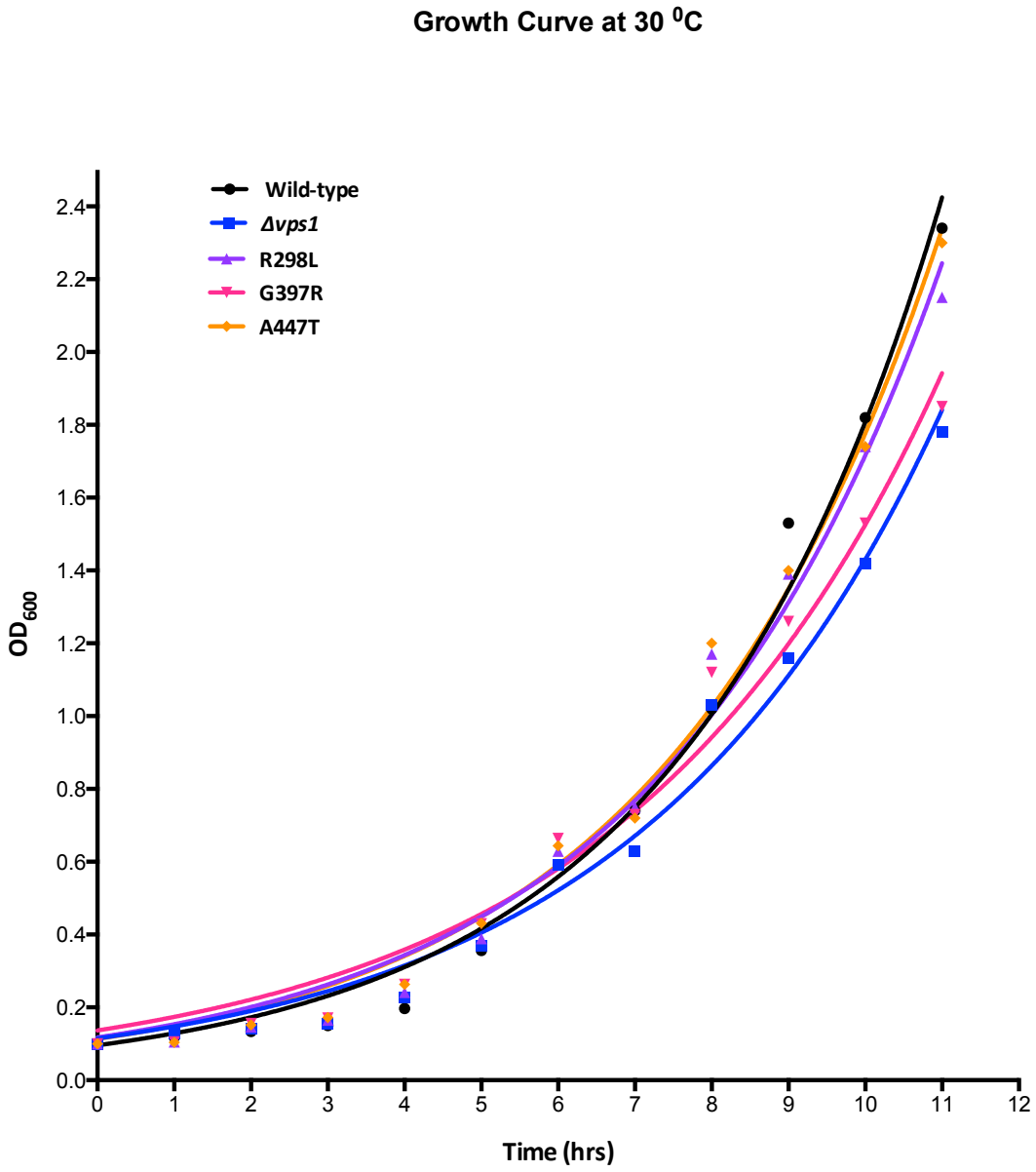

Fig.3.3. Growth of Vps1 mutants in liquid media. An overnight cell culture was re-inoculated into fresh media and the OD_{600} of cells was set at 0.1. Cells were incubated at 30 ^{0}C for a total of 11 hours and a reading of cell density was taken every 1 hour. Graphpad Prism 6 software was used to generate the graph.

3.2.3. Effect of Temperature and Sorbitol on the Growth of Vps1 Mutations

Although growth in liquid media showed some reduction in the growth phenotype in the G397R and the R298L mutants, it was important to further investigate this phenotype. To do so, growth at a higher temperature and in the presence of sorbitol media was analyzed. An overnight culture of *vps1Δ* yeast strain (KAY1095) transformed with a Vps1 wild-type (pKA677) *vps1Δ (*pKA544) , Vps1R298L (pKA798), Vps1G397R (pKA797) and Vps1A447T (pKA796) expression plasmids were re-inoculated into fresh media and the optical density was measured using the spectrophotometer and the OD_{600} was equalized at 0.5. Cell cultures were then serially diluted (1:10, 1:100, 1:1000, 1:10,000 and 1:100,000) and spotted onto selective solid media. The plates were incubated for 3 days at 30 ^{0}C (permissive temperature) and 37 ^{0}C (restrictive temperature).

As expected, the wild-type cells were able to grow normally at both the permissive and the restrictive temperatures unlike the *vps1Δ* cells, which showed a reduction in growth at the restrictive temperature. None of the three mutations affected cell growth at the permissive temperature, however at the restrictive temperature the G397R mutant showed a temperature sensitive phenotype which appeared more severe than that seen in the *vps1Δ* [figure 3.4] further suggesting that this mutant might generate a largely non-functional protein with a dominant negative effect. This growth defect was rescued when the G397R cells were grown on selective media containing 1M of sorbitol which is an osmotic stabilizer suggested to reduce the function of actin in endocytosis [Aghamohammadzadeh and Ayscough 2009].

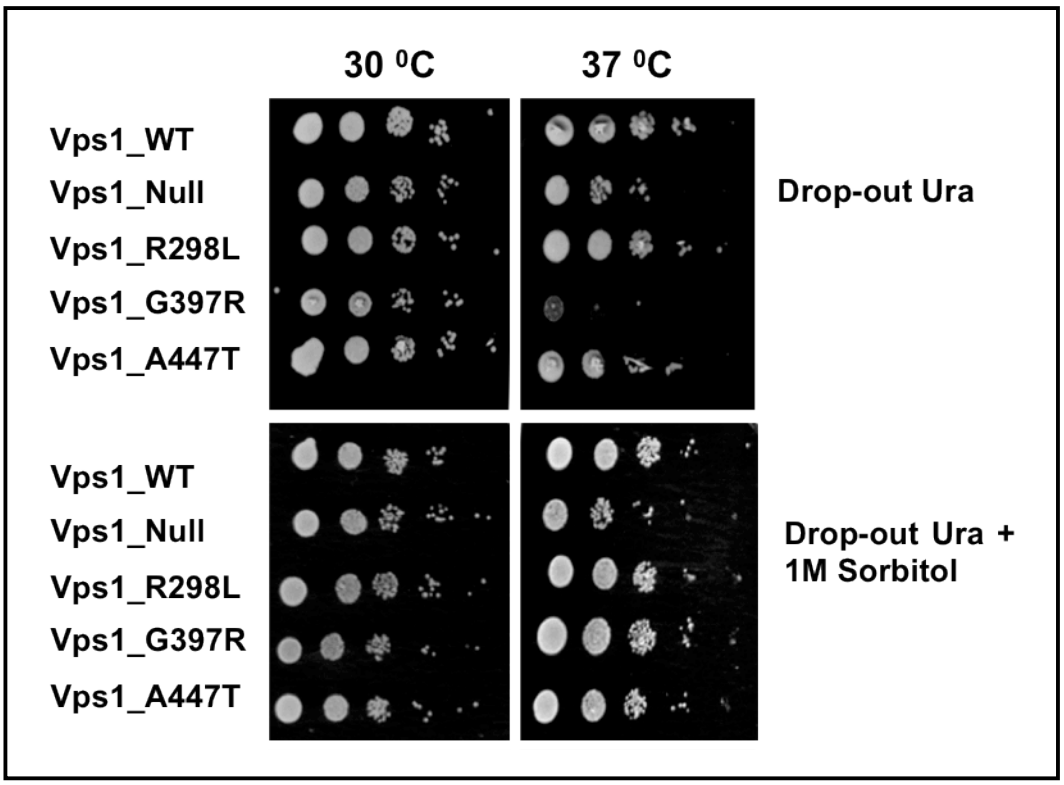

Fig.3.4. Effect of Vps1 mutations on cell growth. An overnight culture was serially diluted and spotted onto selective media +/- 1M sorbitol. Plates were incubated for 3 days at 30 ^{0}C and 37 ^{0}C.

3.2.4. Effect of Vps1 mutations on the trafficking of CPY

Vps1 was originally identified in screens for genes involved in vacuolar protein sorting in *S.cerevisiae* and one of the known trafficking roles it has is in the transport of vesicles between the Golgi and the vacuolar compartments. [Rothman *et al*. 1989, Vater *et al.* 1992]. To test whether this trafficking property was affected by the mutations, a Carboxypeptidase Y (CPY) assay was performed. Carboxypeptidase Y (CPY) is a yeast vacuolar protein whose movement from the endoplasmic reticulum (ER) to the Golgi apparatus can be monitored by the change in protein size from 67 kDa precursor form to 69 kDa form in the Golgi compartment (Stevens et al. 1982). The 69 kDa form of CPY gets trafficked into the vacuole where it undergoes a post-translational modification resulting in a 61 kDa mature protein (Stevens et al. 1982, Bowers and Stevens 2005). Upon successful trafficking of the protein from the Golgi into the vacuole, a 61 kDa band can be detected by Western blot analysis (mCPY), however, in the case of a defect in the trafficking pathway, a 69 kDa band is expected to be detected which would represent the immature form of the protein (pCPY).

A whole cell protein extraction was performed as described in the materials and methods (section 2.5.9) using *vps1Δ* yeast strain (KAY1095) transformed with a Vps1 wild-type (pKA677) *vps1Δ (*pKA544), Vps1R298L (pKA798), Vps1G397R (pKA797) and Vps1A447T (pKA796) expression plasmids. Samples were loaded onto 10% SDS gel and a semi-dry transfer was used to transfer the samples onto PVDF membrane (section 2.5.10). The membrane was incubated with pre-cleaned anti-CPY antibody and the blot was developed using ECL.

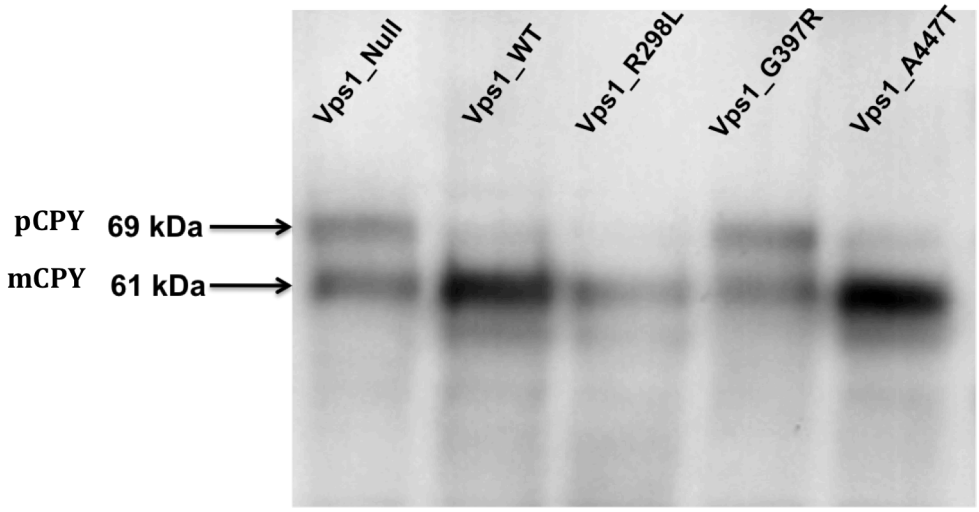

Fig. 3.5. Effect of Vps1 mutations on carboxypeptidase Y (CPY) trafficking. A whole cell protein extraction was performed following preincubation of cells with cycloheximide to stop the synthesis of new CPY protein. Samples were loaded onto 10% SDS gel and transferred onto a PVDF membrane. Pre-cleaned anti-CPY antibody was used and the blot was developed using ECL. The arrows indicate the mature (61 kDa) and precursor (69 kDa) form of CPY.

As expected, in the wild-type cells a band of about 61 kDa was detected representing the mature protein confirming the successful trafficking of CPY. However, in the *vps1Δ* cells as well as showing a 61 kDa band, there was a higher band of about 69 kDa representing the immature form of CPY [figure 3.5]. This suggested that the trafficking process was not totally aberrant but rather less efficient compared to the wild-type. The results from the western blot showed the presence of mature CPY in all of the three mutants indicating that the trafficking role of Vps1 from the late Golgi to the vacuole was at least partially functional. However, similar to *vps1Δ*, the G397R mutant showed a clear higher band of about 69 kDa representing the immature CPY, which again suggested that the efficiency of trafficking of CPY from the late Golgi to the vacuole was reduced in this mutant. The western blot also showed a faint band representing the immature CPY in the wild-type, R298L and A447T mutants which probably was because the cycloheximide was not fully effective or the incubation time was not enough.

3.2.5. Effect of Vps1 mutations on Peroxisomal inheritance

It was previously shown that Vps1 is important in facilitating peroxisome fission in yeast cells and in its absence cells showed a significant reduction in the number of peroxisomes [Hoepfner *et al.* 2001]. In a *vps1Δ* , cells only contained between 1-3 peroxisomes compared to that seen in the wild-type cells, which could have up to 9 peroxisomes seen as large puncta [Hoepfner *et al.* 2001]. In this work the aim was to assess whether the Vps1 mutations could rescue peroxisomal fission defect in yeast cells and thereby fulfil a specific function normally performed by Vps1.

In this experiment a *vps1Δ/ dnm1Δ* yeast strain was used. Dnm1, which is another protein that belongs to the dynamin-like-protein family in yeast, is also able to

participate in regulating peroxisome abundance and therefore, to ensure that any rescue of the peroxisomal fission defects was a result of the Vps1 mutations, it was important to ensure that both endogenous Vps1 and Dnm1 were absent.

A *vps1Δ/dnm1Δ* yeast strain (KAY 1096) was transformed with Vps1 wild-type (pKA677) *vps1Δ (*pKA544), Vps1R298L (pKA798), Vps1G397R (pKA797) and Vps1A447T (pKA796) expression plasmids. These transformants were inoculated for an overnight growth and cell cultures were refreshed and grown until exponential growth phase was reached. Cells were placed on a glass slide and were visualized using fluorescent microscopy at 100x magnification where 30 cells from each sample were examined by eye. This experiment was repeated twice to confirm the observed phenotypes [figure 3.6.a]. The quantification results have shown that 75 % of wild-type cells had more than 10 peroxisomes per cell compared to 53 % for the R298L mutant and 57 % for A447T [figure 3.6.b] suggesting a more intermediate phenotype compared to the wild-type and the null. On the other hand, the G397R mutant was more similar to *vps1Δ*, where 90% of cells had 1-3 peroxisomes per cell confirming the inability of this mutant to rescue peroxisomal fission defects.

A

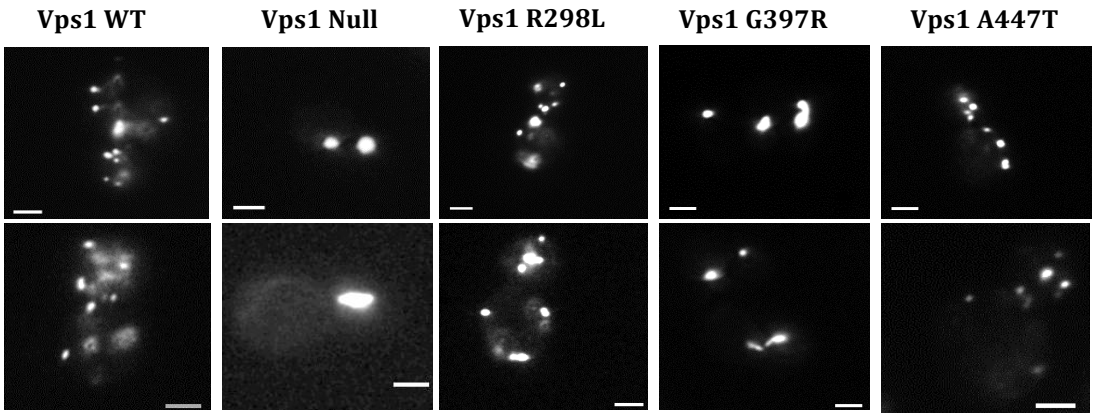

B

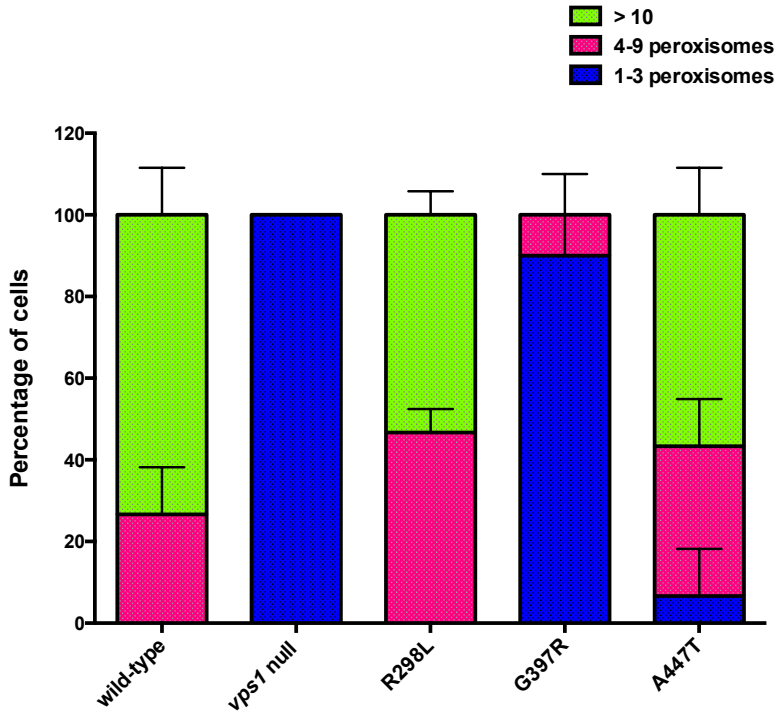

Fig.3.6. Rescue of the peroxisome fission defects by Vps1 mutants. *vps1Δ/dnm1Δ* yeast cells were transformed with expression plasmids containing the Vps1 mutations to assess the rescue of the peroxisomal fission defect. A) Cells visualized using fluorescent microscopy at 100x magnification. Scale bar: 2 μm. B) Quantification of the number of peroxisomes in each Vps1 mutant. Vps1 wild-type and vps1 null were used as controls. 60 cells from each sample from two independent experiments were used in this quantification. Error bars represent mean with SD.

3.2.6. Effect of Vps1 Mutations on endosomal recycling of SNARE reporter Snc1-GFP

Another pathway that Vps1 was shown to function in the trafficking of Snc1 from the late endosomes to the plasma membrane. Snc1 is a vesicle membrane receptor protein (v-SNARE) coded by *SNC1* gene, which is a homolog of vertebrate synaptic vesicle-associated membrane proteins (VAMPs) or synaptobrevins. (Gerst *et al.* 1992). It is involved in endocytosis and in the fusion of Golgi-derived secretory vesicles with the plasma membrane. Mutants in endosomal recycling fail to show clear plasma membrane staining of the reporter.

In this experiment, the yeast strain containing an integrated GFP-Snc1 (KAY1462) was transformed with plasmids containing one of each of the three Vps1 mutations (pKA798 – R298L, pKA797 – G397R and pKA796 – A447T) and the cells were visualised using fluorescent microscopy. Control plasmids were also used (pKA677 for Vps1 wild-type and pKA544 for *vpsIΔ*) The results from this experiment [figure3.7] have shown that in Vps1 wild type, the Snc1-GFP localizes to the plasma membrane with 59 % of budded cells showing plasma membrane staining in the bud, confirming that the receptor was recycled successfully. On the other hand, only 6 % of *vpsIΔ* budded cells showed plasma membrane staining in the bud, suggesting a defect at the endosome / plasma membrane trafficking route. R298L and A447T both showed 48 % of plasma membrane staining in the bud while G397R showed 33 %. This reduction in the percentage of plasma membrane staining in the bud in Vps1 mutants compared to the wild type suggested that the endosomal trafficking pathway could be to some extent defective / less efficient in these mutants, however the defect is less severe than that observed in the null.

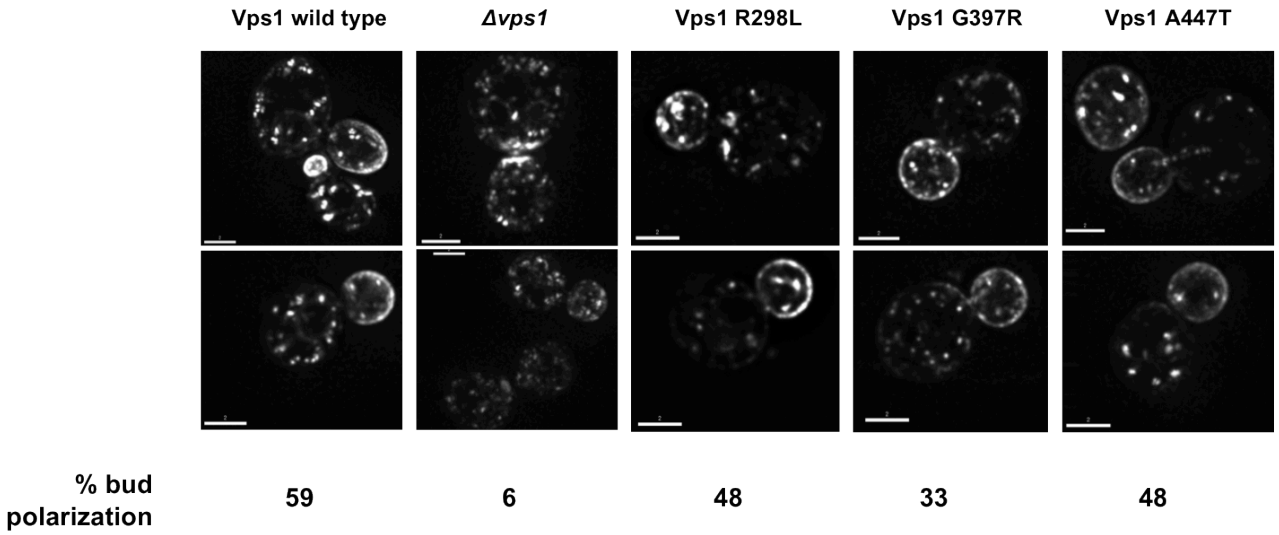

Figure 3.7. Effect of Vps1 mutations on the endosomal trafficking pathway. The Snc1-GFP receptor, which gets recycled from the endosomes to the plasma membrane was used to test for defects in this pathway. Cells with plasmids carrying different Vps1 mutations were examined using DeltaVision microscope and the percentage of bud polarization was counted. N = 50 cells from 2 independent experiments. An unpaired t-test was performed using Graphpad Prism 6 software which gave p values of 0.0046 for *vps1Δ*, 0.1588 for R298L, 0.0256 for G397R and 0.0670 for A447T. Scale Bar: 2 μm.

Surprisingly, the G397R appeared to have a phenotype distinct from the null, which was not the case in almost all of the previous experiments conducted in this project. Possible reasons for this are discussed later in this chapter.

3.2.7. Effect of Vps1 Mutations on Vacuolar Morphology

Vps1 was identified as a vacuolar protein sorting [Vater *et al.* 1992] and was shown to play a role in maintaining vacuolar morphology [Raymond *et al.* 1992, Peters *et al.* 2004]. To determine whether the Vps1 mutations affected the vacuolar morphology in yeast cells FM4-64 staining was used. FM4-64 is a lipophilic styryl dye that stains the vacuole membrane in yeast [Vida and Emr, 1995].

An overnight culture of *vps1Δ* yeast strain (KAY1095) carrying a Vps1 wild-type (pKA677) *vps1Δ (*pKA544), Vps1R298L (pKA798), Vps1G397R (pKA797) and Vps1A447T (pKA796) expression plasmids were re-inoculated in fresh media and treated with FM4-64 for 90 minutes (section 2.6.3). As expected, the FM4-64 staining of the wild-type cells showed the presence of two to five vacuoles all of which are similar in size [figure 3.8]. In contrast, in *vps1Δ* cells a large vacuole surrounded by many fragmented vacuoles could be seen which was typical of Class F vacuolar phenotype [Raymond et al, 1992).

Analysis of R298L and A447T revealed vacuolar morphology similar to that seen in the wild type suggesting that these two mutations do not affect the vacuolar morphology in cells or have major defects in trafficking to the vacuole. On the other hand, G397R was not only significantly different from the wild-type (p-value 0.0070) but it was also significantly different from *vps1Δ* (p-value 0.0082). It mainly showed a fragmented vacuolar phenotype.

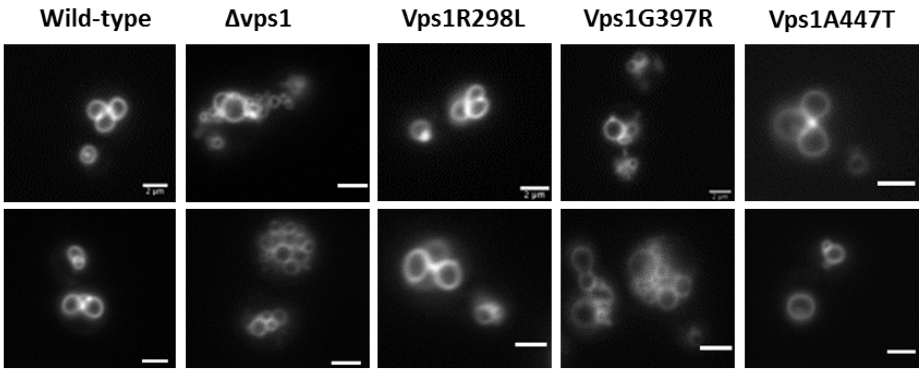

% of normal vacuolar phenotype	87	15	70	4	82

Fig.3.8. Effect of Vps1 mutations on the vacuole morphology. *vps1Δ* cells with plasmids carrying different Vps1 mutations were treated with FM4-64 for 90 minutes at 30 ^{0}C to assess the effect on vacuole morphology. Cells were placed on a glass slide and visualized using fluorescent microscopy at 100x magnification. N = 100 cells from two independent experiments. An unpaired t-test was performed using Graphpad Prism 6 software which gave p values of 0.0095 for *vps1Δ*, 0.2065 for R298L, 0.0070 for G397R and 0.5631 for A447T. Scale Bar: 2 μm.

3.2.8. Effect of Vps1 Mutations on actin cytoskeleton

In yeast there are three different organisations of actin present; actin patches, cables and rings [Aghamohammadzadeh and Ayscough 2009]. Of these, the cortical actin patches are known to be sites of endocytosis. Vps1 was shown to interact with Sla1, a component of the endocytic machinery that is involved in organizing cortical actin [Yu and Cai 2004]. To assess whether Vps1 mutations affect actin structures, rhodamine phalloidin staining was used. Yeast cells were fixed with formaldehyde and stained with rhodamine phalloidin as described in the materials and methods (section 2.6.4). The microscopy analysis was carried out by Iwona Smaczynska-de Rooij.

Analysis of the data [figure 3.9] shows that wild type cells have clear actin cables and 87 % of cells have polarized actin patches in the bud (patch polarization phenotype). Since actin patches are an indication of sites of endocytosis, it was expected for wild type cells to show patch polarization, as most endocytic events take place in the growing bud rather than the mother cell. In the *vps1Δ* only 63 % of cells showed patch polarization. With regards to the Vps1 mutations, none of them seemed to affect actin cables but rather had a relatively minor effect on actin patch polarization. The G397R cells most closely resembled the null phenotype with 65 % of cells showing patch polarization, while both R298L and A447T cells had an intermediate phenotype with 71 % and 77 % of cells showing the polarization phenotype.

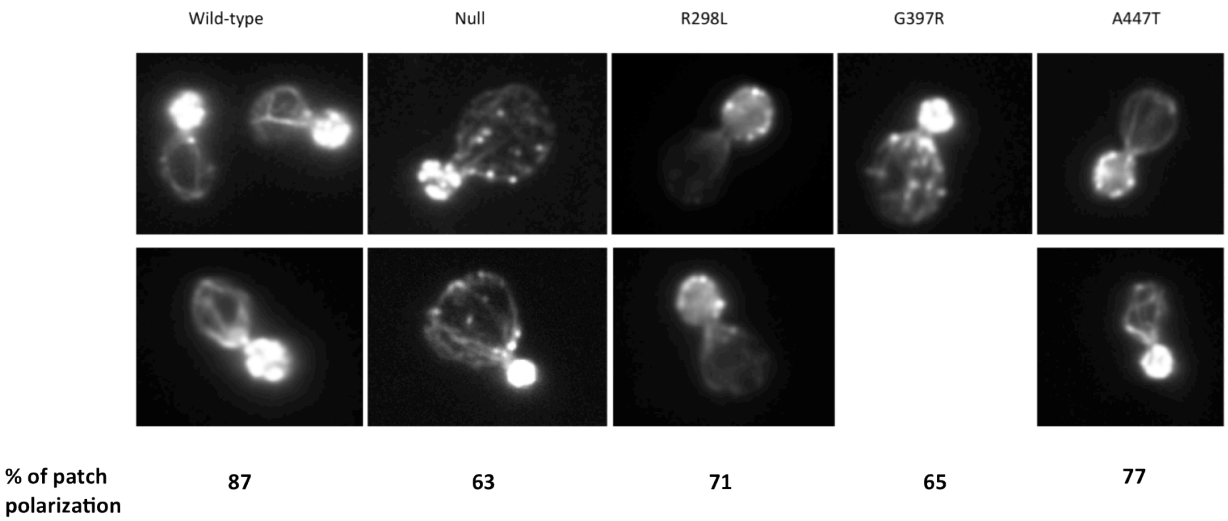

Fig.3.9. Effect of Vps1 mutations on actin cytoskeleton. Rhodamine phalloidin staining was used to determine F-actin organization in *vps1Δ* cells expressing plasmids with Vps1 mutations. Cells were examined using the DeltaVision microscope and the percentage of cells with actin patches polarized at the bud was calculated. N = 100 cells from 2 independent experiments. An unpaired t-test was performed using Graphpad Prism 6 software, which gave p values of 0.0299 for *vps1Δ*, 0.1111 for R298L, 0.0636 for G397R and 0.1425 for A447T. The microscopy work was carried out by Iwona Smaczynska-de Rooij.

3.2.9. Effect of Vps1 Mutations on Fluid Phase Endocytosis

Lucifer yellow (LY) is an aqueous fluorescent dye that was used as a marker to assess fluid phase endocytosis in *vps1Δ* cells carrying Vps1 mutations (Dulic et al 1991). *vps1Δ* yeast cells (KAY1095) carrying a Vps1 wild-type (pKA677) *vps1Δ (*pKA544), Vps1R298L (pKA798), Vps1G397R (pKA797) and Vps1A447T (pKA796) expression plasmids were treated with LY as stated in (section 2.6.2) and incubated at 30 ^{0}C for 15 min to assess early stage endocytosis and 90 min to assess later stages of endocytic trafficking. Cells were visualized using fluorescence microscopy, analysed by eye and placed into appropriate categories.

In wild-type cells at 15 min of incubation with LY dye, 17 % of cells showed predominantly vacuolar staining, which increased to 57 % after 90 min of staining. In contrast, the *vps1Δ* cells showed no vacuolar staining in the first 15 min of staining and after 90 min, 40 % of cells showed endosomal stain with some weaker vacuolar staining. This suggests a defect in the uptake and/or progress through the pathway. Although cells containing the R298L and A447T mutants did show vacuolar staining, this was lower than that observed in wild-type cells, with about 10 % vacuolar staining in R298L and 3 % in A447T after 15 min of staining. This increased to about 32 % in R298L and about 53 % in A447T after 90 min [figure 3.10]. Unlike the other two mutations, the G397R showed a phenotype that was very similar to the *vps1Δ* cells, where in the first 15 min no vacuolar staining was observed but after 90 min over 50 % of cells showed an endosome and vacuole staining [figure 3.10].

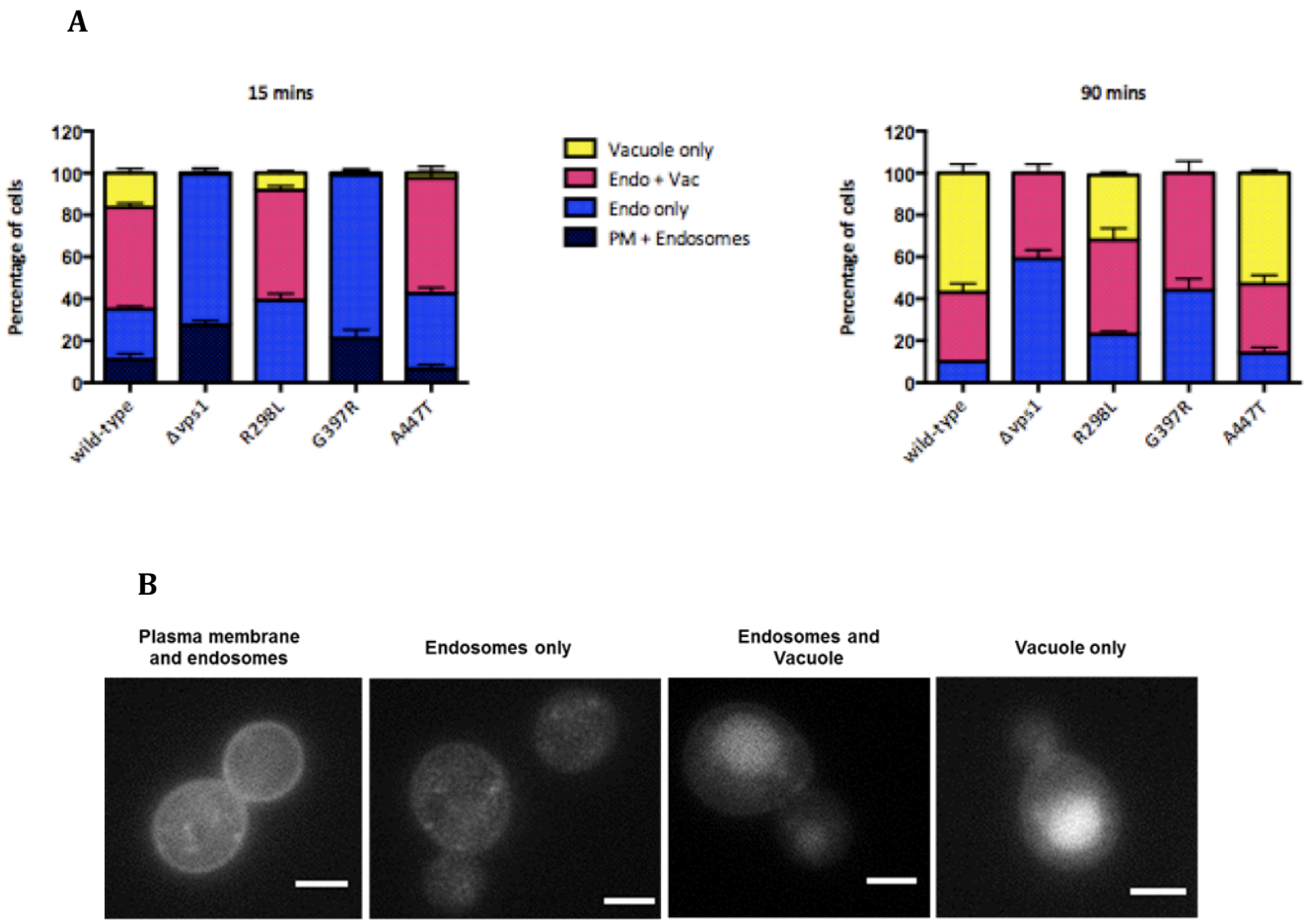

Fig.3.10. Effect of Vps1 mutations on fluid phase endocytosis. *vps1Δ* cells with plasmids carrying different Vps1 disease mutants were treated with Lucifer yellow to assess fluid phase endocytosis. Cells were visualized using fluorescent microscopy at 100x magnification. A) 15 and 90 minutes of staining with Lucifer yellow to asses the early and late stages of endocytosis. B) Examples of different categories of cell staining. N = 100 cells from two independent experiments. Scale Bar: 2 μm.

Although these results show that the R298L and A447T mutants can still perform fluid phase endocytosis, the rate of endocytosis and trafficking of the dye to the vacuole is reduced compared to the wild-type cells suggesting a defect in the process. On the other hand, the G397R mutant clearly resembles the null phenotype suggesting that the protein has lost its function in endocytic trafficking.

3.2.10. Effect of Vps1 mutations on the behaviour of endocytic reporter proteins

Results from the previous experiments have shown that both R298L and A447T have a similar phenotype to the wild-type in all of the tested trafficking roles except for fluid phase endocytosis, which in both cases (although to a greater extent in R298L) the LY uptake seemed to be reduced compared to the wild-type suggesting a delay in the rate of endocytosis in cells. On the other hand, the G397R mutant showed defects in all of its roles investigated including fluid phase endocytosis suggesting that the mutation resulted in a largely non-functional protein even though the protein was still expressed in yeast cells.

Although an obvious starting point would be analyzing the localization and behavior of Vps1-GFP patches, this was not done due to the known problems of GFP tagging in this protein. Previous work has shown that Vps1-GFP was very difficult to localize at the plasma membrane and bright fluorescence could be seen throughout the cells due to its function in other organelles [Peters *et al.* 2004]. Therefore, to gain a deeper insight into the effect of the mutations on endocytosis, three fluorescently tagged endocytic reporter proteins, which are involved at different stages of endocytosis were used. These were, Sla2-GFP, an adaptor protein linking actin filaments to the clathrin coat, Sac6-mRFP, an actin bundling protein

and Rvs167-GFP, a homolog of mammalian amphiphysin involved in vesicle scission.

In this experiment, each yeast strain carrying one of the reporter proteins, Sla2-GFP (KAY1459), Sac6-mRFP (KAY1368) and Rvs167-GFP (KAY1337) were transformed with plasmids carrying the Vps1 mutataion, (pKA798 – R298L, pKA797 – G397R and pKA796-A4447T) using the method described in section 2.3.2.1. Exponentially growing yeast cells carrying the reporter proteins and the Vps1 mutations were used, where 3 µl of cell culture was placed onto a glass slide and images and 1 sec time-lapse recordings were taken. Individual endocytic patches [figure 3.11.a] were analysed for their lifetime, intensity and movement pattern and data were plotted onto appropriate graphs.

3.2.10.1. Analysis of endocytic reporter protein lifetime

Analysis of endocytic reporter lifetime involved measuring the patch intensity from the point of its appearance on the plasma membrane until the disappearance of its fluorescence [fig.3.11.b]. This approach therefore measures a straightforward change in the lifetime of the reporter protein caused by the mutations. Sla2 lifetime in wild-type patches was shown to be about 22 sec whereas the lifetime of *vps1Δ* patches was about 37 sec [fig.3.11.b]. The results obtained from this analysis revealed that all of the three mutations caused a significant increase in the lifetime of Sla2 ($p < 0.0001$) compared to the wild type with the R298L mutation resulting in the highest increase with a lifetime of 48 sec. The A447T mutant had a lifetime of 40 sec while G397R had a lifetime of 34 sec, which was similar to that seen in the *vps1Δ* strain.

In the case of Sac6, the lifetime of the reporter protein was about 15 sec in wild-type patches and 11 sec in *vps1Δ.* R298L and G397R mutations caused a non significant reduction in the lifetime of Sac6 with a lifetime of 14 sec in R298L and 13 sec in G397R, however in A447T, Sac6 had a lifetime of 12 sec, which was slight but significantly different from that in the wild type ($p = 0.0185$).

With the amphiphysin Rvs167, wild type cells had a lifetime of 7.9 sec while *vps1Δ* cells had a lifetime of 6.4 sec. Interestingly, the mutations did not all have the same effect as one another on the lifetime of Rvs167. The lifetime was similar to that in the wild-type cells in the R298L mutant cells, about 8 sec, suggesting that this mutation did not affect the stability of Rvs167 at the plasma membrane, whereas the other mutants showed a reduction in the lifetime of Rvs167 with a lifetime of 7 sec for the G397R ($p = 0.0318$) and 6.5 for the A447T mutants ($p = 0.0020$).

The fact that the major effect of the endocytic mutations was on the lifetime of Sla2 with a significant increase in the reporter protein's lifetime, suggests a defect after the recruitment of Sla2 to the endocytic site, possibly at the onset of invagination. A447T showed a significant change in all of the reporter protein lifetime, initially an increase in Sla2 followed by a decrease in the lifetime of Sac6 and Rvs167 suggesting that the A447T mutation mainly affects endocytosis but not the other roles of Vps1.

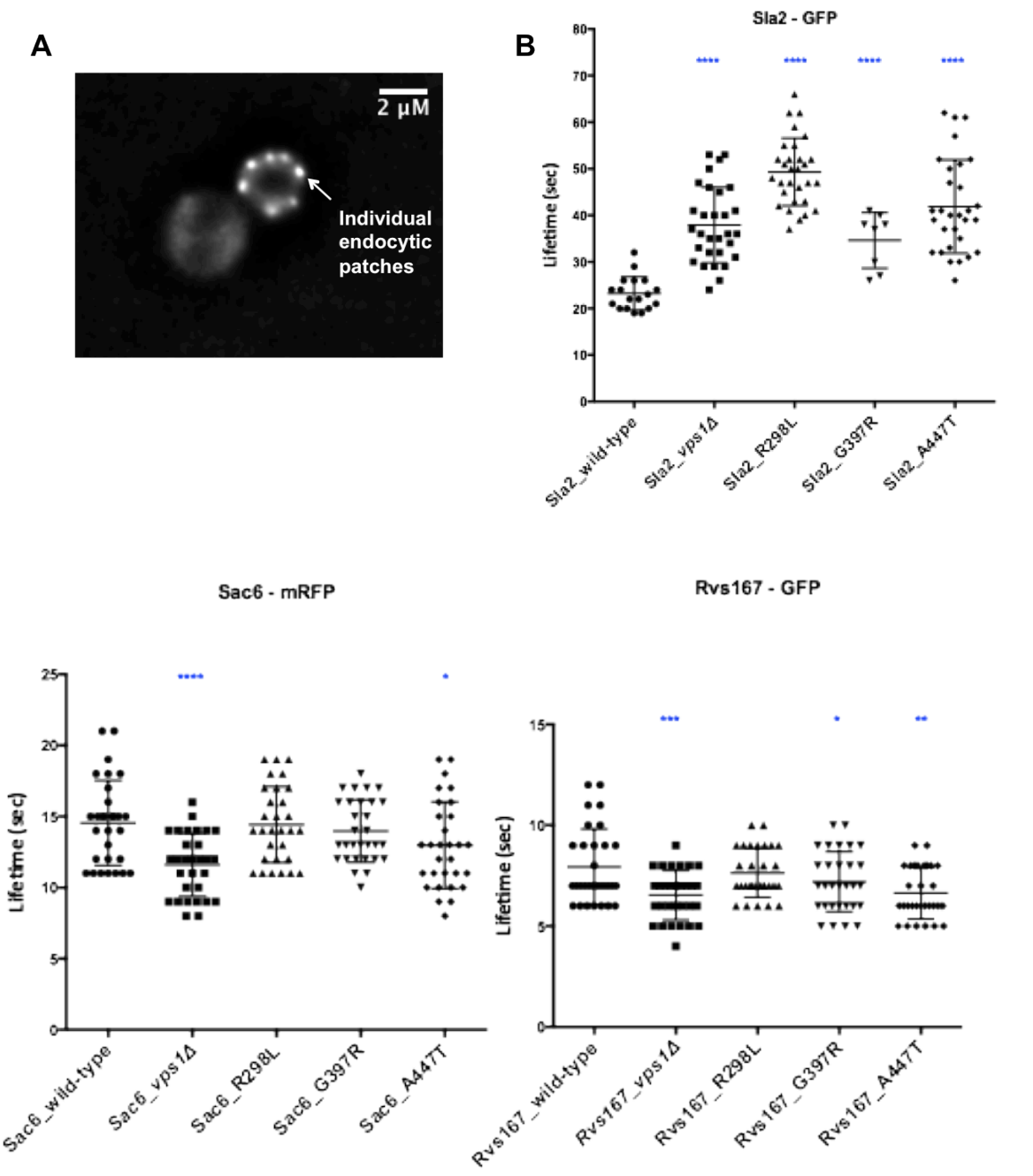

Fig.3.11. Effect of Vps1 mutations on endocytic reporter proteins. Cells carrying the reporter proteins and the Vps1 mutations were grown to exponential phase and images and 1 sec time-lapse video were taken and individual endocytic patches were analysed. a) An example of endocytic patches that were analysed in this experiment. b) The lifetime of the three endocytic reporter proteins, Sla2, Sac6 and Rvs167 in the presence of the Vps1 mutations. Error bars represent mean with SD. Asterisks indicate level of statistical significance of differences compared to the wild-type control from an unpaired t- test.

3.2.10.2. Analysis of Sac6 Patch intensity

Because the lifetime of reporter proteins only gave an overview of the time spent at the membrane with no reference to the level of protein recruited at the endocytic sites, further analysis was undertaken to determine any changes in the reporter protein levels caused by the Vps1 mutations. Since the effect of the three Vps1 mutations on Sla2 lifetime was already clear, this analysis focused on Sac6 and Rvs167.

An intensity profile was generated for individual Sac6 and Rvs167 patches as a reflection of the level of these reporter proteins at the endocytic sites with the aim of highlighting any significant changes in the levels of these proteins in the presence of the Vps1 mutations. The patch intensity reached at 7 sec for Sac6 [figure 3.12.a] and 4 sec for Rvs167 [figure 3.12.b] were plotted on a graph.

Although the data showed a wide distribution of intensity values for each of the strains, the results from the Sac6 graph [figure 3.12.a] showed that at 7 sec 60 % of patches had a pixel value higher than 200 in cells expressing wild type Vps1 compared to the null where 40 % of the patches had a pixel value higher than 200. This indicates that the absence of Vps1 affects the accumulation of Sac6 at the endocytic patches at the time point tested.

Statistical analysis indicated that there was no significant difference in the pixel values between the wild-type and the three Vps1 mutants after performing unpaired t-tests, suggesting that these mutations did not affect the level of Sac6 recruitment to the endocytic sites at the time tested.

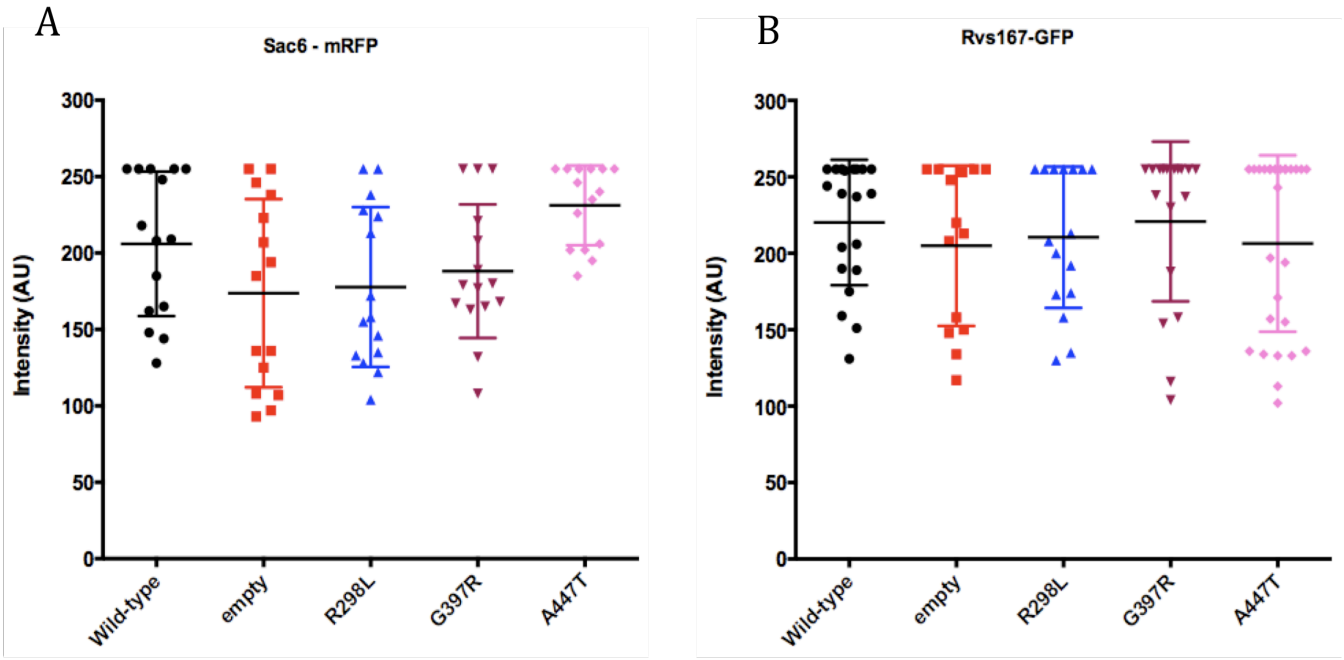

Figure 3.12. Patch intensity of Sac6 and Rvs167 in Vps1 mutants. A) The intensity value reached by individual endocytic patches after 7 sec of Sac6 assembly at endocytic sites in each of the wild-type, *vps1Δ*, R298L, G397R and A447T mutants. Patch intensities were measured using Image J software and plotted using GraphPad Prism 6. N = 15 patches from 5 cells for each sample. Error Bars are mean with SD.

B) The intensity value reached by individual endocytic patches 4 sec afterRvs167 lifetime in each of the wild-type, *vps1Δ*, R298L, G397R and A447T mutants. Patch intensities were measured using Image J software and plotted using GraphPad Prism 6. N = >15 individual endocytic patches from 5 cells for each sample. Error Bars are mean with SD.

However, it was clear that the majority, 87 %, of patches in the A447T mutant reached a pixel value of >200 at the 7 sec time point [figure 3.12.a]. This was higher than that observed in the wild-type patches suggesting that this level of Sac6 was recruited at endocytic sites faster in this mutant compared to the wild-type. In R298L, 40 % of patches reached a pixel value of > 200, while in G397R 33 % reached a pixel value of > 200 which was lower than that observed in the null strain.

While there seems to be clear variations in the level of Sac6 accumulation by the Vps1 mutants compared to wild type, the majority of Rvs167 patches in the wild-type and the null reached the maximum pixel value after 4 sec. This was also true for the three Vps1 mutations where majority of patches had also reached the maximum pixel value after 4 seconds suggesting that these mutations did not affect the level of Rvs167 recruited to the endocytic sites [figure 3.12.b].

3.2.10.3. Analysis of Sac6 patch invagination

The invagination behaviour of Sac6-RFP at the endocytic sites was analysed by tracking the movement of individual patches [fig.3.13]. This analysis revealed that 85 % of wild type cells showed a normal invagination event compared to *vps1Δ* in which the patches would move on the plasma membrane without invaginating inwards. This analysis also showed that Sac6 patches in R298L and G397R were unable to successfully invaginate with only 29 % and 27 % of the patches showing successful invagination respectively. Invagination was higher in the A447T mutant in which 76 % of the endocytic patches were able to successfully invaginate.

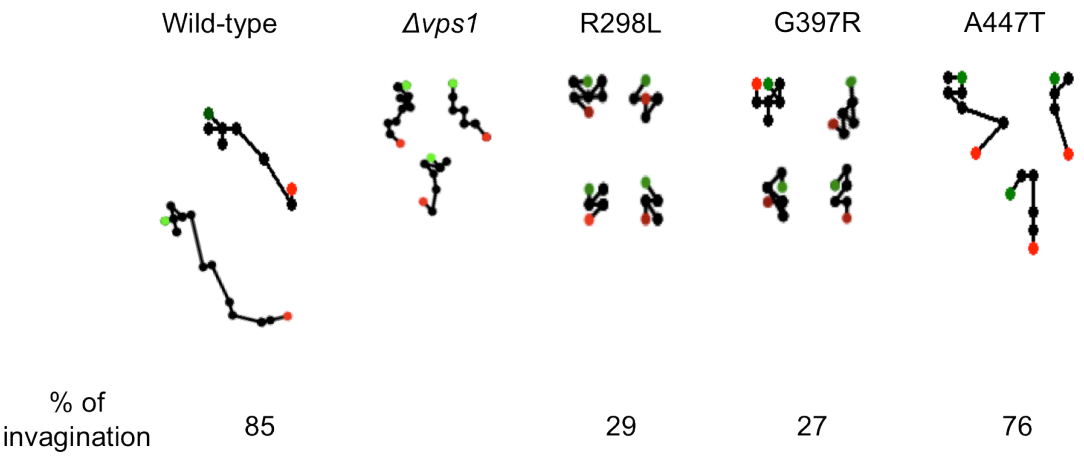

Figure 3.13. Patch tracking of Sac6 endocytic patches. Each endocytic patch was tracked for movement starting with the appearance and ending with the disappearance of its fluorescence. The percentage of invagination events observed in patches was also calculated. Green = start, Red = end. N = 30 cells from two independent experiments. Image J software was used for this analysis.

The data from reporter protein analysis showed that although the lifetime and the patch intensities of Sac6 in the R298L mutant were not greatly aberrant, patch tracking showed that patches in this mutant had a clear defect in invagination. Defective invagination was also found for cells expressing the G397R mutant however this was less surprising considering that this mutant had been shown to be non-functional in most of the functions tested.

3.3. *In-vitro* analysis of Vps1 mutants

Studying the role of Vps1 in living yeast cells and examining the effect of the mutations in the physiological environment has been an important tool in increasing our understanding of the functions in which it is involved. However, yeast cells are complex containing thousands of proteins which makes it challenging to study specific mechanistic defects in the biochemical properties of the protein of interest. *In vitro* studies allow a complementary approach to investigate the proteins of interest and was used here for studying Vps1 and the effect of the three mutations addressed in this project.

3.3.1. Expression and purification of His-tagged Vps1 proteins

The first step towards analyzing the effect of the mutations on the biochemical properties of Vps1 was to purify the proteins from the cells. This was achieved by expressing Vps1 carrying the disease mutations in a His-tagged plasmid construct and purifying the proteins using a His-Trap HP column via nickel binding.

Vps1 disease mutations were introduced into a previously constructed N-terminus His-tagged Vps1 wild-type plasmid construct (pKA 850) via site-directed mutagenesis and this was confirmed by sequencing to ensure that only the

mutations of interest were present (work performed by Iwona Smaczynska-de Rooji). His-tagged Vps1 R298L (pKA 819), G397R (pKA 820) and A447T (pKA 821) plasmid constructs were transformed into *E.coli* chemically competent cells (Section 2.2.2.) for protein expression, and cell cultures were grown in 2 L of 2xYT media + ampicillin. Protein expression was induced by IPTG and cells were harvested by centrifugation (section 2.5.1).

The proteins were purified and eluted into 1 ml fractions using high salt buffer containing 500 mM of imidazole. 10 μl of the first two elution fractions were run on an SDS gel. As it can be seen from [figure 3.14] the three Vps1 mutations were successfully expressed in bacterial cells at similar levels to the wild type protein. The protein concentration was measured using a BSA standard curve (see section 2.5.2) where the concentration of the proteins ranged between 3 to 10 μM.

3.3.2. Effect of Vps1 mutations on Self-assembly

It was reported that dynamins are able to oligomerize into higher ordered structures, which is crucial for performing their cellular functions. Recent work from the Ayscough lab (Palmer *et al.* 2015) has shown that Vps1 forms ring structures which are very similar to those formed by dynamins but slightly smaller in size, 32 nm in diameter compared to 43 nm [Chappie *et al.* 2011, Hinshaw and Schmid, 1995].

To determine whether any of the three mutations affected the oligomerization property in Vps1, a self-assembly experiment was performed, where a non-hydrolysable form of GTP known as GTPγs was used. GTPγs binds to Vps1 in a similar manner to GTP however since it non-hydrolysable, it locks the protein in an

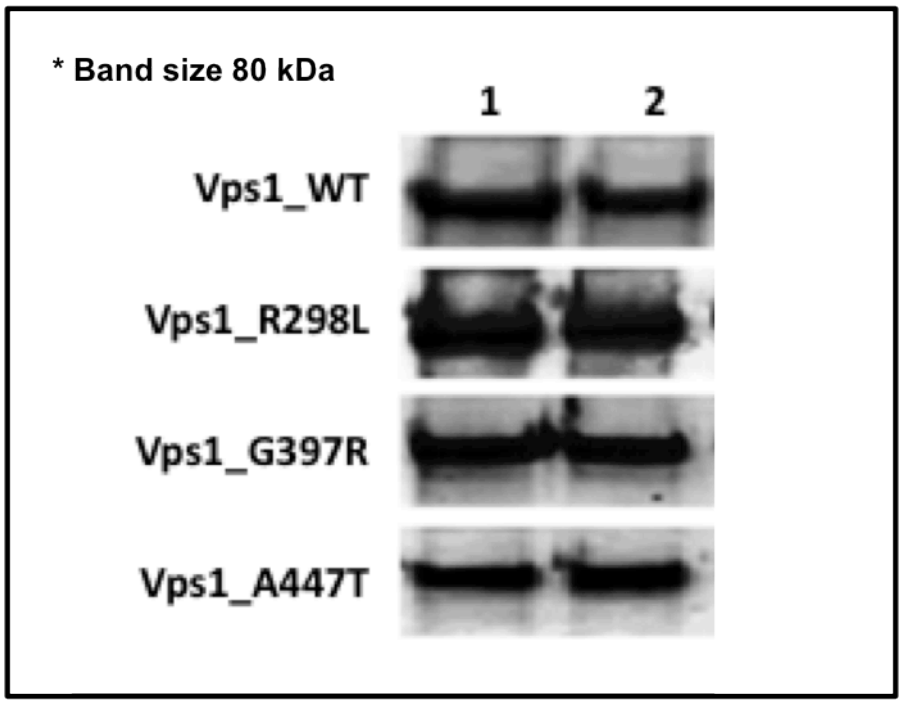

Fig.3.14. Purification of His-tagged Vps1 proteins. Vps1 wild-type, R298L, G397R and A447T proteins purified using the His-trap column and eluted using high salt buffer into 1 ml fractions. Lane 1 and 2 represent the first two elution samples from the purification column. Samples were run on an SDS PAGE and stained with Coomassie.

oligomerized form and so in a pelleting assay, all of the protein oligomers would be expected to pellet upon centrifugation at high speed. In the case of a defect in oligomerization caused by any of the three Vps1 mutations, a reduction in pelleting would be expected.

The experiment was performed as described in the materials and methods (section 2.5.5) where, following protein purification, 10 μM of Vps1 wild-type, R298L, G397R and A447T proteins were spun down at high speed and the supernatant and pellet were carefully separated before they were run on a SDS gel.

Although much of the wild-type protein had pelleted even in the absence of GTPγs [figure 3.15] the presence of GTPγs increased the proportion of protein in the pellet confirming that Vps1 wild type was able to oligomerize. For both R298L and G397R proteins the results did not show an increase in the proportion of protein in the pellet in the presence of GTPγs. This inability to oligomerize could explain why the G397R appeared to be non-functional in almost all of its *in vivo* roles showing a phenotype similar to that of the null. However this was not the case for R298L as previous data in this project showed that it was a functional protein. Electron microscopy (EM) examination of Vps1 wild-type and R298L and A447T has shown an increased level of protein aggregation, which explains the pelleting of the proteins even in the absence of GTPγs. Therefore, due to the aggregative nature of the R298L protein, it was difficult to make clear a conclusion on whether the oligomerization property in this mutant was defective or not and a different approach, possibly further EM examination would be a more appropriate approach to use to make definitive conclusions.

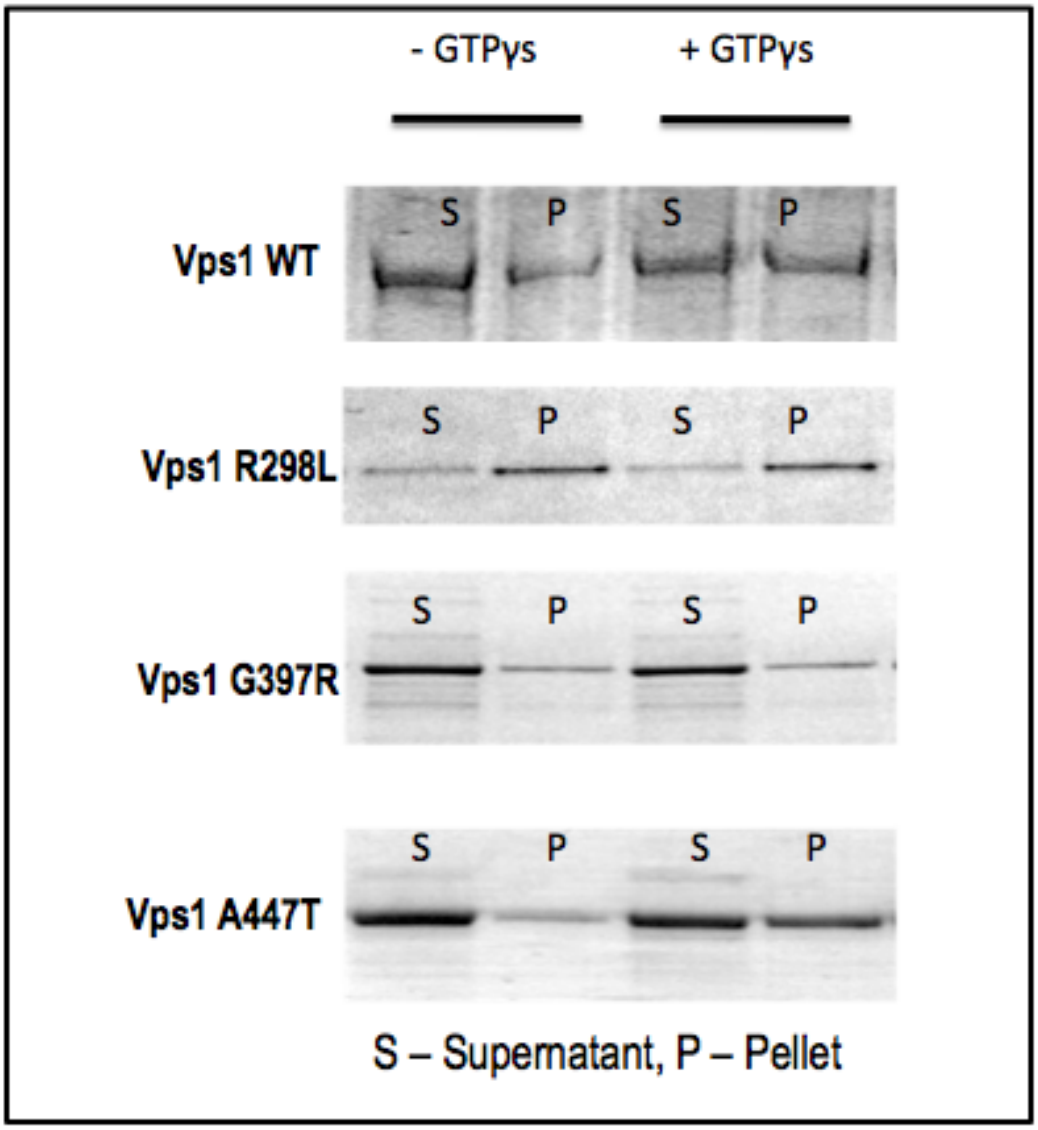

Fig.3.15. Effect of Vps1 mutations on oligomerization. Vps1 wild-type, R298L, G397R and A447T proteins + / - GTPγs were spun down and the pellet and supernatant were separated by SDS PAGE gel and stained with Coomassie. Band size is 80 kDa.

On the other hand, a clear band shift was seen in the A447T protein where a higher proportion of the protein was in the pellet in the presence of GTPγs suggesting that this mutation was not affecting the oligomerization property in Vps1.

3.3.3. Effect of Vps1 mutations on lipid-binding

Another well-documented property of dynamins is their interaction with lipids, which is though to take place via the PH domain. In the case of Vps1 no PH domain is present but instead a region known as Insert B (InsB), which was proposed to play a similar role and despite the absence of the PH domain, Vps1 was shown to bind and tubulate liposomes [Smaczynska-de Rooij et al. 2010]. To test whether any of the three mutations have any effect on the lipid binding property of Vps1, a co-sedimentation assay was performed where 20 μl liposomes and 5 μM Vps1 protein were incubated together and the procedure was performed exactly as described in the materials and methods (section 2.5.6). If Vps1 mutants do not affect this property of the protein, then a higher proportion of the Vps1 protein would be expected to pellet in the presence of liposomes compared to their absence.

As expected, a higher proportion of wild-type protein pelleted down in the presence of liposomes confirming that it was able to bind lipids [figure 3.16]. Similar to the self-assembly assay, the results for both R298L and G397R proteins did not show an increase in the proportion of protein in the pellet in the presence of liposomes. Again this could explain why G397R appeared to be defective in almost all of the *in vivo* experiments performed, unlike the R298L where previous data in this project showed that it was a functional protein. This again made it difficult to make a clear conclusion on whether the lipid binding property in R298L was defective or not.

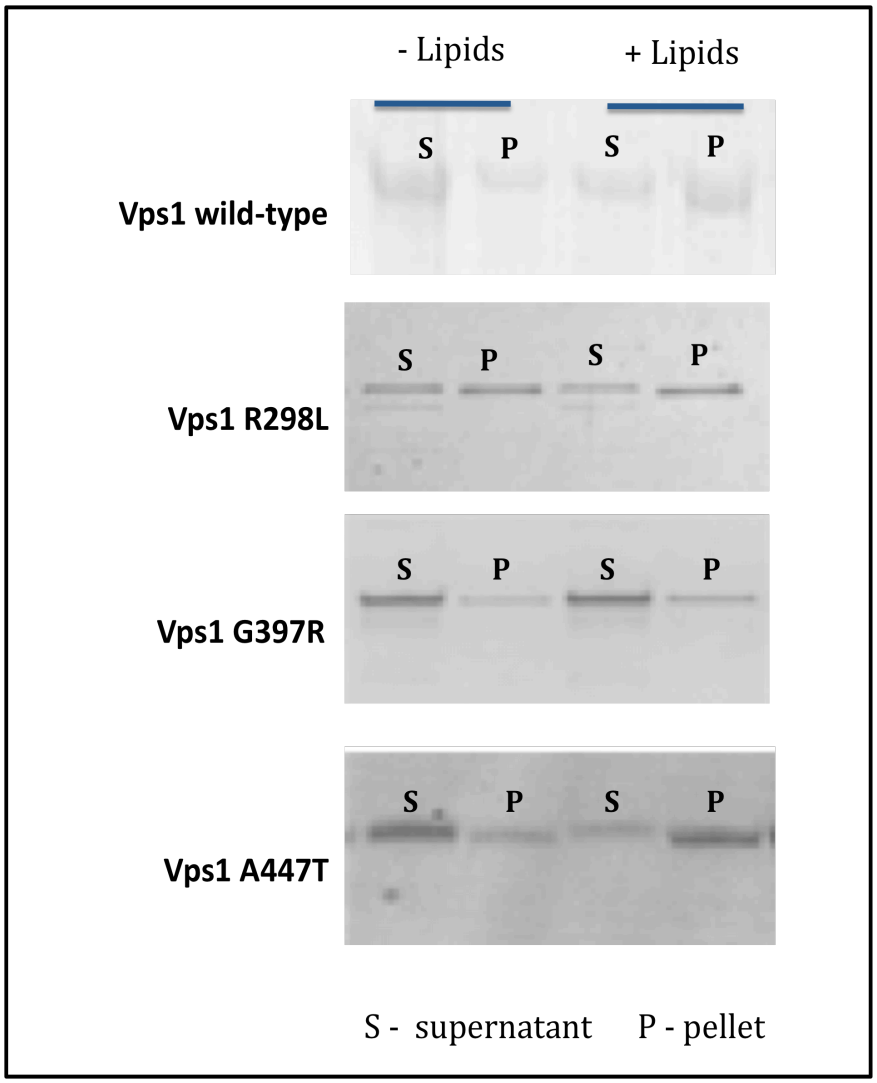

Fig. 3.16. Affect of Vps1 endocytic mutations on binding lipid. Vps1 wild-type, R298L, G397R and A447T proteins + / - liposomes were spun down and the pellet and supernatant were separated by SDS PAGE and stained with Coomassie.Band size is 80 kDa.

On the other hand, a clear band shift could be seen in the A447T protein where the presence of liposomes increased the proportion of protein in the pellet, suggesting that this mutation was not affecting the lipid binding property in Vps1.

Since a direct co-sedimentation assay had its limitation due to the oligomerizing nature of Vps1 proteins, a different approach was used to investigate interaction with lipids. This involved using PIP strips, which are hydrophobic membranes that have been spotted with 100 pmol of 15 different phospholipids (Echelon). The table on the next page (table 2) summarizes the function of some of these phospholipids.

The PIP strip membranes were incubated with Vps1 wild type, R298L, G397R and A447T proteins and the membranes were analysed using western blotting (section 2.5.7). The results [figure 3.17] showed that wild type Vps1 interacted only with the mono-phosphoinositides and phosphatidylethanolamine (PE). In the case of the endocytic mutants, R298L was shown to bind not only to mono-phosphoinositides but also to di- and tri-phosphoinositides. This confirmed the lipid binding ability of the R298L mutant, and also highlighted a marked change in the lipid-binding specificity caused by this mutation. The results have also shown that lipid binding was greatly reduced in G397R mutant with only a very weak interaction evident with PtdIns(3)P. A447T was more similar to the wild type but showed a weaker interaction with PtdIns(5)P.

Phospholipids	Role	Reference
PtdIns(3)P	enriched in the early endosomes and is found in the plasma membrane.	Sbrissa et al. 1996
PtdIns(4)P	important in regulating membrane trafficking at the exit of the Golgi complex. It is also a precursor to PtdIns(4,5)P2.	Godi et al. 2004
PtdIns(5)P	a rare lipid found in the nucleus and is phosphorylated to PtdIns(4,5)P2.	Barlow et al. 2010
PE	found in cell plasma membrane.	Wellner et al. 2012
PtdIns(3,4)P2	generated at the plasma membrane activating a number of cell signalling pathways and playing a role in clathrin-mediated endocytosis.	Posor et al. 2013
PtdIns(3,5)P2	required for retrograde membrane trafficking from lysosomal and late endosomal compartments to the Golgi. Its dysregulation has been linked to several human neuropathies including Charcot-Marie-Tooth disorder.	Ikonomov et al. 2002
PtdIns(4,5)P2	regulates clathrin-mediated endocytosis and was suggested to be required for endocytic membrane invagination.	Czech MP, 2000, Sun and Drubin, 2012
PtdIns(3,4,5)P3	found at the plasma membrane where it controls processes such as phagocytosis, pinocytosis, exocytosis, and cytoskeletal organization and it was shown to regulate endosome fusion.	Czech MP, 2000, Lawe et al., 2000

Table.2. Summary of the function of some of the phospholipids from the PIP strips.

A

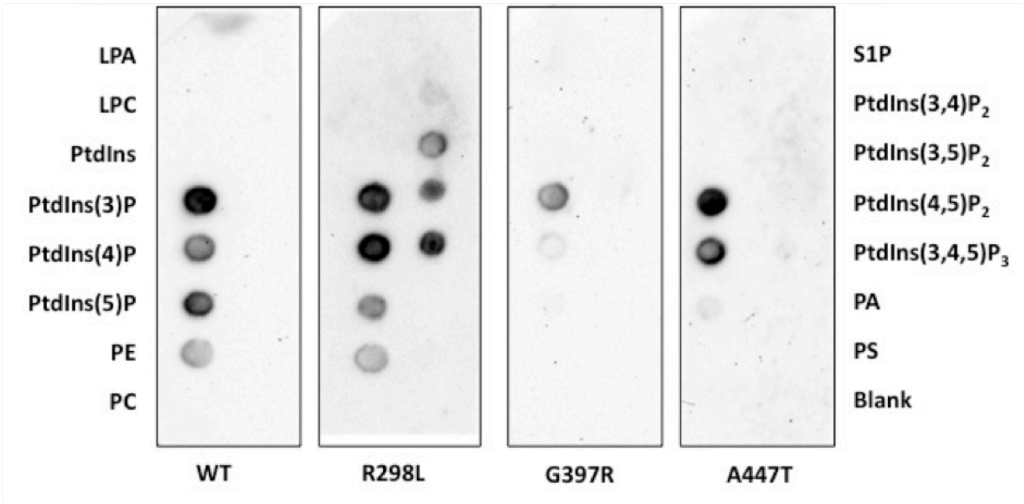

B

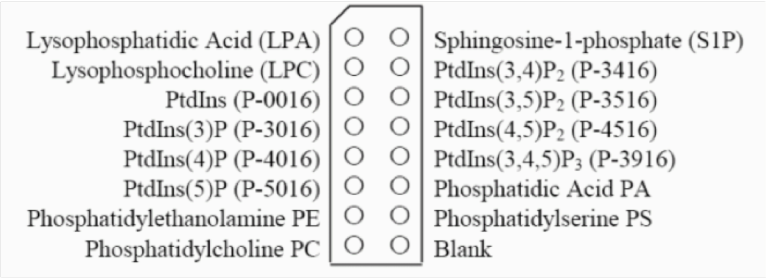

Fig.3.17. Lipid Binding analysis of Vps1 mutants using PIP strips. A) PIP strip membranes incubated with Vps1 wild type, R298L, G397R and A447T proteins. The membranes were blotted and probed with anti-His antibody. B) The identity of the 15 lipids spotted on the PIP strip membrane. Image taken from Echelon website.

Since these results have shown an altered binding specificity of Vps1 R298L toward phosphoinositides compared to the wild type protein, a further investigation into the degree of binding of the R298L mutant towards those phosphoinositides was undertaken using a more sensitive membrane based assay - the PIP arrays. These arrays are hydrophobic membranes that have been spotted with a concentration gradient of eight phosphoinositides. The procedure was performed as described in materials and methods [section 2.5.8] and the membranes were analysed using western blotting. The results from the PIP arrays [figure 3.18] showed that the wild type protein mainly interacted with the mono-phosphoinositides and this interaction increased as the concentration of the phosphoinositides increased. A weak interaction with PI(4,5)P2 was also seen. Supporting the data from the PIP strip, R298L interacted with all of the phosphoinositides on the membrane except for PI.

With most of the phosphoinositides, the interaction increased gradually as the concentration of the phosphoinositides increased, however, in the case of PI(3,5)P2, an interaction could only be seen at concentrations higher than 25 pmol suggesting that the affinity for this phosphoinositides was lower.

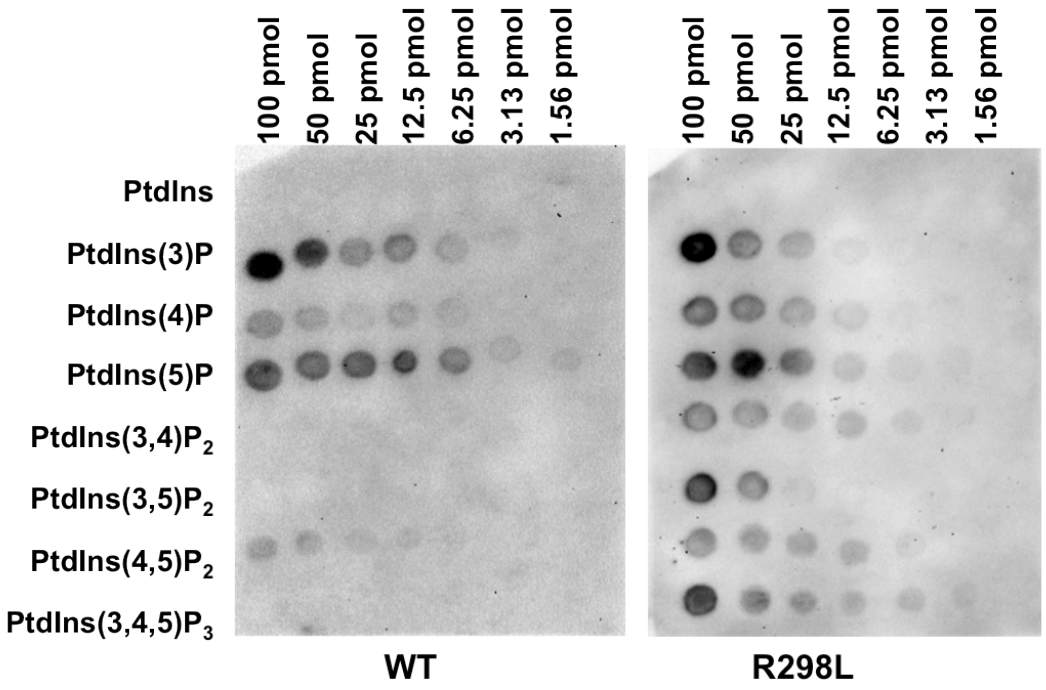

Fig.3.18. PIP array analysis of wild type Vps1 and R298L. Purified Vps1 wild type and Vps1 R298L proteins were incubated with PIP array membranes to check for concentration dependent interaction. The membranes were blotted and probed with anti-His antibody.

3.3.4. Vps1 and actin interaction using Electron Microscopy

Previously in this project the A447T mutant was shown to have a phenotype similar to the wild type in every test performed. However when tested for the level of Sac6 at the endocytic patches (section 3.2.10.2), the majority of A447T patches had high levels of Sac6 at the early stage of endocytosis. Since Sac6 is an actin bundling protein and recent studies have shown that Vps1 can directly interact with actin [Palmer *et al.* 2015], it was decided to investigate whether the A447T mutant affected the interaction with actin. The most direct way of investigating this would have been by performing co-sedimentation assays, however this experiment appeared to be very challenging with the oligomerizing nature of the protein and although initial attempts were undertaken, no consistent results were obtained. Therefore, in order to answer this question, A447T and F-actin were incubated and examined using electron microscopy. The procedure was performed as described in the materials and methods (section 2.7.2) where 1 μM Vps1 wild type /A447T was added to 1.5 μM F-actin. For controls, 1.5 μM F-actin only and 1 μM Vps1 wild type /A447T protein only were used. 5 μl of a 1:10 dilution of each mix was adsorbed onto carbon coated grids and were negatively stained using uranyl formate. The grids were examined using Gatan MultiScan 794 charge-coupled device (CCD) camera on Philips CM100 electron microscope.

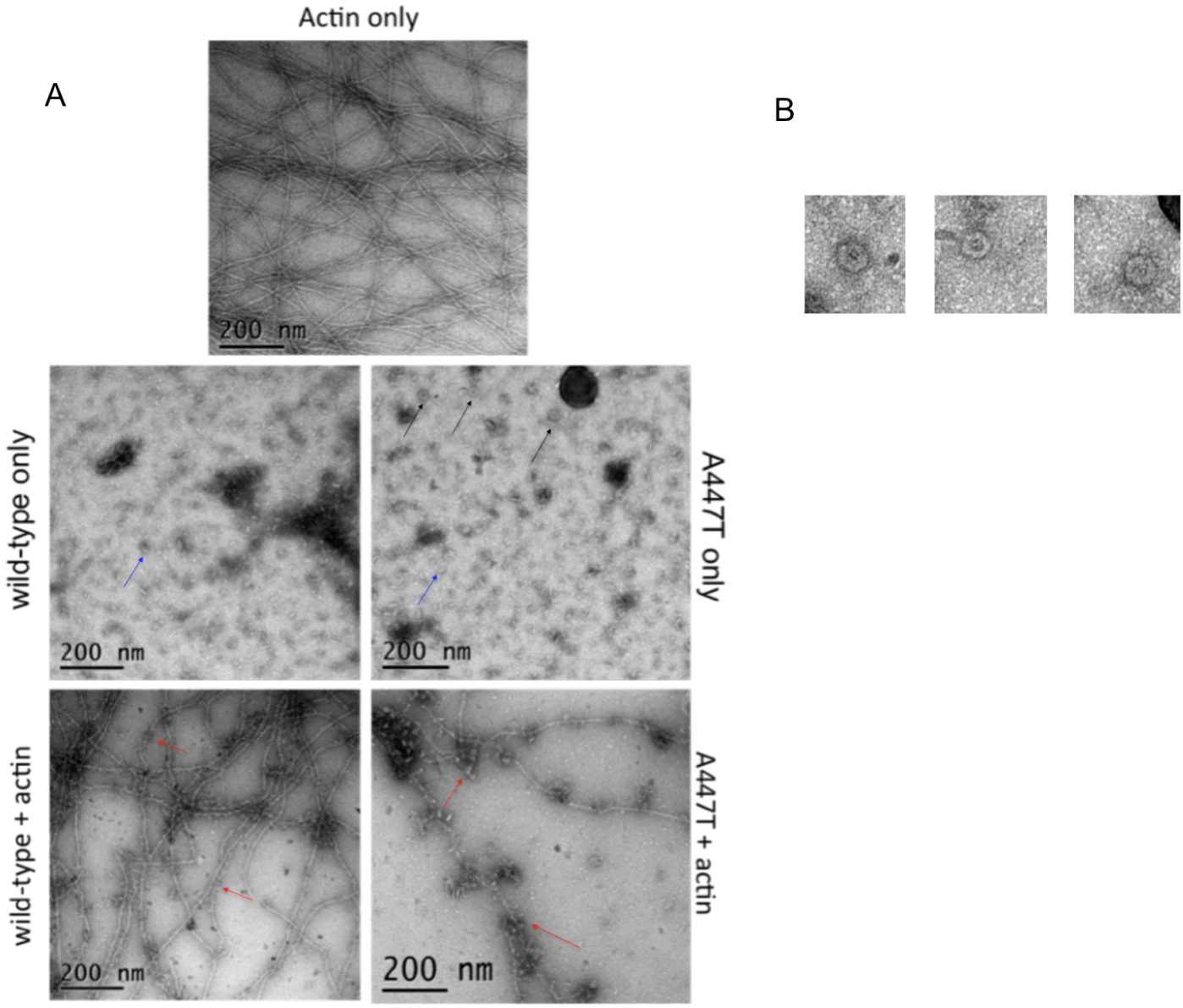

Fig.3.19. EM analysis of Vps1 and actin. Purified Vps1 wild type and A447T were incubated with F-actin and visualized by EM. A) EM images showing Vps1 wild-type and A447T alone or following incubation with F-actin. Blue arrows indicate rod-like shape of Vps1, Black arrows indicate ring structures and red arrows indicate spike-like structures. B) Closer images of ring structures formed by Vps1 A447T mutant proteins.

The EM images [Figure 3.19.a] showed that in the absence of actin, Vps1 wild-type protein formed rod-like shaped structures, with an average length of 8.2 nm. Similar to the wild-type protein, the A447T mutant protein also formed rod-like shaped structures in the absence of actin with an average length of 7.6 nm. In addition, the A447T protein also formed ring-like structures [figure 3.19.b], which were not evident in these conditions for the wild-type protein. These ring structures were very similar to those reported in a recent study by Palmer *et al.* 2015, and had an average diameter of 27.2 nm compared to 32 nm for Vps1 wild-type as reported in the mentioned study.

In the presence of actin however, the wild type Vps1 formed spike-like structures all along the actin filament. The A447T mutant was also able to form similar structures, however these appeared to be larger in size and less frequent. To confirm this observation, the number of spikes formed by both wild-type and A447T proteins per 150 nm length of actin filament was quantified and the results [figure 3.20.a] have shown that the average number of spikes per 150 nm of actin filament in the wild type was about 5 spikes compared to about 2 spikes in the A447T mutant.

The effect of actin on the oligomerization of A447T was further investigated by measuring the length of oligomers (spike-like structures) formed by the wild-type and A447T proteins in the absence of actin, in actin background and on actin filaments [figure 3.20.b]. The results revealed that in the presence of actin the average length of the wild-type oligomers increased from 8.2 nm to 15.5 n.

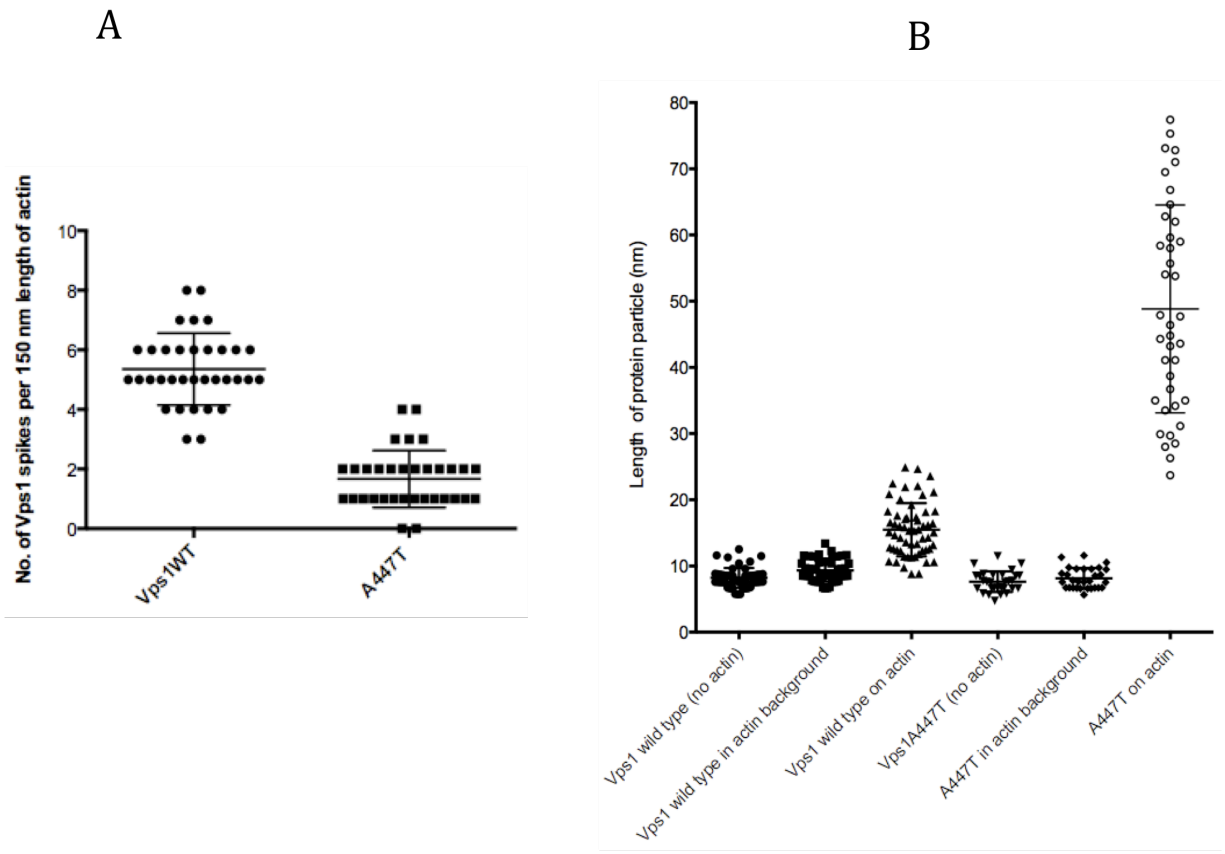

Fig.3.20. Analysis of Vps1 A447T spikes. A) Quantification of the number of Vps1 wild-type and A447T spikes per 150 nm length of actin filament. Error bars are mean with SD. B) Quantification of the effect of actin on Vps1 oligomerization. The length of oligomers formed by the wild-type and A447T proteins were measured in the absence of actin, in actin background and on actin filaments. Error bars are mean with SD.

This was even more dramatic in the A447T mutant where the average length of oligomers increased from 7.6 nm to 48.8 nm suggesting that the A447T mutation is enhancing the protein oligomerization in the presence of actin.

3.4. Discussion

In this part of the study three Vps1 mutations were generated to mimic the equivalent dynamin mutations that cause disease in mammals. The effect of each mutation was analysed in several *in vivo* assays. In addition, the mutant proteins were expressed recombinantly and purified. The effect of the mutations on protein behaviour was also studied biochemically. Importantly all of the three mutants were expressed in yeast cells at levels similar to that in the wild type indicating that none of the mutations caused a major disruption to protein folding. Given that all mutated residues project from the tertiary protein structure (judged by comparison of Vps1 with the Dynamin-1 crystal structure) mutations would not have been predicted to cause a large disruption of protein structure and, as surface residues, would be more likely to affect protein-protein interactions.

The various assays undertaken have indicated that different functions are affected in each of the mutants. Table 3 provides a summary of the Vps1 disease mutant phenotypes. The mutation that caused the greatest effect to function was the G397R mutation. This mutation would introduce a large basic residue in place of a small residue that often confers flexibility to regions of protein. Both the charge and reduced flexibility might be predicted to have a marked change on function. The region in which this mutation is made is the stalk region. This part of dynamin proteins is known to be important in oligomerization. It was therefore not

completely surprising that this mutation had a negative effect on oligomerization *in vitro*. Interestingly the mutation also caused a dramatic reduction in lipid binding. The majority of assays conducted *in vivo* indicated that cells expressing this mutant had a phenotype similar to the null strain therefore indicating the importance of oligomerization and lipid binding in function. Interestingly however the presence of the vps1 G397R protein seemed to confer greater temperature sensitivity and a slower growth rate on cells. This might suggest that there is some level of functionality in the protein. For example, it might still maintain certain protein interactions with other binding partners. In support of this partial function the G397R mutant appeared to have a phenotype distinct from the Vps1 deletion strain for the Snc1 trafficking assay. In the deletion strain there is an accumulation of small vesicles, while in this mutant, material is also observed at the plasma membrane. This might indicate that the G397R protein is still able to interact with a protein at the endocytic site and that this, possibly unregulated interaction acts to inhibit Snc1 recycling from the plasma membrane.

The A447T mutation had a less dramatic effect on the overall function of Vps1. Although neither the normal nor the mutant residues have a charge, threonine is a slightly larger residue with an additional methyl-group and also it has a hybroxyl group which can participate in hydrogen bond interaction. These may therefore result in steric clashes or inappropriate hydrogen bonding, which may disturb the protein conformation. This mutation also lies in the stalk region, however unlike the G397R mutation, it did not affect the oligomerization of the protein neither did it affect the lipid binding. The majority of *in vivo* assays performed revealed a phenotype similar to the wild-type except for endocytosis where the mutation

caused a significant affect on the lifetime of all three reporter proteins tested. Furthermore, the mutation also seemed to enhance the recruitment of Sac6 at endocytic sites suggesting that it may have an essential role during early stages of endocytosis, which was unexpected, as Vps1, like other dynamins is considered to function during the late stages of endocytosis, specifically the scission stage.

When tested for the affect of actin on the A447T oligomerization, it was very clear that actin enhanced greatly the oligomerization of this mutant. The paper by Palmer et al. 2015 revealed that Vps1 forms ring structures which help to bundle and stabilize actin filaments at sites of endocytosis. In this study, similar ring structures were also observed in the A447T mutant but not in the wild-type. The reason behind this could be attributed to the difference in the purification conditions used. In the study described in this thesis, spun protein extracts were used compared to non-spun protein materials which was used in the Palmer study. This extra step of spinning protein extracts allows removal of the non-functional and oligomerized protein as well as all the debris that can affect EM analysis. However it could be that this procedure has also resulted in the destabilization of the ring structures in the wild-type Vps1, hence no rings were observed. The fact that these ring structures were formed in the A447T mutants might suggest that the ring state is more stable and prevalent in this mutant. The exact mechanism of interaction of A447T with actin is still not clear and so further analysis is essential to understand the effect of this mutation on actin, its stabilization and bundling and hence the outcome it has on endocytosis.

Of the three Vps1 mutations analysed in this study, the R298L mutation was the most marked alteration at the level of the amino acid itself, where a large positive hydrophilic residue was substituted for an uncharged hydrophobic residue. This removal of charge might have been expected to have adverse effects on protein stability and folding as well as affecting protein-protein interactions that the protein may have. Although the R298L mutant protein was successfully purified, the protein appeared to have a greater tendency to form aggregates, which made interpretation of some in-vitro work difficult.

As a result, it was difficult to conclude whether this mutation affects the oligomerization of the protein. On the other hand, the data from the PIP strips have revealed significant changes in the lipid binding specificity of R298L. Since this mutation lies in the GTPase domain, it was unexpected for an effect on lipid binding to occur, as this function has been suggested to lie within the Insert B region in the stalk domain. However, one possible explanation could be the during the folding of the protein into its tertiary structure or the dimerization/oligomerization of the protein, the GTPase region somehow comes in close contact with the stalk region and the R298 residue interacts with the Ins B bringing an effect on the function of Ins B.

The GTPase domain in Vps1 contains a region known as Insert A (amino acids 74-117) about which little is known. Though it would be predicted to lie relatively close to the R298L position. It is possible that this region may be involved in lipid binding, and since leucine is a hydrophobic residue, which can be involved in the binding and recognition of hydrophobic ligands such as lipids, the mutant protein

might have increased its affinity for binding lipids. Further structural studies will be essential to understand such outcome from a mutation in the GTPase domain.

The majority of *in vivo* assays performed on cells expressing the R298L mutant revealed phenotypes similar to the wild-type except for endocytosis where the mutation resulted in a significant increase in the lifetime of Sla2 reporter protein and defects in Sac6 endocytic patch invagination suggesting a defect following commitment to invaginate.

Cells carrying the R298L mutation also had low uptake levels of lucifer yellow dye and although data shows that the R298L cells can still perform fluid phase endocytosis, the rate of endocytosis and trafficking of the dye to the vacuole is reduced compared to the wild-type cells suggesting a defect in the process. Unlike the wild-type or the other mutant cells, no plasma membrane staining was observed in the R298L cells after 15 min of staining with lucifer yellow dye. This could be either due to a faster initial uptake of the dye or a defect in the cell wall which could allow an increased access of the dye into the cells. It is also possible that the plasma membrane in this mutant is different, for example, the composition or the arrangement of the plasma membrane might be different compared to wild-type cells in which case this could result in the LY dye being washed off and therefore a reduction in the total amount of dye uptake. A future experiment that could be performed to clarify the level of internalisation is to measure the total fluorescence intensity of LY inside the cells, which should show whether less dye is taken up by the mutant compared to wild-type. Analysis of the cell wall by EM to check for fundamental differences in the cell wall structure could also be attempted.

Experiment	R298L	G397R	A447T
Expression in yeast cells	+	+	+
Cell growth	+	+/-	+
Temperature sensitive	-	+	-
Rescued by sorbitol		+	
CPY	+	-	+
Normal peroxisomes	+	-	+
Snc1-GFP recycling	+	+/-	+
Normal vacuolar phenotype	+	-	+
Lucifer yellow staining	+	-	+
Effect on Sla2 reporter lifetime	- -	-	-
Effect on Sac6 reporter lifetime	+	+	+/-
Effect on Rvs167 reporter lifetime	+	+/-	+/-
Sac6 patch intensity	+	+	+/-
Rvs167 patch intensity	+	+	+
Patch tracking	-	-	+
Protein oligomerization	?	-	+
Lipid binding	?	-	+
PIP strips	+++	-	+
Electron microscopy	ND	ND	+

Table 3. A summary table of the Vps1 disease mutant phenotypes. The experiments performed are listed and the effect of each of the three mutations on the phenotypes was marked as positive (+), negative (-) or no major effect (+/-).

Chapter 4 - Investigating functional complementation of Vps1 by Dynamin-2

Chapter 4 - Investigating functional complementation of Vps1 by Dynamin-2

4.1. Introduction

In yeast, Vps1 is the only dynamin-like protein that functions in endocytosis and various membrane trafficking pathways. Studies of Vps1 suggest that it is likely to function in a similar way to Dynamin-1 or Dynamin-2 in mammalian endocytosis [Yu and Cai 2004, Smaczynska-de Rooij *et al.* 2010, Nannapaneni *et al.* 2010 and Schmid and Frolov, 2011], where recent studies have reported that Dynamin-2 functions not only in endocytosis but also in a number of trafficking pathways [Gonzalez-Jamett *et al.* 2013]. Similar to classical dynamins, Vps1 has a GTPase domain and a stalk region but it does not have a PH domain nor does it have a PRD domain. However, work from the Ayscough lab has shown that the Insert B region is able to interact with amphiphysins via their SH3 domains, therefore performing similar function to the PRD domain. In addition, recent work in the Ayscough lab has shown that Insert B alone can confer lipid binding function, and so perform at least part of the function of the PH domain.

The work in this chapter outlines attempts to investigate whether mammalian Dynamin-2 can complement deletion of *vps1* in any of its membrane trafficking roles. A chimeric construct was also generated comprising vps1 with the Insert B region replaced by the Dynamin-2 PH domain to determine whether this was able to localize and function in yeast.

4.2. Introducing Dynamin-2 in yeast

To confirm whether dynamin is able to function in a similar way to Vps1 in yeast, mammalian *DYN2* gene was cloned into a yeast expression plasmid under a TPI promoter for expression in yeast cells and to check for the rescue of a *vps1* null phenotype.

DYN2 was PCR amplified using the 1150 and 1151 primers, while the plasmid (pKA526) was digested with Xba I and Hind III restriction enzymes. A ligation reaction was set up and transformed into *E.coli* competent cells after which plasmid miniprep was performed. A restriction digestion was used to check for successful ligation of the *DYN2* gene into the plasmid following by plasmid sequencing to confirm the correct ligation as well as the absence of any mutations in the construct sequence. The construct was transformed into yeast cells expressing endogenous Vps1 to check for any changes in cellular phenotype in the presence of the *DYN2* gene, and was also transformed into yeast cells with a *vps1* deletion to check for phenotype rescue.

4.3. Effect of temperature on cell growth

It has been previously shown in this project and elsewhere that *vps1Δ* cells show a temperature sensitivity phenotype when grown at 37 ^{0}C (section 3.2.3). Since it was proposed that Vps1 and Dynamin-2 proteins perform similar functions, it might be expected that the presence of the *DYN2* gene would rescue the temperature sensitive phenotype expressed by *vps1Δ* cells. For this reason a temperature sensitivity test (ts) was performed, where an overnight culture of KAY447 (Vps1 wild type) cells and KAY1095 (*vps1Δ*) cells containing the pKA677 (Vps1 wild-type), pKA544 (empty CEN plasmid), pKA549 (empty plasmid with a TPI promoter) and pKA 1227 (*DYN2* under a TPI promoter) expression plasmids were re-inoculated into fresh media and the optical density was measured using the spectrophotometer where the OD_{600} was equalized at 0.2. Cell cultures were serially diluted (1:10, 1:100, 1:1000, 1:10,000 and 1:100,000) and spotted onto selective solid media. The plates were incubated for 3 days at 30 ^{0}C (permissive temperature) and 37 ^{0}C (restrictive temperature).

As seen in [figure 4.1] the expression of endogenous wild-type Vps1 allowed the cells to grow in both the permissive and restrictive temperatures. The presence of either a CEN based plasmid (pKA544) or a plasmid containing a TPI promoter (pKA549) did not affect the cell growth. In the absence of vps1, re-expression of *VPS1* rescued growth at 37°C as expected while Dyn2 was unable to rescue the ts phenotype of yeast cells indicating that Dyn2 is not able to complement vps1 functions. However, while the empty plasmid pKA544 did not rescue cell growth at 37 ^{0}C, unexpectedly the pKA549 empty plasmid appeared to. This result would need to be repeated to investigate whether this effect was reproducible. It was also noted that the plasmid carrying Dyn2 did not impact on growth of cells with wild type Vps1.

4.4. Expression of Dynamin-2 in yeast

In order to analyze the effect of Dynamin-2 in yeast cells and to determine whether the lack of rescue of *vps1Δ* growth phenotype was attributable to lack of Dynamin-2 protein in cells, it was important to confirm its expression and stability in yeast. Therefore a yeast whole cell protein extraction was performed where KAY447 (Vps1 wild-type) and KAY1095 (*vps1Δ*) yeast cells containing the pKA549 (*vps1Δ*) plasmid or pKA 1227 (Dyn2) were used.

The procedure was performed exactly as described in materials and methods (section 2.5.9). A 10 % mouse brain extract was included as a positive control and an anti-Dyn2 (rabbit) primary antibody and anti-rabbit HRP secondary antibody were used to detect Dynamin2 protein following western blotting.

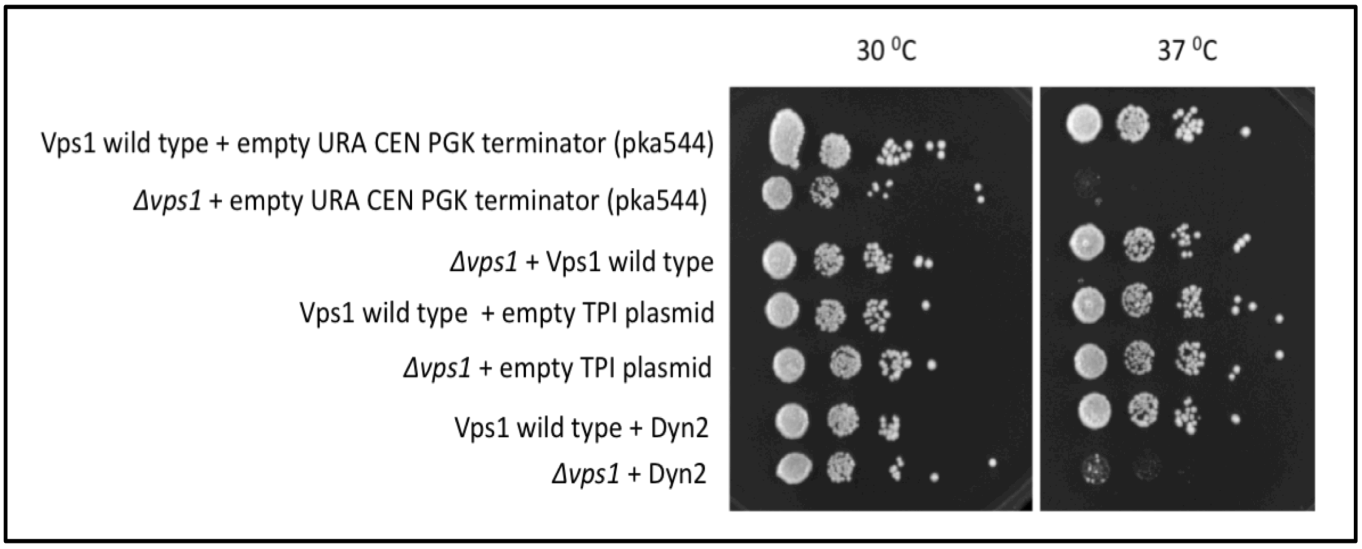

Fig.4.1. Effect of Dyn2 on yeast growth. An overnight culture were serially diluted and spotted onto selective media. Plates were incubated for 3 days at 30 ^{0}C and 37 ^{0}C. A CEN empty plasmid (pKA544), an empty plasmid containing a TPI promoter (pKA549) and a plasmid containing wild-type Vps1 (pKA677) were used as controls.

As expected, Dynamin-2 protein was detected in the mouse brain extract but not in the negative controls, Vps1 wild-type (KAY447) + pKA549 and *vps1Δ*(KAY1095) + pKA549. However, no Dynamin-2 protein was detected in both KAY1095 and KAY447 cells expressing the pKA1227 plasmid [figure 4.2]. A band of about 150 kDa was detected which is most likely a non-specific band of the antibody as it is seen in the strains in which Dynamin-2 has not been introduced. This experiment was repeated three times, however all results indicated no expression of the Dynamin-2 gene in yeast cells.

In order to determine the problem that was preventing Dynamin-2 expression in yeast, a number of factors were considered. First, the functionality of the TPI promoter in the plasmid, which could be tested by cloning a different gene known to function under this promoter and check for its expression using western blotting. This plasmid has been used on many occasions and expression is known to occur for a number of other proteins so it was deemed that the promoter was unlikely to be the main problem in this case. A second step that could be taken would be to check for the production of the Dynamin-2 mRNA, for example by performing northern blotting or reverse transcription-polymerase chain reaction. If the results confirm the production of the Dynamin-2 mRNA then the following step would be checking for defects in the translation of the mRNA, for example due to the presence of rare codons.

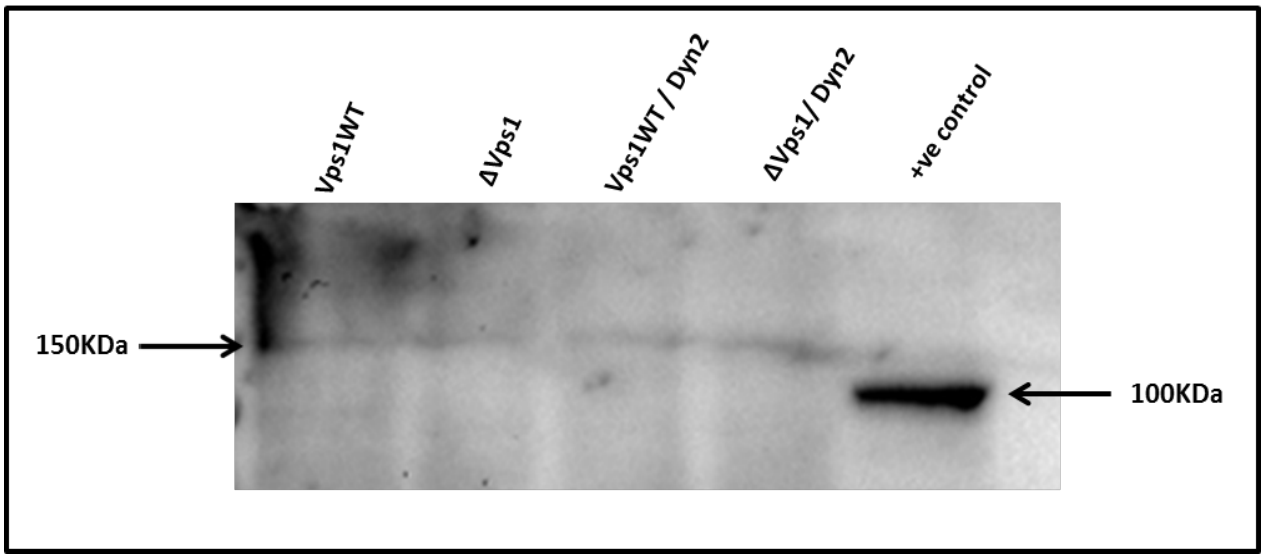

Fig.4.2. Dyn2 expression levels in *S.cerevisiae*. Yeast whole cell protein extraction was performed to check for the expression levels of the Dyn2 protein in yeast cells. Samples were separated using a 10% SDS gel before being transferred onto a PVDF membrane. A Western blot was probed with anti-Dyn2 antibody and 10 % mouse total brain extract was used as a positive control. A band of about 150 kDa can be seen, however this is a non-specific band as it can be seen in the strains in which Dyn2 has not been introduced.

4.5. Checking for rare codons in *S.cerevisiae*

It was mentioned in the previous section that one of the possible reasons for not detecting Dynamin-2 in yeast is due to a problem at the translation stage, which can be caused by the presence of rare codons. Since checking for rare codons does not require experimental procedure, it was decided to analyse the Dynamin-2 sequence for the presence of any rare codons that would potentially cause a problem during translation in yeast. The t-RNAs available for rare codons are usually far less numerous, which results in slowing down of the translation stage and finally can give rise to a premature protein, if any is made at all. The online Bioline calculator tool (http://www.bioline.com/us/media/calculator/01_11.html) was used to check for the presence of rare codons of Dynamin-2 in yeast. The results [figure 4.3] showed the presence of 21 rare codons, all coding for the same amino acid, arginine (Arg) and consisting of the same codon CGG.

4.6. Exchanging Vps1 Insert B domain for Dyn2 PH domain

Introducing Dynamin-2 into yeast would have allowed investigating the functional similarities between Vps1 and dynamin, however the presence of rare codons made this much more challenging to achieve considering time limitations for the project. During the analysis of the sequence, the PH domain of the *DYN2* gene was also checked for rare codons using the Bioline calculator tool. The results [figure 4.4] showed the presence of only two rare codons, which if introduced into yeast, in the context of the rest of the Vps1 protein, may not cause such a drastic reduction in translation.

Fig.4.3. Rare Codons in *S.cerevisiae*. Amino acid sequence of Dyn2 gene in *S.cerevisiae*. The highlighted amino acids are those composed of rare codons and therefore may introduce difficulty during the translation stage. The rare codons were identified using the Bioline rare codon calculator tool (http://www.bioline.com/us/media/calculator/01_11.html).

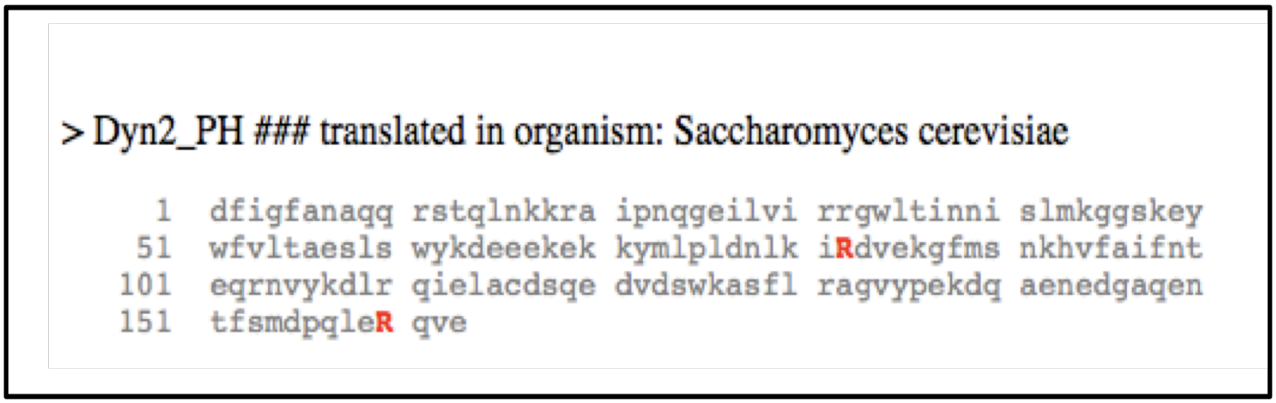

Fig.4.4. Rare Codons in Dyn2 PH domain. Amino acid sequence of the Dyn2 PH domain. The highlighted amino acids are those composed of rare codons. The Bioline rare codon calculator tool (http://www.bioline.com/us/media/calculator/01_11.html) was used to identify rare codons.

The PH domain in dynamin is thought to be essential in the protein interaction with lipids, which is important for its role in endocytosis. Vps1 however has no PH domain yet it was shown both in this project (section 3.3.3) and in a previously published work [Smaczynska-de Rooij *et al.* 2010] to be able to bind lipids. Because of the high conservation across most of the protein, it was thought that this function was most likely attributable to the region showing difference - known as Insert B (InsB) in Vps1.

Despite the absence of any sequence similarity, the Insert B region is thought to function similarly to the PH domain in dynamin and so to study this in greater depth, a chimeric construct was generated in which the Vps1 Insert B region was exchanged for the Dynamin-2 PH domain. Another reason for investigating this chimera is that if expressed it would potentially allow the investigation of many more disease causing mutants, as a large subset of mutations causing both CMN and CMT have been show to lie in the PH domain [figure 4.5] of Dynamin-2 [Kenniston and Lemmon, 2010 and Koutsopoulos *et al.* 2011].

4.7. Creating the chimeric protein

In order to exchange the Vps1_InsB for the Dyn2PH domain [figure 4.6], it was essential to introduce appropriate restriction sites upstream and downstream the InsertB region in Vps1. Upstream of InsertB, a SalI restriction site was introduced by changing residue 532 from proline to valine, while SacI restriction site was introduced downstream of the region by introducing a silent mutation at residue 619 (glutamic acid) and changing valine 620 into leucine.

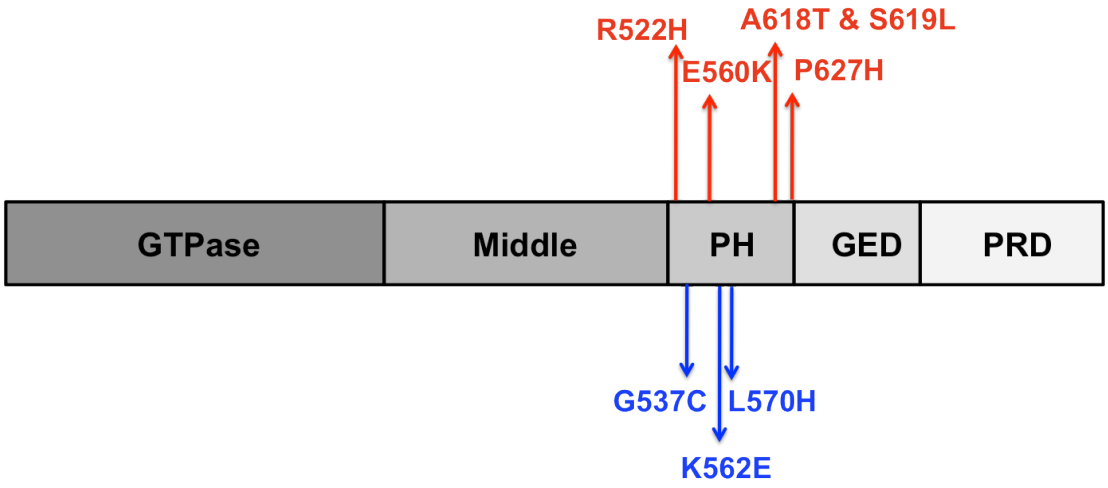

Fig.4.5. Disease mutations in the Dynamin-2 PH domain. Schematic diagram highlighting the disease mutations in the PH domain of the Dynamin-2 protein. Mutations in red represent those implicated in centronuclear myopathy (CNM) while mutations in blue represent those implicated in Charcot-Marie-Tooth (CMT). Information taken from Koutsopoulos et al. 2011 and Kenniston and Lemmon, 2010.

The mutations were introduced by site-directed mutagenesis as described in the materials and methods (section 2.4.5) using the 1138, 1139, 1140 and 1141 primers and pKA677 (Vps1 wild type) and pKA836 (Vps1_GFP) as templates. The procedure was performed as stated in the manual kit. The PCR products were cleaned using the PCR cleaning method (section 2.4.7) and sent for sequencing (University of Dundee) to confirm the successful creation of the SalI and SacI sites and to confirm that no extra mutations were present.

The sequencing results confirmed the successful creation of the SalI and SacI sites, however, sequence analysis revealed the presence of an extra SalI site at the end of the Vps1 gene in pKA677 (Vps1 wild-type). Therefore, before the InsertB could be exchanged for Dyn2PH in this construct, it is essential to remove the extra SalI site, which due to the time limitation was difficult to perform. Therefore, it was decided to continue with the GFP construct of Vps1 that now had the restriction sites introduced (pKA970).

The pKA970 plasmid was digested with SalI and SacI restriction enzymes and the fragments were separated on a 1% agarose gel. A band representing the digested plasmid was excised from the gel extracted and cleaned using the gel extraction method (section 2. 4.3). The PH domain from *DYN2* gene was amplified using PCR and the flanking SalI and SacI restriction sites were introduced using the 1142 and 1143 primers. The PCR amplified Dyn2PH fragment was also digested with SalI and SacI restriction enzymes. A ligation reaction was set up to ligate the Dyn2PH into the digested pKA970 and the successful ligation of the Dyn2PH into pKA970 was confirmed by sequencing using the 832,833, 834 and 835 primers.

A

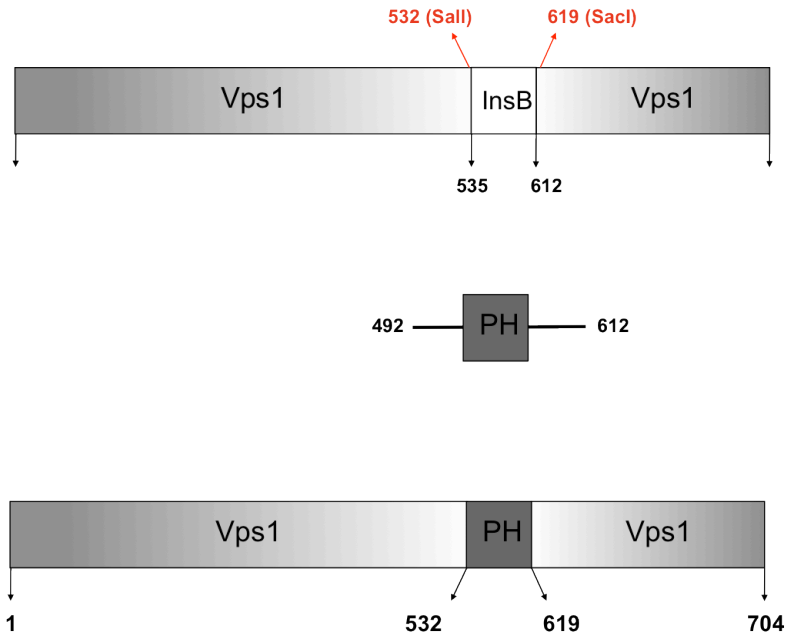

B

ATGGATGAGCATTTAATTTCTACTATTAACAAGCTTCAGGACGCTTTGGCGCCCTTAGGAGGAG
GATCTCAATCTCCTATTGATTTACCACAGATCACTGTTGTCGGTAGGGTTCTCAAGCAATGGTTA
TGGTCGACTTCATTGGATTTGCCAATGCCCAGCAGAGGAGCACGCAGCTGAACAAGAAGAGG
GCCATACCTAACCAGGGGGAGATCTTGGTGATCCGCAGGGGCTGGTTGACCATCAACAACATC
AGCTTGATGAAAGGCGGTTCCAAGGAGTACTGGTTCGTGCTGACTGCTGAGTCGTTGTCTTGG
TACAAGGATGAAGAGGAAAAAGAAAAGAAGTACATGCTGCCACTAGACAACCTCAAAATACGG
GATGTGGAGAAGGGCTTCATGTCCAACAAGCATGTGTTTGCCATCTTCAACACAGAGCAGAGG
AACGTCTACAAGGACCTGCGACAGATCGAACTGGCTTGTGACTCCCAGGAAGATGTGGACAGC
TGGAAGGCTTCGTTCCTGCGAGCTGGGGTCTACCCAGAGAAGGACCAGGCAGAGAACGAGGA
TGGAGCACAAGAGAACACCTTCTCCATGGACCCGCAGCTGGAGCGGCAGGTGGAGCTCATCA
AGTTGTTGATTAGTAGTTATTTCTCTATTGTCAAAAGAACCATTGCCGATATTATACCAAAGGCT
TTGATGCTTAAATTGATTGTGAAAAGTAAAACTGATATTCAGAAAGTTTTACTCGAAAAACTTTAC
G G A A A G C A A G A T A T T G A A G A A T T A A C G A A A G A A A A C G A C
ATAACCATTCAAAGAAGAAAAGAATGTAAG

Fig.4.6. Sequence of Dyn2_PH domain in Vps1. A) Schematic diagram of the exchange of the Vps1 InsB for the Dyn2PH domain. B) The sequence represent a section of the Vps1 nucleotide sequence and the underlined sequence represents the Dyn2_PH nucleotide sequence. The sequence highlighted in red are the 5' SalI and 3' SacI restriction sites introduced to exchange the Vps1_InsB with the Dyn2PH sequence.

4.8. Protein Expression of the Vps1InsBΔ_Dyn2PH chimera

After successfully exchanging Vps1_InsB for the Dyn2 PH domain it was essential to ensure that this exchange did not interfere with the protein production and its stability in yeast. For this reason, a yeast whole cell protein extraction was performed where *vps1Δ* yeast cells (KAY1095) containing the pKA836 (Vps1_GFP), pKA528 (*vps1Δ*_GFP) and pKA970 (Vps1InsBΔ_Dyn2PH-GFP) expression plasmids were used. The procedure was performed as stated in the materials and methods (section 2.5.9). A mouse anti-GFP mouse monoclonal antibody and anti-mouse HRP secondary antibody were used to detect the Vps1InsBΔ_Dyn2PH chimera following western blotting. As expected, no Vps1 protein was detected in the *vps1Δ* cell extract but was expressed in the wild-type cells [figure.4.7]. The loading control has shown that the lane with the chimeric protein contained slightly less extract compared to the wild type and the empty plasmid lanes and this was reflected in the blot which showed the expression of the chimeric protein but to a lesser extent compare to the wild type most likely due to the loading error.

4.9. Investigating the localization of the Vps1ΔInsB Dyn2PH-GFP chimera in yeast cells

In order for a protein to have a direct role in endocytosis, it is expected to, at least partially localize to endocytic sites. Vps1_GFP was previously shown to localize to several internal organelles such as the endosomes and the Golgi (Peters *et al*., 2004

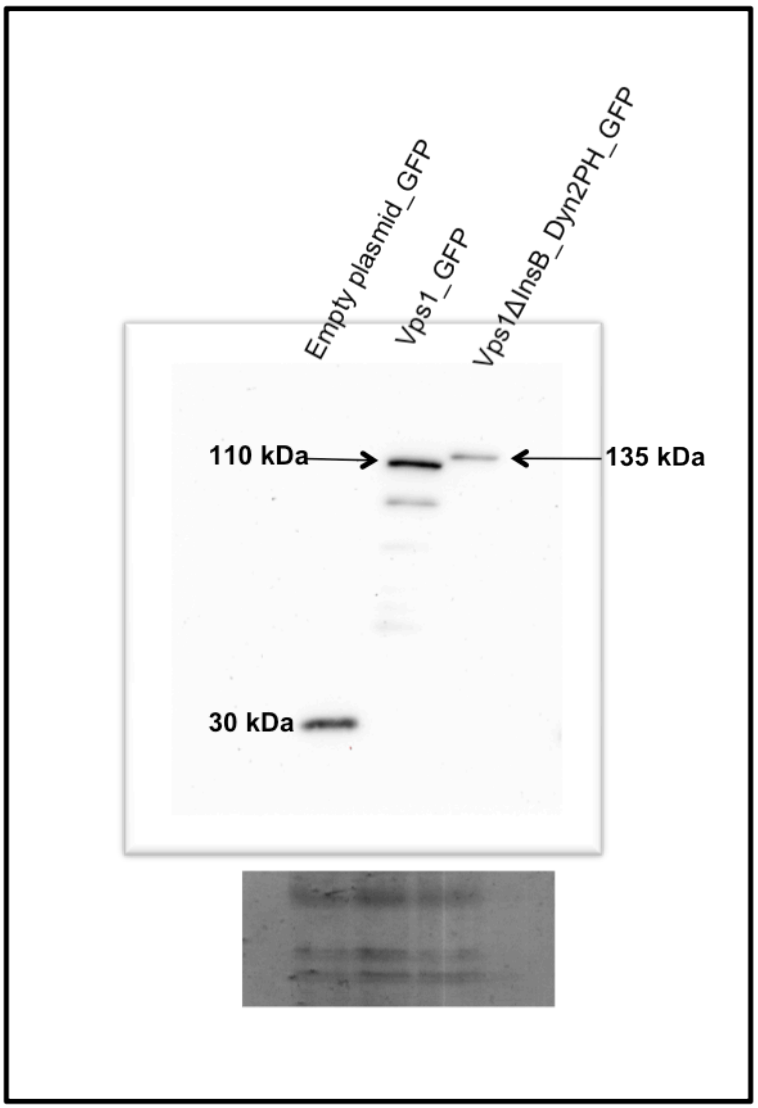

Fig.4.7. Expression of Vps1ΔInsB_Dyn2PH-GFP chimera in yeast. Yeast whole cell protein extraction was performed, where *vps1Δ* yeast cells containing expression plasmids of *vps1Δ*_GFP (pKA528), Vps1_GFP (pKA836) and the Vps1ΔInsB_Dyn2PH-GFP chimera (pKA970) were used. Samples were loaded onto a 10% SDS gel before being transferred onto a PVDF membrane. A Ponceau staining of the membrane was used as a loading control to allow the protein loading to be compared.

and Smaczynska-de Rooij *et al*. 2010) and also was shown to colocalize with the endocytic adaptor protein Sla1 and Abp1 (Smaczynska-de Rooij et a. 2010).

After the expression of the Vps1ΔInsB_Dyn2PH-GFP chimera in yeast was confirmed, it was important to investigate the localization pattern of this construct in yeast cells. For this purpose, Vps1_GFP and Vps1ΔInsB_Dyn2PH-GFP were expressed as the sole source of Vps1 in cells.

The yeast strain KAY1095 was transformed with pKA836 (Vps1_GFP) and pKA970 (Vps1ΔInsB_Dyn2PH-GFP) expression plasmids. These transformants were then inoculated for an overnight growth and cell cultures were refreshed and grown until exponential growth phase was reached. Cells were placed on a glass slide and were visualized using fluorescence microscopy at 100x magnification. As expected, Vps1_GFP showed clear localization to internal organelles most likely endosomes and Golgi. In the cells expressing the chimeric protein all organelle localization was lost [figure 4.8].

Vps1_GFP

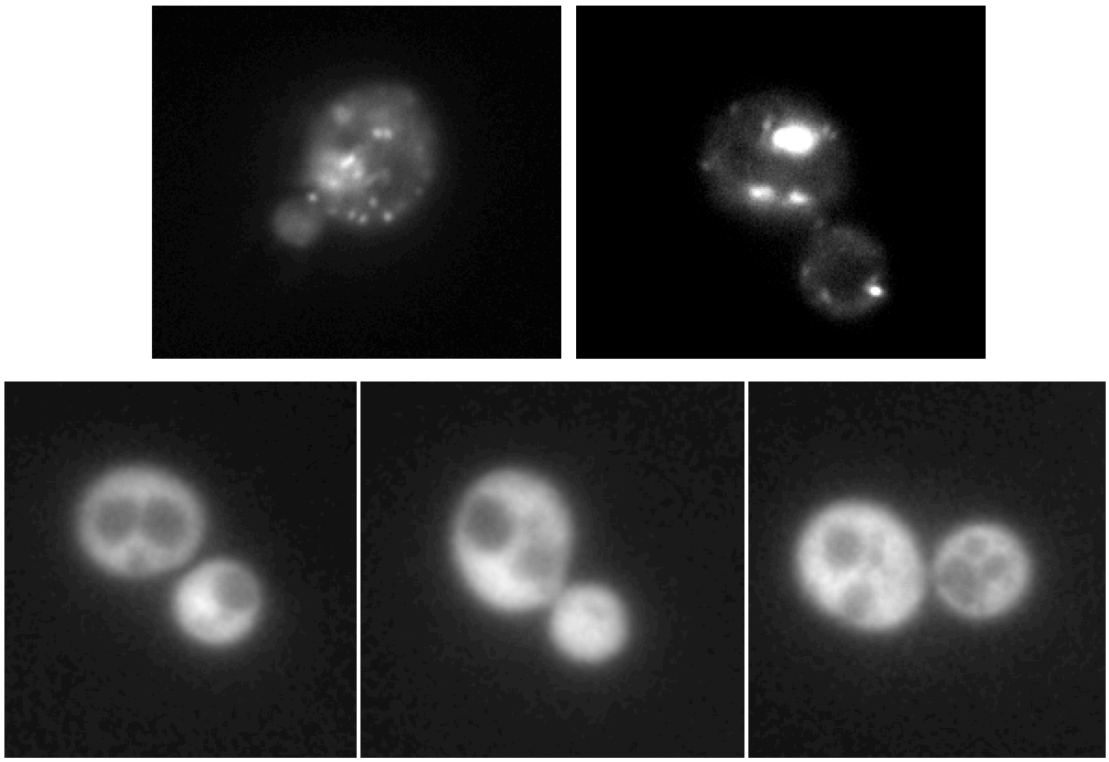

Vps1ΔInsB_Dyn2PH_GFP

Fig.4.8. Localization of Vps1ΔInsB_Dyn2PH-GFP chimera in yeast cells. Yeast cells were transformed with Vps1_GFP and Vps1ΔInsB_Dyn2PH-GFP expression plasmids to assess the effect of exchanging Vps1_InsB with the Dyn2_PH on Vps1 localization. Cells were visualized using fluorescence microscopy at 100x magnification.

4.10. Discussion

In this part of the study the mammalian *DYN2* gene was cloned into a yeast expression plasmid for expression in yeast to check for functional similarity between Dynamin-2 and Vps1 and the ability to rescue a *vps1* null phenotype. The *DYN2* gene however was not expressed in yeast cells, which was attributed, at least in part, to the presence of 21 CGG codons, which encode for Arg. According to the work published by Letzring *et al*. 2010, the CGG codon has only one t-RNA gene copy and accounts for 4 % of the Arg codons in yeast compared to the AGA codon which has 11 t-RNA gene copies and accounts for 47 % of the yeast Arg codons. Therefore the presence of this high number of the CGG codons in Dynamin-2 may explain why no protein could be detected in the western blot, as these codons most likely have prevented effective protein production. One possible way of overcoming this problem might be by growing the cells with the Dynamin-2 plasmid at a lower temperature, possibly below 20 ^{0}C, which should slow down the cellular processes including translation, which might allow more effective incorporation of the CGG encoded arginine. Alternatively or in addition, the CGG codons could be replaced for a more common codon in yeast such as AGA.

Given that only two CGG codons were present in the Dyn2PH domain and the high number of disease mutations occurring in this region [figure 4.5] a different strategy was then adopted. In this approach, the InsertB region in Vps1 was exchanged for the Dyn2PH domain to generate a chimeric protein. A Vps1ΔInsB_Dyn2PH-GFP chimeric protein was successfully created and importantly was shown to be expressed in yeast cells. However, the chimera was not able to localize neither to the plasma membrane nor to the internal organelles.

One possible reason for this loss of localization was suggested to be due to a possible lower level of PtdIns(4,5)P2 to which the PH domain is known to bind to on the plasma membrane. For this reason, an attempt was made to elevate the levels of PtdIns(4,5)P2 in yeast by introducing the chimeric protein into a *sjl1Δ*, *sjl2Δ* yeast strain. The Sjl1/2 proteins belong to the family of synaptojanins, which are phosphatidylinisitol-4,5 bisphosphate phosphatases and are involved in endocytic coat disassembly [Stefan *et al.* 2005 and Goode *et al.* 2015]. Although the Vps1ΔInsB_Dyn2PH-GFP chimera was expected to localize to the plasma membrane and to internal organelles, again no localization was observed (data not shown). It is possible that the GFP tag is interfering with the functioning of the protein and so a co-expression with untagged Vps1_Dyn2PH may facilitate the chimeric protein incorporation at relevant sites.

It is still not clear whether lipid binding is important for the localization of Vps1. It is possible that the PH domain is preventing the formation of higher order structures therefore interfering with the protein function as a whole. Another possible explanation could be that InsertB, but not the PH domain, contains major localization signal that is important in localizing Vps1 into plasma membrane and other organelles. In a work published by Smaczynska-de Rooij *et al.* 2012, the presence of a KxxPxxP motif predicted to bind the Rvs167 SH3 domain was identified within InsertB region. Specifically, when the central proline in the motif was mutagenized, the interaction between Vps1 and Rvs167 was lost. Since Vps1 does not have a PRD domain, which in dynamins is known to be involved in the interaction with SH3 domain, it is possible that in Vps1, the InsertB region is acting

as both the PH and the PRD domains. Therefore, when it was exchanged for the PH domain, the PH domain was not able to rescue all of the functions performed by InsertB, for example interaction with SH3 domain containing proteins, and hence the loss of localization observed. One possible way to approach this problem is to determine the motif or the specific amino acids essential for lipid binding within InsertB and if possible exchange that specific motif for the PH domain and leave the remaining of the InsertB. This should mean that the functions performed by InsertB other than lipid binding should not be affected and the new chimeric protein should be able to maintain its interaction with other protein partners such as Rvs167.

Chapter 5 - Genetic screen to identify suppressors of an endocytic mutant of Vps1

Chapter 5 - Genetic screen to identify suppressors of an endocytic mutant of Vps1

5.1. Introduction

The work described in this thesis and elsewhere indicated that some Vps1 mutations affect all of its known roles while other mutations only affect endocytosis. These latter mutations presumably affect residues only required in this process. In order to gain deeper insight into the function of Vps1 during endocytosis, it was decided to investigate what other genes could rescue Vps1 endocytic mutant phenotype when overexpressed. Because of ease of analysis, it was determined that a primary screen would focus on rescue of temperature sensitivity (ts) associated with one of these mutations and follow up analysis would focus on more specific phenotypes.

5.2. Integration of Vps1 endocytic mutations into the yeast genome

So far, the Vps1 mutations that have been studied were all expressed from a yeast expression plasmid under the control of a Vps1 promoter. Because under various conditions the number of plasmids carrying a mutation of interest can change affecting by that the level of expressed protein in cells, it was essential to integrate the Vps1 endocytic mutations into the yeast genome before the screen was attempted. Integrating the mutations into the yeast genome should result in a more uniform expression of the mutant proteins in cells. For this purpose, a *URA3* deletion cassette and 5-Fluoroorotic acid (5-FOA) selection were used [figure 5.1].

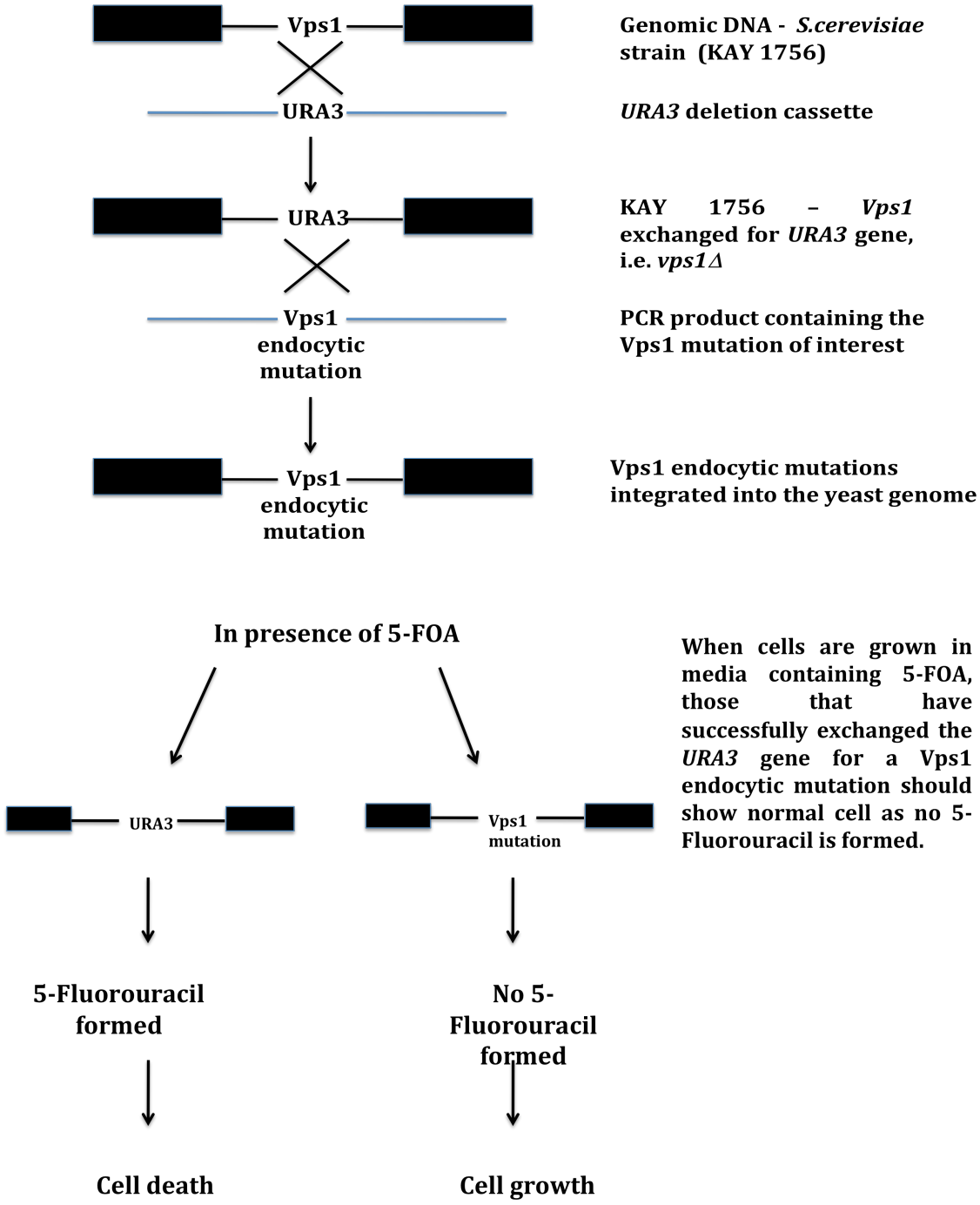

Fig.5.1. Summary of the Vps1 allele exchange. The *URA3* deletion cassette was used to produce a *vps1Δ* strain. PCR fragments containing Vps1 endocytic mutations were then exchanged with the *URA3* gene and the mutations were integrated into the yeast genome. A 5-Fluoroorotic acid (5-FOA) selection was used.

URA3 gene on chromosome V in yeast encodes for orotidine 5-phosphate decarboxylase (ODCase), which is involved in the catalysis of a reaction important in the synthesis of pyrimidine ribonucleotides in yeast RNA [Lacrout F. 1968]. In the presence of 5-FOA, ODCase converts 5-FOA into 5-Fluorouracil, a toxic compound resulting in cell death [Boeke JD, et al. 1984]. In the case of successful integration, the cells would have exchanged the *URA3* gene for the *Vps1* mutation and therefore should be able to grow in the presence of 5-FOA.

In this study, and other studies, a number of Vps1 mutations were studied which showed an effect on endocytosis but not on the other roles of Vps1. A number of these mutations were chosen for this study with the aim of checking for a robust phenotype that could be rescued in a suppressor screen. The mutations selected were Vps1 R298L in the GTPase domain, A447T, RR457-8EE and E461K in the middle/stalk domain, P564A in the Insert B region and K642A and I649K in the GED domain.

Plasmid constructs containing the Vps1 R298L, A447T, RR457-8EE, E461K, I649K, P564A and K642A mutations were used as PCR templates and the 1161 and 1162 oligonucleotides were used for the allele exchange (section 2.4.5). The linear PCR products encoding the mutant gene were transformed into KAY1756 yeast strain using the lithium acetate protocol (section. 2.3.2.2) and the cells were plated on YPD plates and incubated at 30 ^{0}C overnight. The YPD plates were replica plated onto media plates containing 5-FOA, and incubated at 30 ^{0}C until colonies were evident. Once colonies started growing, they were re-streaked onto a fresh media plate containing 5-FOA to confirm the selective

growth and colony PCR was performed to check for the integration of the mutations into the yeast genome. A 2 kbp increase in band size when run on an agarose gel was an indication of successful integration compared to the non-integrated samples.

Once the integration of R298L, A447T, RR457-8EE, E461K, I649K, P564A and K642A was confirmed via colony PCR, using the 712 and 713 oligonucleotides, the generated products were cleaned using a PCR cleaning method (section 2.4.7) and sent for sequencing (University of Dundee) to further demonstrate the integration of the mutations into the genome as well as to determine whether any extra mutations had occurred. The results from both colony PCR and the sequencing have shown that 5 mutations; A447T, RR457-8EE, E461K, I649K and P564A were integrated successfully into the genome, while in the R298L and K642A fragments additional mutations were present.

5.3. Analysis of the Vps1 integrated mutants

5.3.1. Growth at the permissive and restrictive temperature

After successfully integrating the Vps1 endocytic mutations into the genome, it was important to test for their effect on the growth of yeast cells. Therefore a temperature sensitivity test (ts) was performed where yeast strains grown overnight were re-inoculated in fresh YPD media and incubated for 3 hrs at 30 ^{0}C. 0.5 OD_{600} units of cells were serially diluted in a multi-well plate (1:10, 1:100, 1:1000, 1:10,000, 1:100,000) and 5 µl of each sample was spotted onto fresh YPD plates, which were then incubated at 30 ^{0}C and 37 ^{0}C for 3 days.

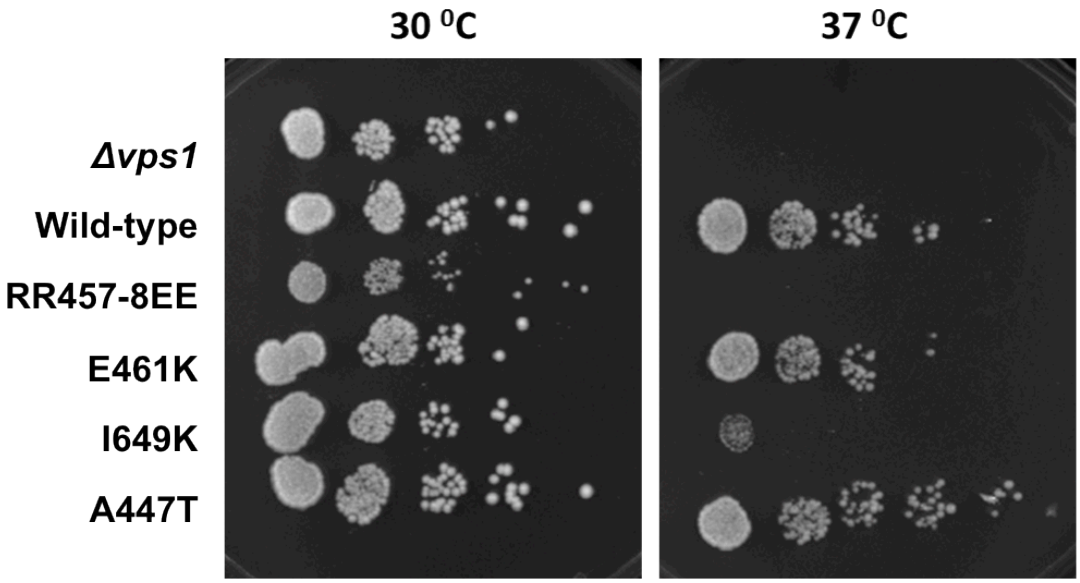

Fig.5.2. Temperature sensitivity test for Vps1 integrated mutants. 0.5 OD_{600} units of cells were serially diluted and plated onto YPD plates and incubated at 30 ^{0}C and 37 ^{0}C. Vps1 wild-type and *vps1Δ* were included as controls.

The results from the plates showed that out of all the mutants tested only RR457-8EE and I649K had a ts phenotype when grown at 37 ^{0}C. The I649K mutant showed a very weak growth 37 ^{0}C whereas the RR457-8EE showed no growth at all [figure 5.2]. Because of their ts phenotype, which allows a ts phenotype suppression screen to be carried out, both RR457-8EE and I649K mutants were chosen as possible candidates for the screen and therefore their phenotypes were analysed further.

5.3.2. Protein Expression of the Vps1 integrated mutants

The growth test performed previously revealed a ts phenotype for both RR457-8EE and I649K mutants when grown at 37 ^{0}C. To confirm that this phenotype was the result of the mutations rather than the proteins not being expressed or being unstable in the cells, a yeast whole cell protein extraction was performed to check for the protein expression in the cells. The method was performed as stated in section 2.5.9. An anti-Vps1 (rat) primary antibody and anti-rat secondary antibody were used to detect the Vps1 protein in a western blot and the results confirmed the expression of the two mutants at similar levels to the wild-type [figure 5.3].

5.3.3. Effect of Vps1 integrated mutants on vacuolar morphology

As well as its role in endocytosis, Vps1 is also involved in the maintenance of vacuole morphology in cells [Raymond *et al.* 1992, Peters *et al.* 2004]. In this experiment the aim was to identify whether integrating the mutations resulted in a vacuolar fission defect. For this purpose the lipophilic dye FM4-64, which stains the vacuole membrane in yeast [Vida and Emr, 1995] was used. An overnight culture was re-inoculated in fresh YPD media and treated with FM4-64 for 60

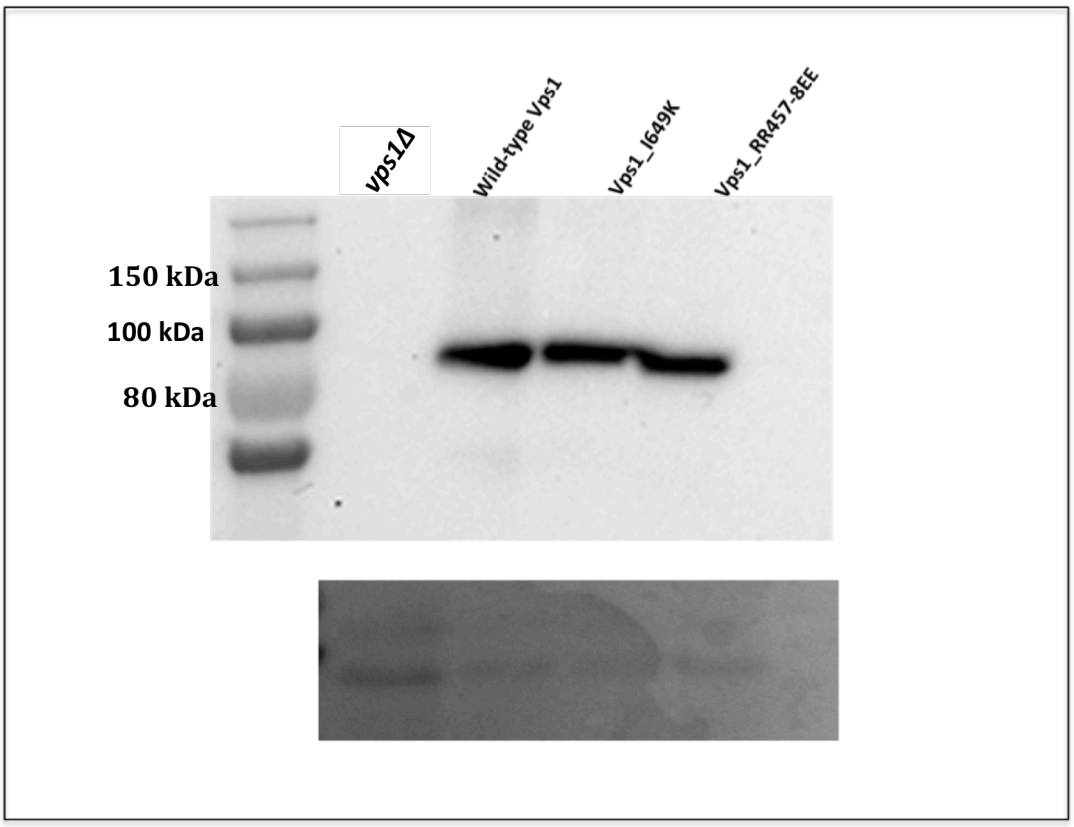

Fig.5.3. Expression levels of the Vps1 integrated mutants. Yeast whole cell extraction was performed to check the expression levels of Vps1 RR457-8EE and I649K in yeast cells. A Ponceau staining of the membrane was used as a loading control to allow the protein loading to be compared.

minutes using the same procedure as described in the materials and methods (section 2.6.3). Cells were visualized using fluorescent microscopy at 100x magnification and vacuolar morphologies were categorized. As expected, the majority of wild-type cells (0ver 70 %) showed normal vacuolar staining which involved the presence of two to five vacuoles all of which were similar in size. On the other hand, 50 % of *vps1Δ* cells had fragmented vacuoles [figure 5.4]. Analysis of the RR457-8EE mutant revealed that about 69% of the cells show a single vacuole or single vacuole + endosomes morphology which was not evident in either the wild-type or in the *vps1Δ*.

This could be an indication of a vacuolar fission defect where the vacuoles are unable to perform fission and therefore appear as a single bright vacuole. In the case of the I649K mutant, 56 % of cells showed a single vacuole or single vacuole + endosomes morphology and about 38 % of cells showed a normal vacuolar morphology. This suggests that similar to the RR457-8EE mutant, this mutation could be affecting the vacuolar fission in cells but probably to a lower extend compared to RR457-8EE. Previous analysis of vacuolar morphology in cells expressing these mutants from plasmids had not noted these mild vacuolar fission defects.

A)

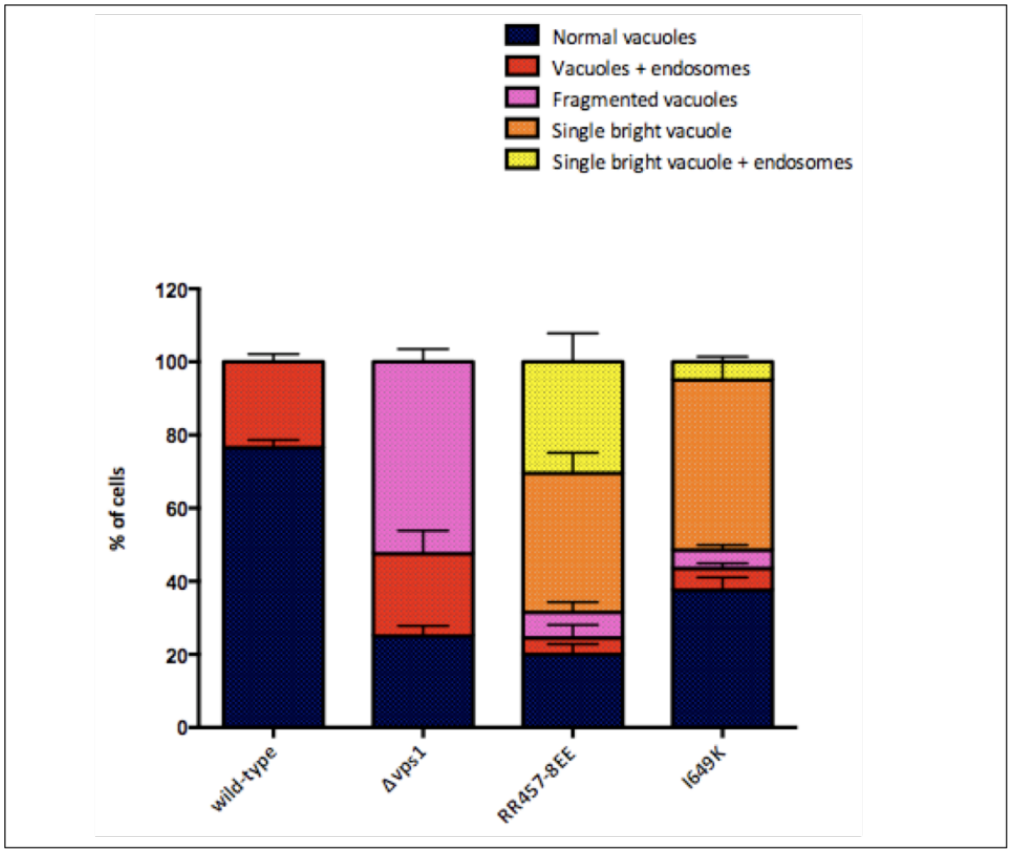

B)

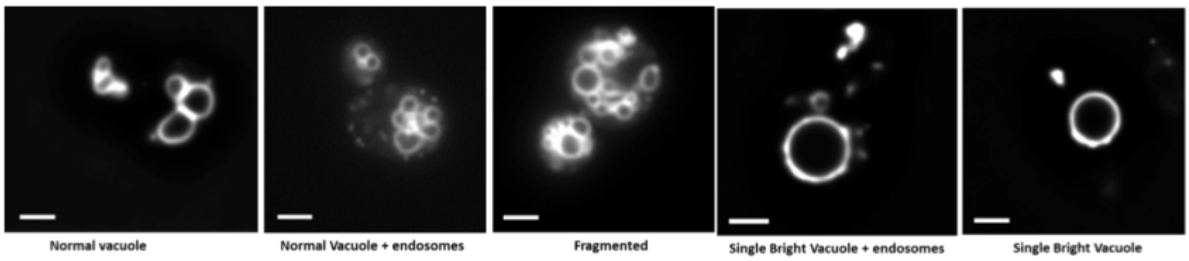

Fig.5.4. Vacuolar morphology in RR457-8EE and I649K integrated mutants. Cells were treated with FM4-64 for 60 minutes at 30 ^{0}C to assess the effect on vacuole morphology. Cells 0-were visualized using fluorescent microscopy at 100x magnification. a) Graph representing the percentage of cells with each of vacuolar categories. N = 80 from two independent experiments. b) Examples of different categories of cell staining. Scale Bar 2 μM

5.3.4. Effect of Vps1 integrated mutants on fluid phase endocytosis

Lucifer yellow (LY) staining was used to test for fluid phase endocytosis in the RR457-8EE and I649K integrated mutants. Cells were incubated with the dye (section 2.6.3) to test for early (15 min) and late endocytic (90 min) defects. Cells were visualized using fluorescence microscopy and were placed into appropriate categories [figure 5.5].

After 15 min of incubation with the LY dye, 52 % of wild-type cells showed vacuolar staining which increased to 90 % after 90 min of staining. In contrast, the *vps1Δ* cells showed only 6.5 % of vacuolar staining after 15 min of staining and 45 % after 90 min of staining. Although the initial uptake of the LY dye in the RR457-8EE mutant was similar to the wild-type, where 6 % of cells showed plasma membrane and endosomal staining after 15 min of staining, the majority of cells appeared to have defects in further trafficking and 70 % of the cells showed endosome only staining. Only 4 % of the RR457-8EE cells had vacuolar staining. This suggests that the trafficking pathway from the endosome to the vacuole could be blocked, hence the accumulation of the LY in the endosomes.

After 90 min of staining 12 % of the RR457-8EE cells still showed endosome staining and only 40 % of the cells had a vacuolar staining, supporting further the suggestion that these cells have defects in vacuolar trafficking. With the I649K cells, 2 % showed vacuole only staining after 15 min however unlike the RR457-8EE cells, 42 % of the I649K cells showed endosome only staining and 35 % showed endosome and vacuole staining.

A)

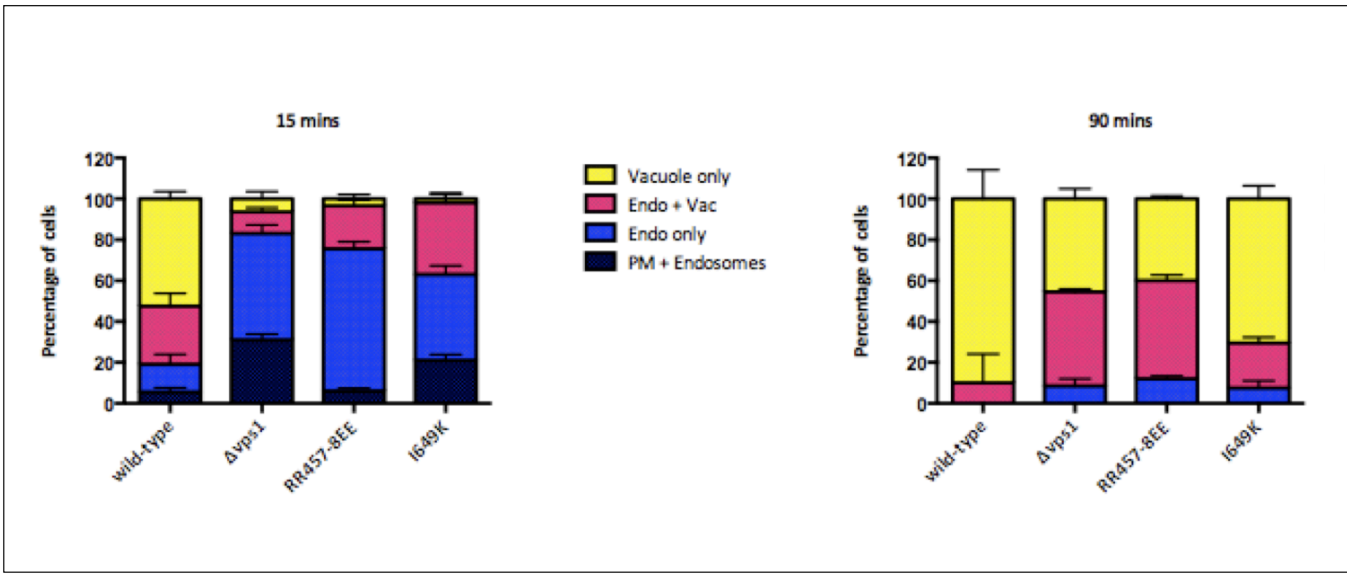

B)

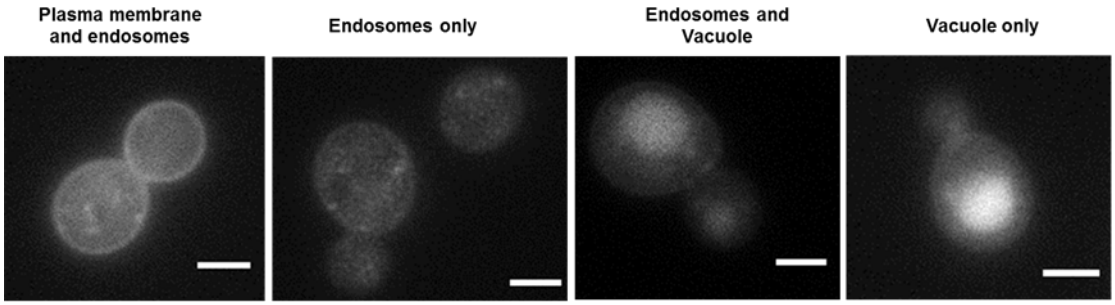

Fig.5.5 Fluid phase endocytosis of the RR457-8EE and I649K integrated mutants. a) Cells were treated with Lucifer yellow to assess fluid phase endocytosis at two time points, 15mins for early endocytosis and 90mins for late endocytosis. Cells were visualized using fluorescent microscopy at 100x magnification. b) Examples of different categories of cell staining. N = 80 cells from two independent experiments. Scale Bar 2 μM.

The graph shows a slow and less efficient trafficking of the dye through the different compartments compared to the wild-type cells, however it is unlikely that any stage of the pathway is blocked. After 90 min of staining, 75 % of cells showed vacuolar staining supporting the suggestion that this mutation seems to only affects the rate of the dye trafficking and if given enough time, the dye would reach finally to the vacuoles.

5.3.5. Further analysis of the TS phenotype of RR457-8EE and I649K

Previously in this project the I649K mutant showed a ts phenotype at 37 ^{0}C. However, data from other projects have observed variability in its growth at 37 ^{0}C, which might make it difficult to interpret any results following the suppression screen. Therefore, the RR457-8EE mutant seemed to be a better candidate for the suppression screen.

For a screen to be performed it was essential to identify the exact temperature at which the RR457-8EE mutant cease to grow. This is because during the screen, the cells may not get rescued by a high copy gene if the level of rescue required is too great. Therefore, a ts test was performed using exactly the same procedure as before (section 5.3.1.) but the cells were incubated at 35 ^{0}C instead of 37 ^{0}C. The results have shown a ts phenotype for the RR457-8EE mutant at 35 ^{0}C, which was more severe than that seen in the *vps1Δ* possibly suggesting a dominant negative effect. The I649K mutant was still able to grow normally at 35 ^{0}C.

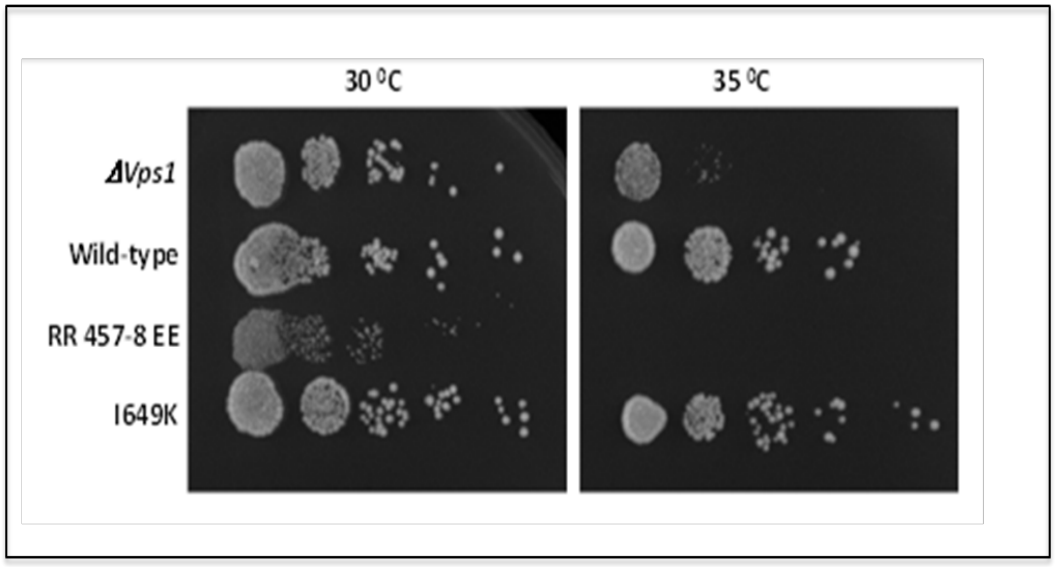

Fig.5.6. Temperature Sensitivity test for the RR457-8EE and I649K integrated mutants. 0.5 OD_{600} units of cells were serially diluted and plated onto YPD plates and incubated at 30 ^{0}C and 35 ^{0}C. Vps1 wild-type and *vps1Δ* were used as controls.

In this experiment the difference in growth of the RR457-8EE mutant at 30 ^{0}C and 35 ^{0}C seemed to be quite dramatic and therefore preferably more analysis should have been carried out to define the exact temperature at which the mutant would start to show the ts phenotype. This however was not possible due to the time limitation especially that these experiments and the suppression screen were performed simultaneously.

5.4. Endoctyic suppressor screen using the YEp24 library

Yeast episomal plasmid 24 (YEp24) is a 7,769bp shuttle vector used for gene overexpression in *S.cerevisiae*, but is also able to replicate in *E. coli* [Parent et al. 1985]. It is a high copy number plasmid and it contains the ampicillin *(ampR),* the tetracycline *(tetR)* and *URA3* marker for selection [figure 5.7] [Parent et al. 1985]. In this work, a YEp24 genomic library, which was created via blunt end cloning of genomic fragments at the BamHI site, was used to perform the endocytic suppression screen.

For the screen, 100 ml of log phase RR457-8EE mutant cells (OD600 0.5) were transformed with 5 µl of the YEp24 library (1mg/ml) using the lithium acetate transformation method (section 2.3.2.2) with 10 min heat shock at 40 ^{0}C. Cells were resuspended in 4 ml of drop-out URA and recovered for 40 min before being plated onto drop-out URA plates. Cells were plated onto 21 plate, in which 10 were incubated straight at 34 ^{0}C, 10 were left at room temp overnight then moved to 34 ^{0}C and 1 was incubated at 21 ^{0}C to test for transformation efficiency.

Fig.5.7. YEp24 Map. The map shows the different features and the unique restriction sites of the YEp24 plasmid. EcoRI restriction enzyme cuts the plasmid at 1 and 2241 bp.

The plate at 21 ^{0}C indicated that there should be 50-100,000 transformants over the 20 plates however only 11 transformants grew with no difference between the plates that were left at room temperature before incubation and the plates that were incubated straight at 34 ^{0}C.

Each of these 11 colonies were extracted using the Zymoprep yeast plasmid miniprep I (section 2.3.3.) where the final pellet was resuspended in 35µl of TE buffer. A PCR test was performed using the plasmids as templates to check for the presence of the Vps1 gene in the extracted plasmid, as in most screens it might be expected to isolate the gene mutated. The results showed no band representing Vps1 confirming that the growth of the 11 colonies was rescued by another gene or genes. To make a bacterial stock of the rescued plasmids each of the 11 plasmids extracted from yeast cells were transformed into XL-gold bacterial competent cells, plated onto YPD + ampicillin plates and incubated overnight at 37 ^{0}C. Plates were covered with cells from which 4 colonies from each of the 11 samples were picked up at random (total of 44 samples) and bacterial plasmid minipreps were performed (section 2.4.1).

To confirm that the extracted plasmids were not empty, each of the 44 plasmids were digested for 2 hrs at 37 ^{0}C with EcoR1 restriction enzyme which cuts the YEp24 plasmid at two sites, 1 and 2241 bp. The digested samples were run on a 0.8% agarose gel for 30 min at 110V. As expected, the empty YEp24 plasmid showed two bands, the first band being about 2300 bp and another band of about 5500 bp.

All of the digested plasmids resulted in different band sizes compared to the control which confirmed that the rescued plasmids were not empty and that the growth rescue observed was due to the presence of another gene or genes [figure 5.8].

5.4.1. Confirming Suppression by isolated plasmids

Plasmid 1 from each of the samples B1-B8, B10-B11 and plasmid 1 and 4 from B9 were picked and re-transformed into the integrated RR457-8EE mutant using the lithium acetate transformation method to confirm the rescue of the ts phenotype previously observed. Cells were plated onto drop-out URA plates and incubated at 30 ^{0}C. The plates were covered with colonies and 2 random colonies from each plate were inoculated into liquid drop-out URA media and grown overnight at 30 ^{0}C. OD600 0.4 of the overnight refreshed culture were diluted at 1/100 and 1/1000, plated onto drop-out URA plates and incubated at 35 ^{0}C to check for the growth rescue. The results have shown successful growth of cells containing the plasmids [figure 5.9].

After confirming the ts phenotype rescue, the following step was to identify what genes were present in the plasmids. This was achieved by sequencing, where plasmid 1 from each of the samples B1-B8, B10-B11 and plasmid 1 and 4 from B9 were sent for sequencing using the 1282 and OKA152 primers. Each of the sequences obtained were analysed using the basic local alignment search tool (BLAST) and the results came with a DNA fragment on chromosome VII.

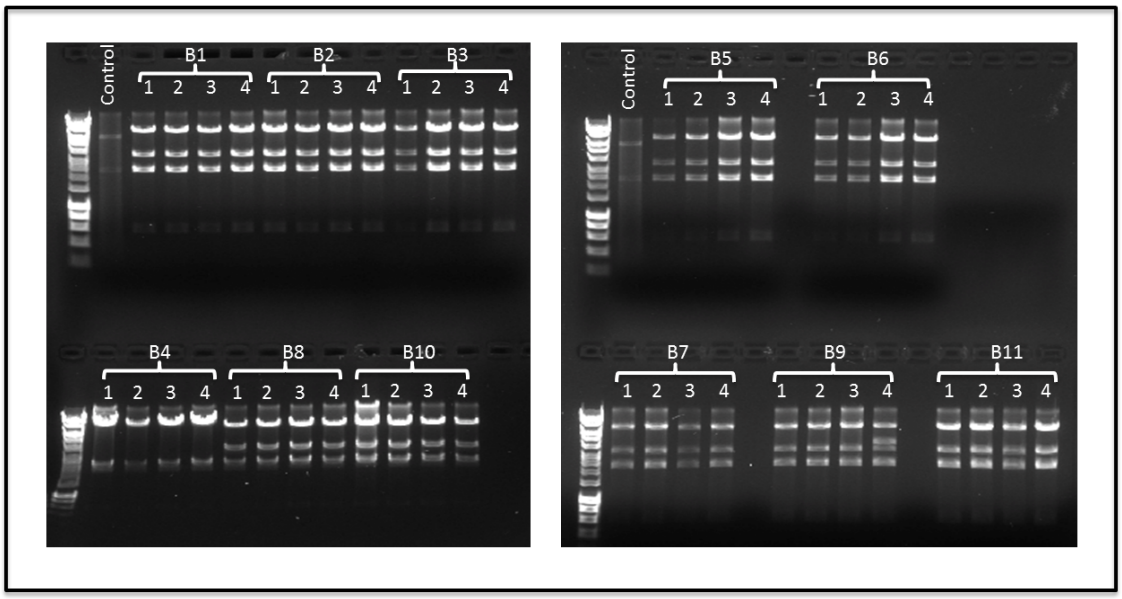

Fig.5.8. Test digest for the YEp24 screen recovered plasmids. Each of the 11 recovered plasmids (B1 – B11) were transformed into XL-gold competent cells from which 4 random colonies were picked for plasmid miniprep. The minipreped plasmids were digested with EcoRI. Yep24 empty plasmid was included as a control. Bioline Hyperladder I marker was used.

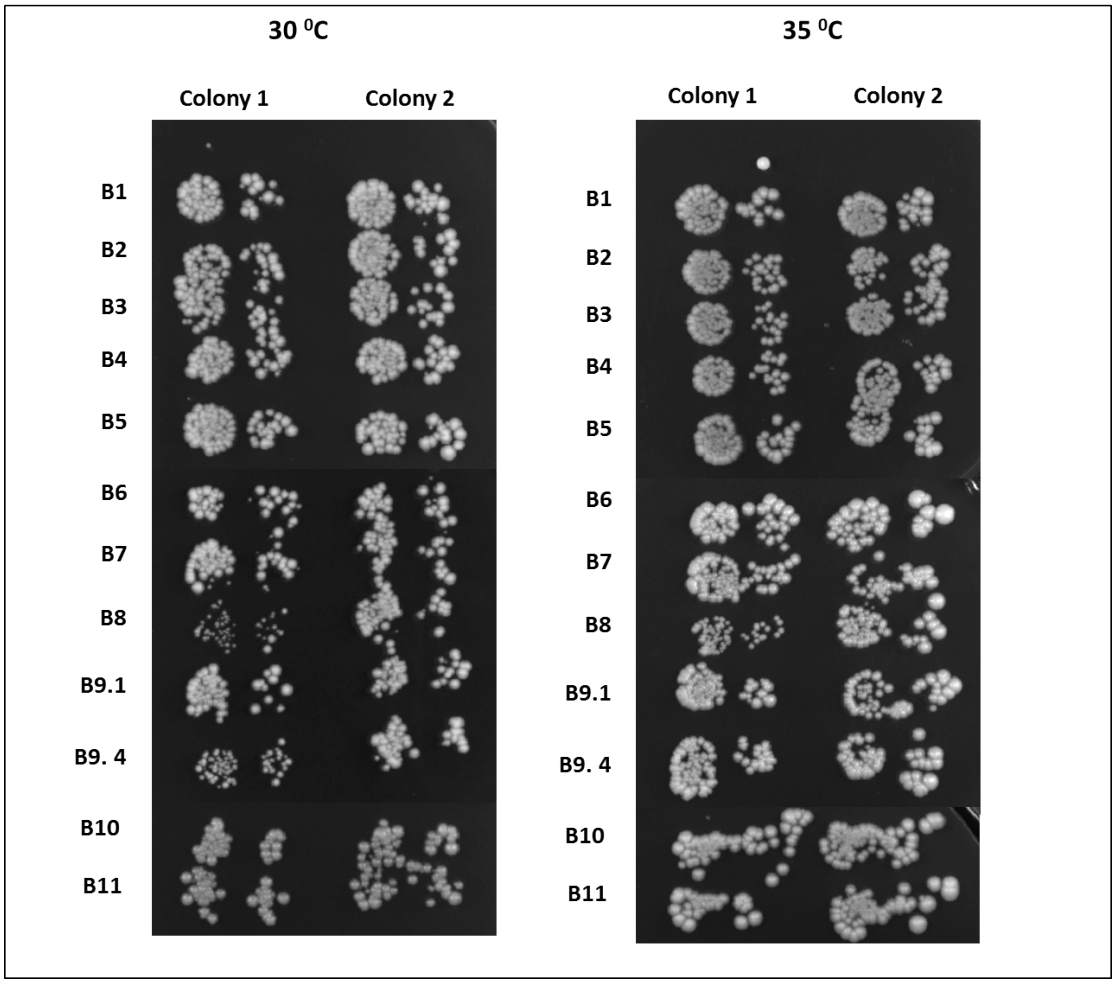

Fig.5.9. Confirming the ts phenotype rescue. Two random colonies from each of B1-B11 plasmids in the RR457-8EE mutant were picked and grown at 30 C^0 as control and at 35 ^{0}C to confirm the rescue of the ts phenotype.

The BLAST analysis revealed that plasmids B1 – B11 all contained fragments of the same region in chromosome VII with only few base pair differences. This region was shown to code for 3 genes, PBP1, ATF2 and ERG1. Unlike the other plasmids, B4 fragment was greater in size and was shown to span through a larger area on chromosome VII which codes for 7 genes in its sequence, PBP1, ATF2, ERG1, CBP4, RGB2, YIP1 and part of MSM1 [figure 5.10]

5.5. Discussion

In total, 7 genes were identified in the YEp24 screen for suppressors of the ts phenotype in RR457-8EE. Out of the 7 genes, 3 were present in all of the 11 plasmids rescued and these were *PBP1, ATF2* and *ERG1*. In addition, the B4 fragment also contained 4 additional genes in their sequences, which were *CBP4, RGB2, YIP1* and only about 250 base pair of *MSM1*.

The fact that the same region was picked up 11 times in a screen suggests its importance in the phenotype rescue of the Vps1 RR457-8EE mutation. However, from the initial search on the functions of these genes using the Saccharomyces Genome Database (SGD) [Table 4], it appears to be unlikely for all of the genes to be required for the rescue of the ts phenotype in RR457-8EE. Amongst those that are unlikely to be involved in the rescue are *CBP4* and *MSM1*, which are both mitochondrial proteins and would probably not be able to suppress an endocytic defect in the cell. On the other hand, *PBP1*, which is involved in Processing-body-dependent granule assembly, might be a good candidate for the rescue especially that a genetic interaction with Vps1 has been previously reported [Hoppins *et al.* 2011].

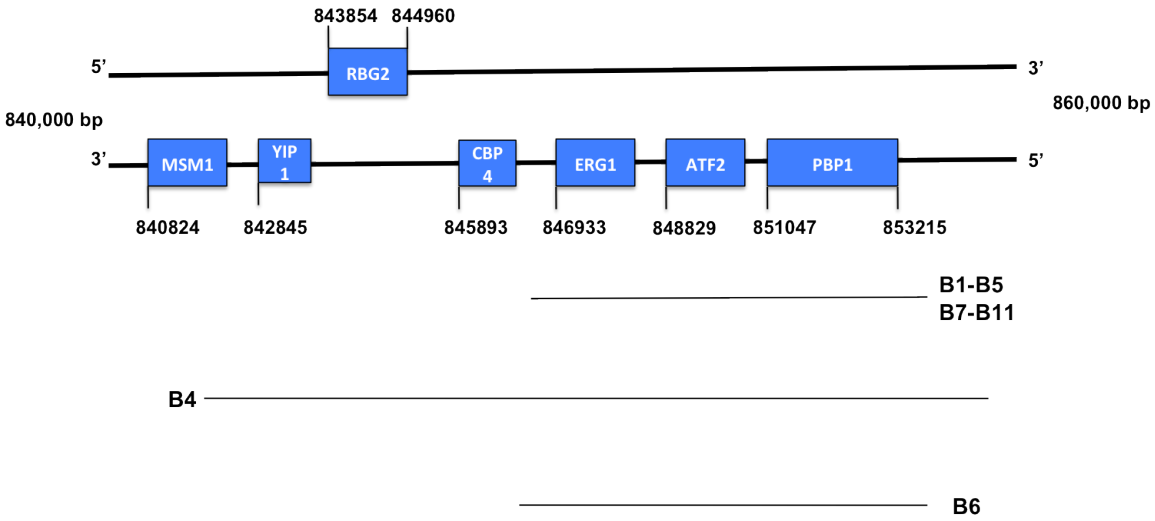

Fig.5.10. Genes identified in the screen. A schematic diagram represents the region on yeast chromosome VII that was identified in the YEp24 screen. The diagram represents the size of the fragments from each of the 11 plasmids rescued in the screen. This region contained 7 protein-coding genes PBP1, ATF2, ERG1, CBP4, RBG2, YIP1 and MSM1.

Processing bodies (P-bodies) which appear as dense foci in the cell cytoplasm have fundamental roles in mRNA degradation and also they can be a place for storing and protecting mRNA from harmful conditions until they are needed for translation [Buchan et al. 2008]. It is possible that the temperature used in the screen put the cells in stress and the overexpression of the *PBP1* protein allowed the protection of the essential mRNAs until the cells were adapted to their environment and were ready to progress forward.

In order to understand which of the genes rescued the ts phenotype, it is essential to introduce each of the genes from the screen separately into the RR457-8EE mutant and check for ts phenotype rescue. This can be achieved via restriction digestion of the genes and ligating them into a high copy plasmid before introducing them into the RR457-8EE integrated mutant. Not only ts suppression can be checked for, but also if any of these genes can rescue the endocytic and vacuolar defects observed in the RR457-8EE mutant.

Although this screen aimed to identify suppressors of an endocytic mutation when integrated, the RR457-8EE mutation was shown to have also affected the role of the protein in vacuolar fission/morphology. However, because the YEp24 genomic screen and the test for vacuolar morphology were performed simultaneously, it was decided to continue with the screen based on the ts phenotype. The ts phenotype of the RR457-8EE mutant was rescued, however it is still unclear whether this was due to an endocytic rescue or it was a result of rescuing/inducing other pathways within the cell that would make it survive the stressful environment.

Gene Name	Gene size	Function	Interaction with Vps1
PBP1 (Pab1p-Binding Protein)	2169 bp	Component of glucose deprivation induced stress granules; involved in P-body-dependent granule assembly; upon DNA replication stress the protein increases in abundance and relative distribution to the nucleus [Buchan et al. 2008, Tkach et al. 2012]	Genetic
ATF2 (AcetylTransFerase)	1608 bp	Encodes for alcohol acetyltransferase [Nagasawa et al. 1998]	None
ERG1 (ERGosterol biosynthesis)	1491 bp	Encodes for Squalene epoxidase a protein that catalyzes the epoxidation of squalene into 2,3-oxidosqualene and also plays an essential role in the ergosterol-biosynthesis pathway [Jandrositz et al. 1991, Satoh et al. 1993]	None
CBP4 (Cytochrome B mRNA Processing)	513 bp	Mitochondrial protein required for assembly of cytochrome bc1 complex [Crivellone 1994]	None
RBG2 (Ribosome interacting GTPase)	1107 bp	Plays a role in translation; forms a complex with Gir2p; has similarity to mammalian developmentally regulated GTP-binding protein [Li and Trueb 2000, Daugeron et al. 2011]	None
YIP1	747 bp	Integral membrane protein; required for the biogenesis of ER-derived COPII transport vesicles; localizes to the Golgi, the ER, and COPII vesicles [Heidtman et al. 2003]	None
MSM1 (Mitochondrial aminoacyl-tRNA Synthetase, Methionine)	1728 bp	Functions as a monomer in mitochondrial protein synthesis [Tzagoloff et al. 1989]	None

Table.4. Summary of the genes identified in the suppressor screen. Information was used from the Saccharomyces Genome Database (SGD).

In the future it would be important to determine if the screen genes would also be able to rescue the ts phenotype in *vps1Δ* as well as the other defects such as membrane trafficking, peroxisomal inheritance and vacuolar defects. This would answer the question of whether these genes can only contribute to the endocytic role of Vps1 or they can also rescue its other roles.

One of the questions that puts itself forward is whether the genes identified in the screen can also rescue defects caused by deletion of other endocytic genes such as *las17Δ* and *sla2Δ.* This information would clarify whether these gene/genes have a specific role at a specific stage of endocytosis or whether they have a more general endocytic role. Growth tests, ts tests, vacuole morphology, peroxisomal inheritance are all simple tests that can be done as a starting point to learn more about the genes that came up in the screen and their effect on Vps1.

Due to time limitations further work was not undertaken, however, future work can reveal important relationships and interactions either direct or indirect between the rescued genes and Vps1. The results from this project will be a valuable addition to the Vps1 interaction chart unraveling new genes that can affect its function.

Chapter 6 – Discussion of Future Directions

6. Discussion

The work presented in this thesis was aimed towards addressing the role of Vps1 in endocytosis and also aimed to determine whether studies of Vps1 could be useful to inform about defects in mammalian dynamins caused by point mutations. Work in chapter 3 describes how mutations corresponding to disease causing mutations in Dynamin-1 (R256L and A408T) and Dynamin-2 (G358R) were generated in yeast Vps1. These studies focussed on mutations in highly conserved regions of the protein that could allow effective identification of the homologous residues. However, many disease causing mutations fall in the PH domain of dynamin. Like other dynamin-like proteins, Vps1 does not have a PH domain, instead at the equivalent position in its primary sequence is a different domain referred to as InsertB. Thus in Chapter 4 attempts were made to introduce either full-length Dynamin-2 or to generate a chimera Vps1ΔInsB_Dyn2_PH. The aim here was to be able to subsequently model the PH domain mutations in a manipulable system. Finally, a number of previous studies in the lab, coupled with work outlined in chapter 3, had allowed generation of a number of mutations that were defective in endocytosis but able to perform other functions associated with Vps1 including Snc1 recycling, Golgi to vacuole trafficking and peroxisome fission. These mutations suggest that certain functions of Vps1 were only important during endocytosis. The generation of stable cells with integrated mutations allowed a screen to be carried out to identify genes, which when overexpressed rescue the temperature sensitivity associated with one of these endocytic mutations and thereby could indicate cell processes or pathways that might impact on Vps1 function during endocytosis.

Analysis of Dynamin Disease causing Mutations generated in Vps1

This work started with investigating the effect of three disease mutations on the cellular role of Vps1. All three mutations have been linked to various neurological diseases.

The G397R mutation in Vps1 is the equivalent mutation to G358R in Dynamin-2 that causes Charcot Marie tooth disorder. G358R was described to lie in the C-terminus of the $L1N^s$ loop which is one of the main contributors to interface 3 which was shown to be essential along with interface 1 for the assembly of Dynamin-3 dimers into tetramers [Reubold *et al.* 2015]. This mutation was shown to dimerise but was unable to bind liposomes, it also had a dominant-negative effect on CME [Koutsopoulos *et al.* 2011, Sidiropoulos *et al.* 2012, Reubold *et al.* 2015]. It was suggested that the arginine side chain interferes with the proper binding conformation of $L1N^s$. Interestingly, the G358R mutant was still recruited to clathrin-coated pits, however these remained stable at the membrane surface suggesting that interface 3 is important for the function of dynamin at the clathrin-coated pits, but not in its recruitment [Reubold *et al.* 2015].

The work carried out in this thesis suggest that the G397R mutation does not cause an inherent stability in the protein as levels of expression were similar to those of Vps1 in wild type cells but the protein was no longer able to interact with lipids effectively and that oligomerisation was reduced. The recent data published by Reubold *et al.* 2015 and the results described here suggest that the oligomerisation and lipid binding are the main defects in the G358R/G397R mutant which when expressed in humans probably affects all functions of the protein hence leading to disease. It has been reported (unpublished work from the lab by Marklew et al.) that oligomerisation is important for lipid binding by

the dynamin PH domain. The result here might also suggest that oligomerisation is important for lipid binding in Vps1 and the primary defect in the mutant is oligomerisation.

The other two mutations analysed were based on Dynamin-1 mutations causing epilepsy in mice (A408T) or exercise-induced collapse in Labrador retrievers (R256L). These mutations reflect the importance of Dynamin-1 in neuronal cells and in particular in endocytic recycling at the synapse. The process of synaptic vesicle recycling involves the coupling of both exocytosis and endocytosis. The fusion of synaptic vesicles containing neurotransmitters with the plasma membrane of the presynaptic terminal results in the addition of new membrane to it. This extra membrane is retrieved back into the cytoplasm of the nerve terminal via endocytosis [Saheki and Camilli 2012]. At low levels of activity in neurons it was shown that neither Dynamin-1, nor Dynamin-1 and 3 together were essential for clathrin-mediated endocytosis to take place. The high level of Dynamin-1 present at synapses is however required during extensive neuronal activity to balance out the high rate of exocytosis taking place [Lou *et al.* 2008, Saheki and Camilli 2012]. The synaptic vesicles need to be urgently recycled so it can pack more neurotransmitters for release outside the synaptic plasma membrane. The role of Dynamin-1 becomes very critical where it is required to perform its role at a very high rate, hence its uniquely high GTPase activity. Therefore, it is not surprising that any defects to the dynamin will have adverse effects on the synaptic recycling pathway, which eventually leads to various neurological disorders.

It was interesting that the two mutations in Vps1 were able to rescue all functions of the protein apart from endocytosis. Despite the complexity of the

neuronal cells it seems that the Vps1 mutations were causing defects that might at some level recapitulate the defects caused by the disease mutations. In this respect it is interesting that the mutations had distinct effects with the R298L/R256L mutation in the GTPase domain having an unexpected effect on lipid binding. It will be interesting to note whether this mutation in mammalian dynamin-1 also influences the range of PI head groups that the protein is able to interact with. The A447T/A408T mutation had more subtle, but still significant effects on endocytosis. The fitful mutation is known to disrupt transferrin uptake in mammalian cells [Boumil *et al.* 2010] and more recently it was shown to lie close to the oligomerisation interface [Reubold *et al.* 2015]. Although the protein was shown to be defective in its oligomerization, the A447T mutation in Vps1 showed no such defects. In fact, stable ring structures of this mutant were observed by EM, further confirming its ability to form higher ordered structures. The work published recently by Dhindsa *et al.* 2015 reported using electron microscopy that fitful mice had a significant decrease in the number of vesicles and an increase in its size in synapses compared to wild type. This observation was consistent with the previously proposed idea by [Patterson *et al.* 2008] that the mutation affected the synaptic vesicle recycling resulting in a defect in endocytosis. If an increased oligomerising potential was also found with Dynamin-1 this might be predicted to be able to have a detrimental effect on the rapid recycling required at synapses when at exercise but not during normal level of function.

Introduce full-length Dynamin-2 and generation of a Vps1ΔInsB_Dyn2_PH chimera in yeast.

This work started with introducing the full length Dynamin-2 into yeast to check for complementation of *vps1* deletion. However, most likely due to the presence of large number of rare codons, Dynamin-2 could not be expressed in yeast. A Vps1ΔInsB_Dyn2PH-GFP chimera was created in yeast with the aim of modeling human disease mutations in the PH domain in yeast. Since many of the disease related mutations in Dynamin-2 were located in the PH domain, creating a construct that can allow the study of these mutations in a simpler model will definitely be of a great value. It is interesting how mutations in a very close proximity can cause the onset of different neurological disorders, as is the case with Dynamin-2 PH mutations that cause Charcot-Marie-Tooth and Centronuclear myopathy. Modeling these mutation in yeast will allow studying the basic effect of these mutations on the biochemical property of the protein and hence a comparison can be made between these mutations. The effect of these mutations on the protein's role in endocytosis and/or its other roles can be addressed especially that there has been growing evidence that Dynamin-2 is not simply involved in endocytosis [Yang et al. 2001 and Nicoziani et al. 2001] which makes yeast a good model to expand on these studies.

Although in this work the Vps1ΔInsB_Dyn2PH-GFP chimeric protein was expressed in yeast cells, it failed to localize to the plasma membrane or to the internal organelles. As was discussed previously in section 4.10 one of the possible reasons behind this could be that the InsertB region, but not the PH domain, contains sequence that is not only important for lipid binding but also for the interaction of Vps1 with other partner proteins. The deletion of InsertB resulted in

the loss this sequence and this in turn could have lead to the loss in the localization observed in the chimeric protein. Therefore, before this chimera could be used, it is important to identify the residues within InsertB that are essential for lipid binding and those essential for the protein's interaction with other partners. Once this is achieved, the PH domain can be substituted for the residues/motifs that are required for lipid binding. This theoretically should ensure that the localization of the new chimeric protein is not affected. Once a stable construct is created, further studies described above can be undertaken.

Genetic screen for a suppressor of a Vps1 endocytic mutant

To fully understand the role and function of Vps1 in endocytosis screens can be performed to identify proteins, which might act to perform equivalent functions. Chapter 5 of this thesis describes a suppressor screen that was performed to identify rescuers of the temperature sensitive phenotype caused by the Vps1 RR456-7EE endocytic mutation. Results obtained from the screen revealed a region on yeast chromosome VII that coded for 7 different genes. Although the temperature sensitive phenotype of the RR457-8EE mutant was rescued, it is still unclear which of the 7 genes was the major contributor to this effect. Once identified, it would particularity be interesting to test whether this gene/genes can also rescue the temperature sensitive phenotype associated with *vps1Δ* as well as the other defects such as membrane trafficking, peroxisomal inheritance and vacuolar defects. If the interaction between the suppressor gene/genes and the Vps1 is specific to endocytosis, then none of the other defects exhibited by *vps1Δ* would be expected to be rescued. Testing the effect of the suppressor gene/genes on other endocytic protein deletions such as *las17Δ* and *sla2Δ* would reveal

interesting information on whether the Vps1/suppressor rescue is specific to a specific stage of endocytosis.

The integrated Vps1 mutants form a stable construct and performing a suppressor screen that would rescue specifically an endocytic defect rather than simply temperature sensitivity would definitely be more informative. For instance, an invertase assay can be used to assess endocytosis, which involves the use of a construct where the SNARE protein Snc1 is fused at its N-terminus to a *SUC2* gene which has an invertase activity and GFP at its C-terminus [Burston et al. 2009].

Snc1 normally gets internalized into the cell via endocytosis and gets recycled back to the plasma membrane. When grown on appropriate media, colonies of wild-type Vps1 would appear orange/brown in colour, however in the presence of an endocytic defect, the colonies will appear dark brown in colour due to a delay in the Snc1 internalization [Smaczynska-de Rooij et al. 2010]. In the case of the *vps1Δ*, the Snc1 construct fails to get recycled back to the plasma membrane and therefore the colonies appear white in colour. If a suppressor gene rescues an endocytic Vps1 mutation, then the change in colony colour from dark brown to orange would be expected. Therefore the rescue of an endocytic defect can be easily monitored in a colormetric manner.

Overall the work described in this thesis has investigated the use of Vps1 as a model for mammalian dynamin function and understanding diseases associated with mutations in dynamin. The yeast work suggests interesting avenues for future research and also indicates that it might be a useful model to understand the growing breadth of membrane fission events with which Dynamin-2 is associated.

References

Aderem, A. and D. M. Underhill (1999). "Mechanisms of phagocytosis in macrophages." Annu Rev Immunol **17**: 593-623.

Aghamohammadzadeh, S. and K. R. Ayscough (2009). "Differential requirements for actin during yeast and mammalian endocytosis." Nat Cell Biol **11**(8): 1039-1042.

Aghamohammadzadeh, S., R. Smaczynska-de, II and K. R. Ayscough (2014). "An Abp1-dependent route of endocytosis functions when the classical endocytic pathway in yeast is inhibited." PLoS One **9**(7): e103311.

Alexander, C., M. Votruba, U. E. Pesch, D. L. Thiselton, S. Mayer, A. Moore, M. Rodriguez, U. Kellner, B. Leo-Kottler, G. Auburger, S. S. Bhattacharya and B. Wissinger (2000). "OPA1, encoding a dynamin-related GTPase, is mutated in autosomal dominant optic atrophy linked to chromosome 3q28." Nat Genet **26**(2): 211-215.

Anderson, S. L., J. M. Carton, J. Lou, L. Xing and B. Y. Rubin (1999). "Interferon-induced guanylate binding protein-1 (GBP-1) mediates an antiviral effect against vesicular stomatitis virus and encephalomyocarditis virus." Virology **256**(1): 8-14.

Ayscough, K. R., J. J. Eby, T. Lila, H. Dewar, K. G. Kozminski and D. G. Drubin (1999). "Sla1p is a functionally modular component of the yeast cortical actin cytoskeleton required for correct localization of both Rho1p-GTPase and Sla2p, a protein with talin homology." Mol Biol Cell **10**(4): 1061-1075.

Ayscough, K. R., J. Stryker, N. Pokala, M. Sanders, P. Crews and D. G. Drubin (1997). "High rates of actin filament turnover in budding yeast and roles for actin in establishment and maintenance of cell polarity revealed using the actin inhibitor latrunculin-A." J Cell Biol **137**(2): 399-416.

Barlow, C. A., R. S. Laishram and R. A. Anderson (2010). "Nuclear phosphoinositides: a signaling enigma wrapped in a compartmental conundrum." Trends Cell Biol **20**(1): 25-35.

Bethoney, K. A., M. C. King, J. E. Hinshaw, E. M. Ostap and M. A. Lemmon (2009). "A possible effector role for the pleckstrin homology (PH) domain of dynamin." Proc Natl Acad Sci U S A **106**(32): 13359-13364.

Bitoun, M., A. C. Durieux, B. Prudhon, J. A. Bevilacqua, A. Herledan, V. Sakanyan, A. Urtizberea, L. Cartier, N. B. Romero and P. Guicheney (2009). "Dynamin 2 mutations associated with human diseases impair clathrin-mediated receptor endocytosis." Hum Mutat **30**(10): 1419-1427.

Bitoun, M., S. Maugenre, P. Y. Jeannet, E. Lacene, X. Ferrer, P. Laforet, J. J. Martin, J. Laporte, H. Lochmuller, A. H. Beggs, M. Fardeau, B. Eymard, N. B. Romero and P. Guicheney (2005). "Mutations in dynamin 2 cause dominant centronuclear myopathy." Nat Genet **37**(11): 1207-1209.

Boeke, J. D., J. Trueheart, G. Natsoulis and G. R. Fink (1987). "5-Fluoroorotic acid as a selective agent in yeast molecular genetics." Methods Enzymol **154**: 164-175.

Bohm, J., V. Biancalana, E. T. Dechene, M. Bitoun, C. R. Pierson, E. Schaefer, H. Karasoy, *et al.* (2012). "Mutation spectrum in the large GTPase dynamin 2, and genotype-phenotype correlation in autosomal dominant centronuclear myopathy." Hum Mutat **33**(6): 949-959.

Bonifacino, J. S. and B. S. Glick (2004). "The mechanisms of vesicle budding and fusion." Cell **116**(2): 153-166.

Boucrot, E., A. P. Ferreira, L. Almeida-Souza, S. Debard, Y. Vallis, G. Howard, L. Bertot, N. Sauvonnet and H. T. McMahon (2015). "Endophilin marks and controls a clathrin-independent endocytic pathway." Nature **517**(7535): 460-465.

Boumil, R. M., V. A. Letts, M. C. Roberts, C. Lenz, C. L. Mahaffey, Z. W. Zhang, T. Moser and W. N. Frankel (2010). "A missense mutation in a highly conserved alternate exon of dynamin-1 causes epilepsy in fitful mice." PLoS Genet **6**(8).

Bowers, K. and T. H. Stevens (2005). "Protein transport from the late Golgi to the vacuole in the yeast Saccharomyces cerevisiae." Biochim Biophys Acta **1744**(3): 438-454.

Buchan, J. R., D. Muhlrad and R. Parker (2008). "P bodies promote stress granule assembly in Saccharomyces cerevisiae." J Cell Biol **183**(3): 441-455.

Bui, H. T., M. A. Karren, D. Bhar and J. M. Shaw (2012). "A novel motif in the yeast mitochondrial dynamin Dnm1 is essential for adaptor binding and membrane

recruitment." J Cell Biol **199**(4): 613-622.

Burston, H. E., L. Maldonado-Baez, M. Davey, B. Montpetit, C. Schluter, B. Wendland and E. Conibear (2009). "Regulators of yeast endocytosis identified by systematic quantitative analysis." J Cell Biol **185**(6): 1097-1110.

Cao, H., F. Garcia and M. A. McNiven (1998). "Differential distribution of dynamin isoforms in mammalian cells." Mol Biol Cell **9**(9): 2595-2609.

Cerveny, K. L., Y. Tamura, Z. Zhang, R. E. Jensen and H. Sesaki (2007). "Regulation of mitochondrial fusion and division." Trends Cell Biol **17**(11): 563-569.

Chappie, J. S., S. Acharya, Y. W. Liu, M. Leonard, T. J. Pucadyil and S. L. Schmid (2009). "An intramolecular signaling element that modulates dynamin function *in vitro* and *in vivo*." Mol Biol Cell **20**(15): 3561-3571.

Chappie, J. S., J. A. Mears, S. Fang, M. Leonard, S. L. Schmid, R. A. Milligan, J. E. Hinshaw and F. Dyda (2011). "A pseudoatomic model of the dynamin polymer identifies a hydrolysis-dependent powerstroke." Cell **147**(1): 209-222.

Chin, Y. H., A. Lee, H. W. Kan, J. Laiman, M. C. Chuang, S. T. Hsieh and Y. W. Liu (2015). "Dynamin-2 mutations associated with centronuclear myopathy are hypermorphic and lead to T-tubule fragmentation." Hum Mol Genet.

Chircop, M., B. Sarcevic, M. R. Larsen, C. S. Malladi, N. Chau, M. Zavortink, C. M. Smith, A. Quan, V. Anggono, P. G. Hains, M. E. Graham and P. J. Robinson (2011). "Phosphorylation of dynamin II at serine-764 is associated with cytokinesis." Biochim Biophys Acta **1813**(10): 1689-1699.

Claeys, K. G., S. Zuchner, M. Kennerson, J. Berciano, A. Garcia, K. Verhoeven, E. Storey, J. R. Merory, H. M. Bienfait, M. Lammens, E. Nelis, J. Baets, E. De Vriendt, Z. N. Berneman, I. De Veuster, J. M. Vance, G. Nicholson, V. Timmerman and P. De Jonghe (2009). "Phenotypic spectrum of dynamin 2 mutations in Charcot-Marie-Tooth neuropathy." Brain **132**(Pt 7): 1741-1752.

Coue, M., S. L. Brenner, I. Spector and E. D. Korn (1987). "Inhibition of actin polymerization by latrunculin A." FEBS Lett **213**(2): 316-318.

Crivellone, M. D. (1994). "Characterization of CBP4, a new gene essential for the expression of ubiquinol-cytochrome c reductase in Saccharomyces cerevisiae." J Biol Chem **269**(33): 21284-21292.

Czech, M. P. (2000). "PIP2 and PIP3: complex roles at the cell surface." Cell **100**(6): 603-606.

D'Avino, P. P., M. S. Savoian and D. M. Glover (2005). "Cleavage furrow formation and ingression during animal cytokinesis: a microtubule legacy." J Cell Sci **118**(Pt 8): 1549-1558.

Daugeron, M. C., M. Prouteau, F. Lacroute and B. Seraphin (2011). "The highly conserved eukaryotic DRG factors are required for efficient translation in a manner redundant with the putative RNA helicase Slh1." Nucleic Acids Res **39**(6): 2221-2233.

Doherty, G. J. and H. T. McMahon (2009). "Mechanisms of endocytosis." Annu Rev Biochem **78**: 857-902.

Dulic, V., M. Egerton, I. Elguindi, S. Raths, B. Singer and H. Riezman (1991). "Yeast endocytosis assays." Methods Enzymol **194**: 697-710.

Durieux, A. C., A. Vignaud, B. Prudhon, M. T. Viou, M. Beuvin, S. Vassilopoulos, B. Fraysse, A. Ferry, J. Laine, N. B. Romero, P. Guicheney and M. Bitoun (2010). "A centronuclear myopathy-dynamin 2 mutation impairs skeletal muscle structure and function in mice." Hum Mol Genet **19**(24): 4820-4836.

Faelber, K., Y. Posor, S. Gao, M. Held, Y. Roske, D. Schulze, V. Haucke, F. Noe and O. Daumke (2011). "Crystal structure of nucleotide-free dynamin." Nature **477**(7366): 556-560.

Ferguson, S. M., G. Brasnjo, M. Hayashi, M. Wolfel, C. Collesi, S. Giovedi, A. Raimondi, L. W. Gong, P. Ariel, S. Paradise, E. O'Toole, R. Flavell, O. Cremona, G. Miesenbock, T. A. Ryan and P. De Camilli (2007). "A selective activity-dependent requirement for dynamin 1 in synaptic vesicle endocytosis." Science **316**(5824): 570-574.

Ferguson, S. M. and P. De Camilli (2012). "Dynamin, a membrane-remodelling GTPase."

Nat Rev Mol Cell Biol **13**(2): 75-88.

Ferguson, S. M., A. Raimondi, S. Paradise, H. Shen, K. Mesaki, A. Ferguson, O. Destaing, G. Ko, J. Takasaki, O. Cremona, O. T. E and P. De Camilli (2009). "Coordinated actions of actin and BAR proteins upstream of dynamin at endocytic clathrin-coated pits." Dev Cell **17**(6): 811-822.

Fischer, D., M. Herasse, M. Bitoun, H. M. Barragan-Campos, J. Chiras, P. Laforet, M. Fardeau, B. Eymard, P. Guicheney and N. B. Romero (2006). "Characterization of the muscle involvement in dynamin 2-related centronuclear myopathy." Brain **129**(Pt 6): 1463-1469.

Ford, M. G., S. Jenni and J. Nunnari (2011). "The crystal structure of dynamin." Nature **477**(7366): 561-566.

Francy, C. A., F. J. Alvarez, L. Zhou, R. Ramachandran and J. A. Mears (2015). "The mechanoenzymatic core of dynamin-related protein 1 comprises the minimal machinery required for membrane constriction." J Biol Chem **290**(18): 11692-11703.

Frohlich, C., S. Grabiger, D. Schwefel, K. Faelber, E. Rosenbaum, J. Mears, O. Rocks and O. Daumke (2013). "Structural insights into oligomerization and mitochondrial remodelling of dynamin 1-like protein." Embo j **32**(9): 1280-1292.

Gammie, A. E., L. J. Kurihara, R. B. Vallee and M. D. Rose (1995). "DNM1, a dynamin-related gene, participates in endosomal trafficking in yeast." J Cell Biol **130**(3): 553-566.

Gerst, J. E., L. Rodgers, M. Riggs and M. Wigler (1992). "SNC1, a yeast homolog of the synaptic vesicle-associated membrane protein/synaptobrevin gene family: genetic interactions with the RAS and CAP genes." Proc Natl Acad Sci U S A **89**(10): 4338-4342.

Godi, A., A. Di Campli, A. Konstantakopoulos, G. Di Tullio, D. R. Alessi, G. S. Kular, T. Daniele, P. Marra, J. M. Lucocq and M. A. De Matteis (2004). "FAPPs control Golgi-to-cell-surface membrane traffic by binding to ARF and PtdIns(4)P." Nat Cell Biol **6**(5): 393-404.

Goffeau, A., B. G. Barrell, H. Bussey, R. W. Davis, B. Dujon, H. Feldmann, F. Galibert, J. D. Hoheisel, C. Jacq, M. Johnston, E. J. Louis, H. W. Mewes, Y. Murakami, P. Philippsen, H. Tettelin and S. G. Oliver (1996). "Life with 6000 genes." Science **274**(5287): 546, 563-

547.

Gold, E. S., D. M. Underhill, N. S. Morrissette, J. Guo, M. A. McNiven and A. Aderem (1999). "Dynamin 2 is required for phagocytosis in macrophages." J Exp Med **190**(12): 1849-1856.

Gonzalez-Jamett, A. M., V. Haro-Acuna, F. Momboisse, P. Caviedes, J. A. Bevilacqua and A. M. Cardenas (2014). "Dynamin-2 in nervous system disorders." J Neurochem **128**(2): 210-223.

Gonzalez-Jamett, A. M., F. Momboisse, V. Haro-Acuna, J. A. Bevilacqua, P. Caviedes and A. M. Cardenas (2013). "Dynamin-2 function and dysfunction along the secretory pathway." Front Endocrinol (Lausanne) **4**: 126.

Goode, B. L., J. A. Eskin and B. Wendland (2015). "Actin and endocytosis in budding yeast." Genetics **199**(2): 315-358.

Gu, C., S. Yaddanapudi, A. Weins, T. Osborn, J. Reiser, M. Pollak, J. Hartwig and S. Sever (2010). "Direct dynamin-actin interactions regulate the actin cytoskeleton." Embo j **29**(21): 3593-3606.

Hansen, C. G. and B. J. Nichols (2010). "Exploring the caves: cavins, caveolins and caveolae." Trends Cell Biol **20**(4): 177-186.

Haucke, V. (2015). "Cell biology: On the endocytosis rollercoaster." Nature **517**(7535): 446-447.

Hayden, J., M. Williams, A. Granich, H. Ahn, B. Tenay, J. Lukehart, C. Highfill, S. Dobard and K. Kim (2013). "Vps1 in the late endosome-to-vacuole traffic." J Biosci **38**(1): 73-83.

Heidtman, M., C. Z. Chen, R. N. Collins and C. Barlowe (2003). "A role for Yip1p in COPII vesicle biogenesis." J Cell Biol **163**(1): 57-69.

Henley, J. R., E. W. Krueger, B. J. Oswald and M. A. McNiven (1998). "Dynamin-mediated internalization of caveolae." J Cell Biol **141**(1): 85-99.

Heymann, J. A. and J. E. Hinshaw (2009). "Dynamins at a glance." J Cell Sci **122**(Pt 19):

3427-3431.

Hinshaw, J. E. and S. L. Schmid (1995). "Dynamin self-assembles into rings suggesting a mechanism for coated vesicle budding." Nature **374**(6518): 190-192.

Hoepfner, D., M. van den Berg, P. Philippsen, H. F. Tabak and E. H. Hettema (2001). "A role for Vps1p, actin, and the Myo2p motor in peroxisome abundance and inheritance in Saccharomyces cerevisiae." J Cell Biol **155**(6): 979-990.

Hoppins, S., S. R. Collins, A. Cassidy-Stone, E. Hummel, R. M. Devay, L. L. Lackner, B. Westermann, M. Schuldiner, J. S. Weissman and J. Nunnari (2011). "A mitochondrial-focused genetic interaction map reveals a scaffold-like complex required for inner membrane organization in mitochondria." J Cell Biol **195**(2): 323-340.

Ikonomov, O. C., D. Sbrissa, K. Mlak, M. Kanzaki, J. Pessin and A. Shisheva (2002). "Functional dissection of lipid and protein kinase signals of PIKfyve reveals the role of PtdIns 3,5-P2 production for endomembrane integrity." J Biol Chem **277**(11): 9206-9211.

Ingerman, E., E. M. Perkins, M. Marino, J. A. Mears, J. M. McCaffery, J. E. Hinshaw and J. Nunnari (2005). "Dnm1 forms spirals that are structurally tailored to fit mitochondria." J Cell Biol **170**(7): 1021-1027.

Ishida, N., Y. Nakamura, K. Tanabe, S. A. Li and K. Takei (2011). "Dynamin 2 associates with microtubules at mitosis and regulates cell cycle progression." Cell Struct Funct **36**(2): 145-154.

Jandrositz, A., F. Turnowsky and G. Hogenauer (1991). "The gene encoding squalene epoxidase from Saccharomyces cerevisiae: cloning and characterization." Gene **107**(1): 155-160.

Jeannet, P. Y., G. Bassez, B. Eymard, P. Laforet, J. A. Urtizberea, A. Rouche, P. Guicheney, M. Fardeau and N. B. Romero (2004). "Clinical and histologic findings in autosomal centronuclear myopathy." Neurology **62**(9): 1484-1490.

Jones, B. A. and W. L. Fangman (1992). "Mitochondrial DNA maintenance in yeast requires a protein containing a region related to the GTP-binding domain of dynamin."

Genes Dev **6**(3): 380-389.

Jones, S. M., K. E. Howell, J. R. Henley, H. Cao and M. A. McNiven (1998). "Role of dynamin in the formation of transport vesicles from the trans-Golgi network." Science **279**(5350): 573-577.

Kaksonen, M., C. P. Toret and D. G. Drubin (2005). "A modular design for the clathrin- and actin-mediated endocytosis machinery." Cell **123**(2): 305-320.

Kenniston, J. A. and M. A. Lemmon (2010). "Dynamin GTPase regulation is altered by PH domain mutations found in centronuclear myopathy patients." Embo j **29**(18): 3054-3067.

Kim, Y. W., D. S. Park, S. C. Park, S. H. Kim, G. W. Cheong and I. Hwang (2001). "Arabidopsis dynamin-like 2 that binds specifically to phosphatidylinositol 4-phosphate assembles into a high-molecular weight complex *in vivo* and *in vitro*." Plant Physiol **127**(3): 1243-1255.

Koutsopoulos, O. S., C. Koch, V. Tosch, J. Bohm, K. N. North and J. Laporte (2011). "Mild functional differences of dynamin 2 mutations associated to centronuclear myopathy and Charcot-Marie Tooth peripheral neuropathy." PLoS One **6**(11): e27498.

Kuravi, K., S. Nagotu, A. M. Krikken, K. Sjollema, M. Deckers, R. Erdmann, M. Veenhuis and I. J. van der Klei (2006). "Dynamin-related proteins Vps1p and Dnm1p control peroxisome abundance in Saccharomyces cerevisiae." J Cell Sci **119**(Pt 19): 3994-4001.

Lacroute, F. (1968). "Regulation of pyrimidine biosynthesis in Saccharomyces cerevisiae." J Bacteriol **95**(3): 824-832.

Lander, E. S., L. M. Linton, B. Birren, C. Nusbaum, M. C. Zody, J. Baldwin, K. Devon, K. Dewar, M. Doyle, *et al.* (2000). "The FYVE domain of early endosome antigen 1 is required for both phosphatidylinositol 3-phosphate and Rab5 binding. Critical role of this dual interaction for endosomal localization." J Biol Chem **275**(5): 3699-3705.

Le Roy, C. and J. L. Wrana (2005). "Clathrin- and non-clathrin-mediated endocytic regulation of cell signalling." Nat Rev Mol Cell Biol **6**(2): 112-126.

Letzring, D. P., K. M. Dean and E. J. Grayhack (2010). "Control of translation efficiency in yeast by codon-anticodon interactions." Rna **16**(12): 2516-2528.

Lewis, M. J., B. J. Nichols, C. Prescianotto-Baschong, H. Riezman and H. R. Pelham (2000). "Specific retrieval of the exocytic SNARE Snc1p from early yeast endosomes." Mol Biol Cell **11**(1): 23-38.

Li, B. and B. Trueb (2000). "DRG represents a family of two closely related GTP-binding proteins." Biochim Biophys Acta **1491**(1-3): 196-204.

Lin, H. C., B. Barylko, M. Achiriloaie and J. P. Albanesi (1997). "Phosphatidylinositol (4,5)-bisphosphate-dependent activation of dynamins I and II lacking the proline/arginine-rich domains." J Biol Chem **272**(41): 25999-26004.

Liu, Y. W., V. Lukiyanchuk and S. L. Schmid (2011). "Common membrane trafficking defects of disease-associated dynamin 2 mutations." Traffic **12**(11): 1620-1633.

Liu, Y. W., S. Neumann, R. Ramachandran, S. M. Ferguson, T. J. Pucadyil and S. L. Schmid (2011). "Differential curvature sensing and generating activities of dynamin isoforms provide opportunities for tissue-specific regulation." Proc Natl Acad Sci U S A **108**(26): E234-242.

Lou, X., S. Paradise, S. M. Ferguson and P. De Camilli (2008). "Selective saturation of slow endocytosis at a giant glutamatergic central synapse lacking dynamin 1." Proc Natl Acad Sci U S A **105**(45): 17555-17560.

Lukehart, J., C. Highfill and K. Kim (2013). "Vps1, a recycling factor for the traffic from early endosome to the late Golgi." Biochem Cell Biol **91**(6): 455-465.

Marks, B., M. H. Stowell, Y. Vallis, I. G. Mills, A. Gibson, C. R. Hopkins and H. T. McMahon (2001). "GTPase activity of dynamin and resulting conformation change are essential for endocytosis." Nature **410**(6825): 231-235.

Marsh, M. and A. Helenius (2006). "Virus entry: open sesame." Cell **124**(4): 729-740.

Masud Rana, A. Y., M. Tsujioka, S. Miyagishima, M. Ueda and S. Yumura (2013). "Dynamin contributes to cytokinesis by stabilizing actin filaments in the contractile ring." Genes Cells **18**(8): 621-635.

McLaughlin, S., J. Wang, A. Gambhir and D. Murray (2002). "PIP(2) and proteins: interactions, organization, and information flow." Annu Rev Biophys Biomol Struct **31**: 151-175.

McMahon, H. T. and E. Boucrot (2011). "Molecular mechanism and physiological functions of clathrin-mediated endocytosis." Nat Rev Mol Cell Biol **12**(8): 517-533.

McPherson, J. D., M. Marra, L. Hillier, R. H. Waterston, A. Chinwalla, J. Wallis, M. Sekhon, *et al.* (2001). "A physical map of the human genome." Nature **409**(6822): 934-941.

Mellman, I. and Y. Yarden (2013). "Endocytosis and cancer." Cold Spring Harb Perspect Biol **5**(12): a016949.

Mettlen, M., T. Pucadyil, R. Ramachandran and S. L. Schmid (2009). "Dissecting dynamin's role in clathrin-mediated endocytosis." Biochem Soc Trans **37**(Pt 5): 1022-1026.

Mooren, O. L., T. I. Kotova, A. J. Moore and D. A. Schafer (2009). "Dynamin2 GTPase and cortactin remodel actin filaments." J Biol Chem **284**(36): 23995-24005.

Morton, W. M., K. R. Ayscough and P. J. McLaughlin (2000). "Latrunculin alters the actin-monomer subunit interface to prevent polymerization." Nat Cell Biol **2**(6): 376-378.

Muhlberg, A. B., D. E. Warnock and S. L. Schmid (1997). "Domain structure and intramolecular regulation of dynamin GTPase." Embo j **16**(22): 6676-6683.

Nagasawa, N., T. Bogaki, A. Iwamatsu, M. Hamachi and C. Kumagai (1998). "Cloning and nucleotide sequence of the alcohol acetyltransferase II gene (ATF2) from Saccharomyces cerevisiae Kyokai No. 7." Biosci Biotechnol Biochem **62**(10): 1852-1857.

Nakata, T., A. Iwamoto, Y. Noda, R. Takemura, H. Yoshikura and N. Hirokawa (1991). "Predominant and developmentally regulated expression of dynamin in neurons." Neuron **7**(3): 461-469.

Nannapaneni, S., D. Wang, S. Jain, B. Schroeder, C. Highfill, L. Reustle, D. Pittsley, A. Maysent, S. Moulder, R. McDowell and K. Kim (2010). "The yeast dynamin-like protein Vps1:vps1 mutations perturb the internalization and the motility of endocytic vesicles

and endosomes via disorganization of the actin cytoskeleton." Eur J Cell Biol **89**(7): 499-508.

Newpher, T. M., R. P. Smith, V. Lemmon and S. K. Lemmon (2005). "*In vivo* dynamics of clathrin and its adaptor-dependent recruitment to the actin-based endocytic machinery in yeast." Dev Cell **9**(1): 87-98.

Nicoziani, P., F. Vilhardt, A. Llorente, L. Hilout, P. J. Courtoy, K. Sandvig and B. van Deurs (2000). "Role for dynamin in late endosome dynamics and trafficking of the cation-independent mannose 6-phosphate receptor." Mol Biol Cell **11**(2): 481-495.

Nothwehr, S. F., E. Conibear and T. H. Stevens (1995). "Golgi and vacuolar membrane proteins reach the vacuole in vps1 mutant yeast cells via the plasma membrane." J Cell Biol **129**(1): 35-46.

Obar, R. A., C. A. Collins, J. A. Hammarback, H. S. Shpetner and R. B. Vallee (1990). "Molecular cloning of the microtubule-associated mechanochemical enzyme dynamin reveals homology with a new family of GTP-binding proteins." Nature **347**(6290): 256-261.

Okamoto, P. M., J. S. Herskovits and R. B. Vallee (1997). "Role of the basic, proline-rich region of dynamin in Src homology 3 domain binding and endocytosis." J Biol Chem **272**(17): 11629-11635.

Olichon, A., L. J. Emorine, E. Descoins, L. Pelloquin, L. Brichese, N. Gas, E. Guillou, C. Delettre, A. Valette, C. P. Hamel, B. Ducommun, G. Lenaers and P. Belenguer (2002). "The human dynamin-related protein OPA1 is anchored to the mitochondrial inner membrane facing the inter-membrane space." FEBS Lett **523**(1-3): 171-176.

Palmer, S. E., R. Smaczynska-de, II, C. J. Marklew, E. G. Allwood, R. Mishra, S. Johnson, M. W. Goldberg and K. R. Ayscough (2015). "A dynamin-actin interaction is required for vesicle scission during endocytosis in yeast." Curr Biol **25**(7): 868-878.

Parent, S. A., C. M. Fenimore and K. A. Bostian (1985). "Vector systems for the expression, analysis and cloning of DNA sequences in S. cerevisiae." Yeast **1**(2): 83-138.

Parton, R. G. and M. A. del Pozo (2013). "Caveolae as plasma membrane sensors,

protectors and organizers." Nat Rev Mol Cell Biol **14**(2): 98-112.

Parton, R. G. and K. Simons (2007). "The multiple faces of caveolae." Nat Rev Mol Cell Biol **8**(3): 185-194.

Patterson, E. E., K. M. Minor, A. V. Tchernatynskaia, S. M. Taylor, G. D. Shelton, K. J. Ekenstedt and J. R. Mickelson (2008). "A canine DNM1 mutation is highly associated with the syndrome of exercise-induced collapse." Nat Genet **40**(10): 1235-1239.

Pearse, B. M. (1975). "Coated vesicles from pig brain: purification and biochemical characterization." J Mol Biol **97**(1): 93-98.

Peters, C., T. L. Baars, S. Buhler and A. Mayer (2004). "Mutual control of membrane fission and fusion proteins." Cell **119**(5): 667-678.

Platta, H. W. and H. Stenmark (2011). "Endocytosis and signaling." Curr Opin Cell Biol **23**(4): 393-403.

Posor, Y., M. Eichhorn-Gruenig, D. Puchkov, J. Schoneberg, A. Ullrich, A. Lampe, R. Muller, S. Zarbakhsh, F. Gulluni, E. Hirsch, M. Krauss, C. Schultz, J. Schmoranzer, F. Noe and V. Haucke (2013). "Spatiotemporal control of endocytosis by phosphatidylinositol-3,4-bisphosphate." Nature **499**(7457): 233-237.

Praefcke, G. J. and H. T. McMahon (2004). "The dynamin superfamily: universal membrane tubulation and fission molecules?" Nat Rev Mol Cell Biol **5**(2): 133-147.

Raimondi, A., S. M. Ferguson, X. Lou, M. Armbruster, S. Paradise, S. Giovedi, M. Messa, N. Kono, J. Takasaki, V. Cappello, E. O'Toole, T. A. Ryan and P. De Camilli (2011). "Overlapping role of dynamin isoforms in synaptic vesicle endocytosis." Neuron **70**(6): 1100-1114.

Ramachandran, R. (2011). "Vesicle scission: dynamin." Semin Cell Dev Biol **22**(1): 10-17.
Ramachandran, R., T. J. Pucadyil, Y. W. Liu, S. Acharya, M. Leonard, V. Lukiyanchuk and S. L. Schmid (2009). "Membrane insertion of the pleckstrin homology domain variable loop 1 is critical for dynamin-catalyzed vesicle scission." Mol Biol Cell **20**(22): 4630-4639.

Ramachandran, R., M. Surka, J. S. Chappie, D. M. Fowler, T. R. Foss, B. D. Song and S. L.

Schmid (2007). "The dynamin middle domain is critical for tetramerization and higher-order self-assembly." Embo j **26**(2): 559-566.

Raymond, C. K., I. Howald-Stevenson, C. A. Vater and T. H. Stevens (1992). "Morphological classification of the yeast vacuolar protein sorting mutants: evidence for a prevacuolar compartment in class E vps mutants." Mol Biol Cell **3**(12): 1389-1402.

Renard, H. F., M. Simunovic, J. Lemiere, E. Boucrot, M. D. Garcia-Castillo, S. Arumugam, V. Chambon, C. Lamaze, C. Wunder, A. K. Kenworthy, A. A. Schmidt, H. T. McMahon, C. Sykes, P. Bassereau and L. Johannes (2015). "Endophilin-A2 functions in membrane scission in clathrin-independent endocytosis." Nature **517**(7535): 493-496.

Reubold, T. F., K. Faelber, N. Plattner, Y. Posor, K. Ketel, U. Curth, J. Schlegel, R. Anand, D. J. Manstein, F. Noe, V. Haucke, O. Daumke and S. Eschenburg (2015). "Crystal structure of the dynamin tetramer." Nature **525**(7569): 404-408.

Robertson, A. S., E. Smythe and K. R. Ayscough (2009). "Functions of actin in endocytosis." Cell Mol Life Sci **66**(13): 2049-2065.

Rothman, J. H., I. Howald and T. H. Stevens (1989). "Characterization of genes required for protein sorting and vacuolar function in the yeast Saccharomyces cerevisiae." Embo j **8**(7): 2057-2065.

Saheki, Y. and P. De Camilli (2012). "Synaptic vesicle endocytosis." Cold Spring Harb Perspect Biol **4**(9): a005645.

Salim, K., M. J. Bottomley, E. Querfurth, M. J. Zvelebil, I. Gout, R. Scaife, R. L. Margolis, R. Gigg, C. I. Smith, P. C. Driscoll, M. D. Waterfield and G. Panayotou (1996). "Distinct specificity in the recognition of phosphoinositides by the pleckstrin homology domains of dynamin and Bruton's tyrosine kinase." Embo j **15**(22): 6241-6250.

Satoh, T., M. Horie, H. Watanabe, Y. Tsuchiya and T. Kamei (1993). "Enzymatic properties of squalene epoxidase from Saccharomyces cerevisiae." Biol Pharm Bull **16**(4): 349-352.

Sbrissa, D., O. C. Ikonomov and A. Shisheva (2000). "PIKfyve lipid kinase is a protein kinase: downregulation of 5'-phosphoinositide product formation by autophosphorylation." Biochemistry **39**(51): 15980-15989.

Schmid, S. L. and V. A. Frolov (2011). "Dynamin: functional design of a membrane fission catalyst." Annu Rev Cell Dev Biol **27**: 79-105.

Sever, S., H. Damke and S. L. Schmid (2000). "Garrotes, springs, ratchets, and whips: putting dynamin models to the test." Traffic **1**(5): 385-392.

Sherman, F. (2002). "Getting started with yeast." Methods Enzymol **350**: 3-41.

Shpetner, H. S., J. S. Herskovits and R. B. Vallee (1996). "A binding site for SH3 domains targets dynamin to coated pits." J Biol Chem **271**(1): 13-16.

Shpetner, H. S. and R. B. Vallee (1989). "Identification of dynamin, a novel mechanochemical enzyme that mediates interactions between microtubules." Cell **59**(3): 421-432.

Sidiropoulos, P. N., M. Miehe, T. Bock, E. Tinelli, C. I. Oertli, R. Kuner, D. Meijer, B. Wollscheid, A. Niemann and U. Suter (2012). "Dynamin 2 mutations in Charcot-Marie-Tooth neuropathy highlight the importance of clathrin-mediated endocytosis in myelination." Brain **135**(Pt 5): 1395-1411.

Smaczynska-de, R., II, E. G. Allwood, S. Aghamohammadzadeh, E. H. Hettema, M. W. Goldberg and K. R. Ayscough (2010). "A role for the dynamin-like protein Vps1 during endocytosis in yeast." J Cell Sci **123**(Pt 20): 3496-3506.

Smaczynska-de, R., II, E. G. Allwood, R. Mishra, W. I. Booth, S. Aghamohammadzadeh, M. W. Goldberg and K. R. Ayscough (2012). "Yeast dynamin Vps1 and amphiphysin Rvs167 function together during endocytosis." Traffic **13**(2): 317-328.

Smirnova, E., L. Griparic, D. L. Shurland and A. M. van der Bliek (2001). "Dynamin-related protein Drp1 is required for mitochondrial division in mammalian cells." Mol Biol Cell **12**(8): 2245-2256.

Smirnova, E., D. L. Shurland, S. N. Ryazantsev and A. M. van der Bliek (1998). "A human dynamin-related protein controls the distribution of mitochondria." J Cell Biol **143**(2): 351-358.

Staeheli, P., O. Haller, W. Boll, J. Lindenmann and C. Weissmann (1986). "Mx protein: constitutive expression in 3T3 cells transformed with cloned Mx cDNA confers selective resistance to influenza virus." Cell **44**(1): 147-158.

Stefan, C. J., S. M. Padilla, A. Audhya and S. D. Emr (2005). "The phosphoinositide phosphatase Sjl2 is recruited to cortical actin patches in the control of vesicle formation and fission during endocytosis." Mol Cell Biol **25**(8): 2910-2923.

Stevens, T., B. Esmon and R. Schekman (1982). "Early stages in the yeast secretory pathway are required for transport of carboxypeptidase Y to the vacuole." Cell **30**(2): 439-448.

Sun, Y. and D. G. Drubin (2012). "The functions of anionic phospholipids during clathrin-mediated endocytosis site initiation and vesicle formation." J Cell Sci **125**(Pt 24): 6157-6165.

Swanson, J. A. and C. Watts (1995). "Macropinocytosis." Trends Cell Biol **5**(11): 424-428.

Sweitzer, S. M. and J. E. Hinshaw (1998). "Dynamin undergoes a GTP-dependent conformational change causing vesiculation." Cell **93**(6): 1021-1029.

Takei, K., V. I. Slepnev, V. Haucke and P. De Camilli (1999). "Functional partnership between amphiphysin and dynamin in clathrin-mediated endocytosis." Nat Cell Biol **1**(1): 33-39.

Tanabe, K. and K. Takei (2009). "Dynamic instability of microtubules requires dynamin 2 and is impaired in a Charcot-Marie-Tooth mutant." J Cell Biol **185**(6): 939-948.

Taylor, M. J., D. Perrais and C. J. Merrifield (2011). "A high precision survey of the molecular dynamics of mammalian clathrin-mediated endocytosis." PLoS Biol **9**(3): e1000604.

Thompson, H. M., A. R. Skop, U. Euteneuer, B. J. Meyer and M. A. McNiven (2002). "The large GTPase dynamin associates with the spindle midzone and is required for cytokinesis." Curr Biol **12**(24): 2111-2117.

Tkach, J. M., A. Yimit, A. Y. Lee, M. Riffle, M. Costanzo, D. Jaschob, J. A. Hendry, J. Ou, J.

Moffat, C. Boone, T. N. Davis, C. Nislow and G. W. Brown (2012). "Dissecting DNA damage response pathways by analysing protein localization and abundance changes during DNA replication stress." Nat Cell Biol **14**(9): 966-976.

Tong, A. H., G. Lesage, G. D. Bader, H. Ding, H. Xu, X. Xin, J. Young, G. F. Berriz, R. L. Brost, M. Chang, Y. Chen, X. Cheng, G. Chua, H. Friesen, D. S. Goldberg, J. Haynes, C. Humphries, G. He, S. Hussein, L. Ke, N. Krogan, Z. Li, J. N. Levinson, H. Lu, P. Menard, C. Munyana, A. B. Parsons, O. Ryan, R. Tonikian, T. Roberts, A. M. Sdicu, J. Shapiro, B. Sheikh, B. Suter, S. L. Wong, L. V. Zhang, H. Zhu, C. G. Burd, S. Munro, C. Sander, J. Rine, J. Greenblatt, M. Peter, A. Bretscher, G. Bell, F. P. Roth, G. W. Brown, B. Andrews, H. Bussey and C. Boone (2004). "Global mapping of the yeast genetic interaction network." Science **303**(5659): 808-813.

Traub, L. M. (2009). "Tickets to ride: selecting cargo for clathrin-regulated internalization." Nat Rev Mol Cell Biol **10**(9): 583-596.

Trowbridge, I. S., J. F. Collawn and C. R. Hopkins (1993). "Signal-dependent membrane protein trafficking in the endocytic pathway." Annu Rev Cell Biol **9**: 129-161.

Tzagoloff, A., A. Vambutas and A. Akai (1989). "Characterization of MSM1, the structural gene for yeast mitochondrial methionyl-tRNA synthetase." Eur J Biochem **179**(2): 365-371.

van der Bliek, A. M. (1999). "Functional diversity in the dynamin family." Trends Cell Biol **9**(3): 96-102.

van der Bliek, A. M. and E. M. Meyerowitz (1991). "Dynamin-like protein encoded by the Drosophila shibire gene associated with vesicular traffic." Nature **351**(6325): 411-414.

van der Bliek, A. M., T. E. Redelmeier, H. Damke, E. J. Tisdale, E. M. Meyerowitz and S. L. Schmid (1993). "Mutations in human dynamin block an intermediate stage in coated vesicle formation." J Cell Biol **122**(3): 553-563.

Vater, C. A., C. K. Raymond, K. Ekena, I. Howald-Stevenson and T. H. Stevens (1992). "The VPS1 protein, a homolog of dynamin required for vacuolar protein sorting in Saccharomyces cerevisiae, is a GTPase with two functionally separable domains." J Cell Biol **119**(4): 773-786.

Vida, T. A. and S. D. Emr (1995). "A new vital stain for visualizing vacuolar membrane

dynamics and endocytosis in yeast." J Cell Biol **128**(5): 779-792.

Vizeacoumar, F. J., J. C. Torres-Guzman, Y. Y. Tam, J. D. Aitchison and R. A. Rachubinski (2003). "YHR150w and YDR479c encode peroxisomal integral membrane proteins involved in the regulation of peroxisome number, size, and distribution in Saccharomyces cerevisiae." J Cell Biol **161**(2): 321-332.

Wang, D., J. Sletto, B. Tenay and K. Kim (2011). "Yeast dynamin implicated in endocytic scission and the disassembly of endocytic components." Commun Integr Biol **4**(2): 178-181.

Warnock, D. E., J. E. Hinshaw and S. L. Schmid (1996). "Dynamin self-assembly stimulates its GTPase activity." J Biol Chem **271**(37): 22310-22314.

Warren, D. T., P. D. Andrews, C. W. Gourlay and K. R. Ayscough (2002). "Sla1p couples the yeast endocytic machinery to proteins regulating actin dynamics." J Cell Sci **115**(Pt 8): 1703-1715.

Wellner, N., T. A. Diep, C. Janfelt and H. S. Hansen (2013). "N-acylation of phosphatidylethanolamine and its biological functions in mammals." Biochim Biophys Acta **1831**(3): 652-662.

Williams, M. and K. Kim (2014). "From membranes to organelles: emerging roles for dynamin-like proteins in diverse cellular processes." Eur J Cell Biol **93**(7): 267-277.

Wilsbach, K. and G. S. Payne (1993). "Vps1p, a member of the dynamin GTPase family, is necessary for Golgi membrane protein retention in Saccharomyces cerevisiae." Embo j **12**(8): 3049-3059.

Wu, F. and P. J. Yao (2009). "Clathrin-mediated endocytosis and Alzheimer's disease: an update." Ageing Res Rev **8**(3): 147-149.

Yang et al. 2001 Golgi vesicle budding

Yarar, D., C. M. Waterman-Storer and S. L. Schmid (2005). "A dynamic actin cytoskeleton functions at multiple stages of clathrin-mediated endocytosis." Mol Biol Cell **16**(2): 964-975.

Yoon, Y., K. R. Pitts and M. A. McNiven (2001). "Mammalian dynamin-like protein DLP1 tubulates membranes." Mol Biol Cell **12**(9): 2894-2905.

Yu, X. and M. Cai (2004). "The yeast dynamin-related GTPase Vps1p functions in the organization of the actin cytoskeleton via interaction with Sla1p." J Cell Sci **117**(Pt 17): 3839-3853.

Zhang, M. (2008). "Endocytic mechanisms and drug discovery in neurodegenerative diseases." Front Biosci **13**: 6086-6105.

Zuchner, S., M. Noureddine, M. Kennerson, K. Verhoeven, K. Claeys, P. De Jonghe, J. Merory, S. A. Oliveira, M. C. Speer, J. E. Stenger, G. Walizada, D. Zhu, M. A. Pericak-Vance, G. Nicholson, V. Timmerman and J. M. Vance (2005). "Mutations in the pleckstrin homology domain of dynamin 2 cause dominant intermediate Charcot-Marie-Tooth disease." Nat Genet **37**(3): 289-294.